UNIVERSIDAD NACIONAL AUTÓNOMA DE MÉXICO

Maestría y Doctorado en Ciencias Bioquímicas

CARACTERIZACIÓN DE LA RESPUESTA INMUNOLÓGICA DE LINFOCITOS T CD8+ CONTRA LA PROTEÍNA E1 DE VIRUS DE PAPILOMA HUMANO TIPO-18

TESIS

QUE PARA OPTAR POR EL GRADO DE:

Doctor en Ciencias

PRESENTA:
ALFREDO AMADOR MOLINA

TUTOR PRINCIPAL
DRA. MARCELA LIZANO SOBERÓN
Instituto de Investigaciones Biomédicas

MIEMBROS DEL COMITÉ TUTOR
DRA. LETICIA ROCHA ZAVALETA
Instituto de Investigaciones Biomédicas
DRA. YVONNE ROSENSTEIN AZOULAY
Instituto de Biotecnología

Ciudad de México. Marzo, 2019

Amador Molina Alfredo
Estudiante de Doctorado en Ciencias Bioquímicas
P r e s e n t e

Los miembros del Subcomité Académico en reunión ordinaria del día 14 de enero del presente año, conocieron su solicitud de asignación de **JURADO DE EXAMEN** para optar por el grado de **DOCTORADO EN CIENCIAS**, con la réplica de la tesis **"Caracterización de la respuesta inmune de linfocitos T CD+8 contra la proteína E1 de virus de papiloma humano tipo 18"**, dirigida por el/la Dr(a). **Lizano Soberón Marcela.**

De su análisis se acordó nombrar el siguiente jurado integrado por los doctores:

PRESIDENTE	Ortega Soto Enrique
VOCAL	Carrero Sánchez Julio César
VOCAL	Ortiz Sánchez Elizabeth
VOCAL	Espinoza Gutiérrez Bertha Josefina
SECRETARIO	Licona Limón Paula

Sin otro particular por el momento, aprovecho la ocasión para enviarle un cordial saludo.

A t e n t a m e n t e
"POR MI RAZA, HABLARÁ EL ESPÍRITU"
Cd. Universitaria, Cd. Mx., a 14 de enero de 2019.
COORDINADORA

Dra. ANA BRÍGIDA CLORINDA ARIAS ÁLVAREZ

contacto: mdcbq@posgrado.unam.mx   Tel. 5623 7006

AGRADECIMIENTOS

ÍNDICE DE TABLAS Y FIGURAS

Página

RESUMEN

La respuesta inmunológica mediada por linfocitos T CD8+ es la principal respuesta empleada por el hospedero para eliminar infecciones por virus del papiloma humano (VPH). Sin embargo, el VPH puede evadir el sistema inmune a través de diferentes mecanismos, y llevar hacia una persistencia de la infección, la cual es un requisito para el desarrollo de cáncer cervical. Para el tratamiento efectivo de mujeres con citología normal, pero con lesiones persistentes de VPH de alto riesgo, o con lesiones intraepiteliales de bajo grado, se requiere de nuevas estrategias dirigidas contra blancos inmunológicos que permitan un amplio espectro de protección cruzada contra diferentes tipos de VPH de alto riesgo.

La helicasa E1 es una de las proteínas más conservadas entre los virus del papiloma y se expresa tempranamente durante una infección por VPH; por lo tanto, su expresión durante la replicación viral hace de esta proteína un blanco inmunológico potencial.

En el presente estudio, se examinó la respuesta inmune de linfocitos T CD8+ específicas de E1 en un modelo de ratón, utilizando α-galactosilceramida (α-GalCer) como adyuvante. Encontramos que los ratones inmunizados junto con E1 combinado con α-GalCer presentaron una respuesta de linfocitos T CD8+ antígeno-específica, que se correlacionó con la inhibición del crecimiento de células de melanoma B16-F0 injertadas, que expresan VPH-18/E1, tanto en un modelo profiláctico como terapéutico. Además, α-GalCer promueve una respuesta de linfocitos NK, que potencia la respuesta antitumoral específica de antígeno de los linfocitos T CD8+.

Los linfocitos T CD8+ de ratones inmunizados con VPH-18/E1 más α-GalCer, reconocieron antígenos de E1 de los tipos de VPH-53, 33, 31, 16 y 11, con lo que demostramos que esta inmunización genera una reacción cruzada contra otros tipos virales.

De esta manera el presente trabajo propone a la proteína E1 como un prometedor blanco inmunológico para nuevas estrategias terapéuticas relacionadas a la eliminación de lesiones tanto de bajo grado como de alto grado.

ABSTRACT

CD8+ T cell-mediated immune response plays a major role in the clearance of virus-infected cells, including human papillomavirus (HPV). For the effective treatment of women with normal cytology but persistent high risk-HPV infection or with low-grade intraepithelial lesions, novel strategies based in viral immunological targets which allow a wide spectrum of cross-protection, would be useful. The helicase E1 is one of the most conserved proteins among papillomaviruses and is expressed early during an HPV infection; therefore, its expression during viral replication makes this protein a potential immunological target. In the present study, we examined E1-specific CD8+ T cell immune responses in a mouse model, using α-galactosylceramide (α-GalCer) as an adjuvant. We found that mice immunized with E1 combined with α-GalCer elicited an E1-antigen specific CD8+ T cell response, which correlated with growth inhibition of grafted melanoma B16-F0 cells expressing E1, both in prophylactic and therapeutic protocols. Furthermore, α-GalCer promote an NK cell response, which potentiates the antigen-specific antitumor response by CD8+ T cells.

In addition, CD8+ T cells raised against HPV18 E1-antigen presented cross-reactivity against E1 protein from HPV53, 33, 16 and 31, and poor cross-reactivity was observed for HPV11 and none for HPV6.

This outcome may be relevant for the design of broad spectrum immune-protective agents against HPV infections.

INTRODUCCIÓN

- **EPIDEMIOLOGÍA Y ETIOLOGIA DEL CANCER CERVICOUTERINO.**

Se estima que anualmente se diagnostican a nivel mundial cerca de 569,847 nuevos casos de cáncer cervicouterino (CaCu) y 311,365 muertes al año, siendo el cuarto cáncer más frecuente en mujeres, después del cáncer de mama, colorectal y pulmón a nivel mundial (IARC).

Particularmente en México, el CaCu es la segunda causa de muerte en mujeres por cáncer, antecedido solo por cáncer de mama [1].

Se ha demostrado que los virus del papiloma humano (VPH) de alto riesgo son el principal factor etiológico asociado con el desarrollo de lesiones cervicales y con cáncer cervicouterino [2].

El cérvix es la porción fibromuscular inferior del útero. Su estroma está compuesto de tejido fibromuscular denso, así como de tejido vascular, linfático y nervioso que juntos conforman un complejo plexo. El cérvix está dividido en dos zonas: el **ectocérvix**, que está tapizado por epitelio estratificado escamoso no queratinizado y el **endocérvix,** que está recubierto por uno de tipo cilíndrico mucosecretor no estratificado [3, 4].

Normalmente, el ectocérvix lo constituyen múltiples capas de células. En su porción inferior, ordenadas en una sola capa, se localizan las células basales, con un núcleo prominente y poco citoplasma, ancladas a la membrana basal. Las células basales se dividen y maduran para formar la siguiente capa de células denominadas células parabasales. La maduración y diferenciación de estas células conduce a la formación de la capa intermedia de células poligonales, de núcleo pequeño y abundante citoplasma. La continuada maduración de las células intermedias da lugar a las células que conforman la capa superficial, que fenotípicamente son grandes y aplanadas, con núcleos picnóticos y citoplasma transparente [3].

Estudios efectuados para caracterizar el microambiente inmunológico en el cérvix normal, han demostrado la presencia de linfocitos intraepiteliales en el ectocérvix, siendo la población de linfocitos CD8+ la más abundante; aunado a esto, el fenotipo de mayor frecuencia ha sido el de memoria (CD45RO+). Restringidas principalmente a la lámina propia, se han localizado linfocitos T vírgenes (CD45RA+), y en un grupo amplio de

muestras ectocervicales analizadas hubo escasas células NK; CD57+ y CD56+ (0 a 2 por cada 100) [5]

En la lámina propia y epitelio glandular hay escasos linfocitos CD4+ y CD8+ (0 a 2 por cada 100). En el caso de linfocitos intraepiteliales CD8+, hay una concentración en el rango de 1 a 5 por cada 100 células epiteliales, mientras que para el caso de células CD4+, la concentración es de 0 a 4 [5].

La transición entre los epitelios ecto- y endocervical se denomina unión escamo-columnar **(UEC)** o **"Zona de transformación"**, caracterizada por ser un área dinámica, sujeta a fenómenos proliferativos y de remodelación que transforman el epitelio cilíndrico mucosecretor en epitelio estratificado escamoso **(3, 5)** (Figura 1) [3, 4].
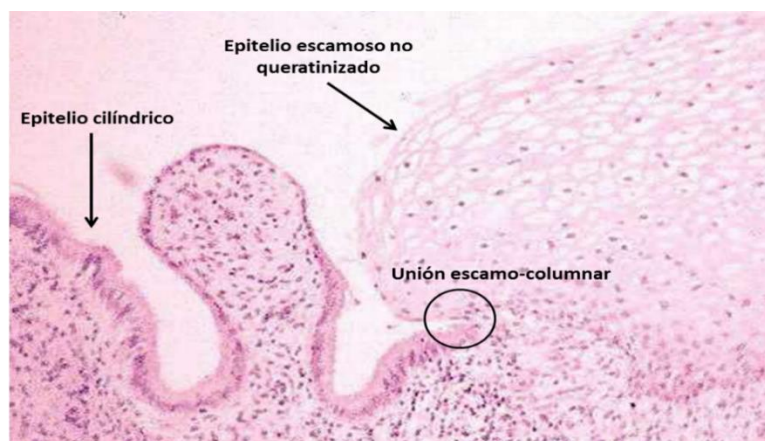
Figura 1. Unión escamo-columnar del epitelio cervical. El círculo de color negro engloba la interfaz en la que se da el cambió de un epitelio escamoso no queratinizado a un epitelio cilíndrico. Esta es la zona de mayor susceptibilidad para el desarrollo de cáncer cervical. Tomado de Eifel L, 2009 [4].

En la zona de transformación se han reportado las concentraciones más elevadas de macrófagos y linfocitos T CD4+ y CD8+. Estos datos proveen evidencia de que la zona de transformación funciona como una barrera inmunológica dinámica, lo cual es de gran interés puesto que ésta es la zona blanco para la infección por VPH.

- **BIOLOGIA MOLECULAR DEL VPH**

De acuerdo con el comité internacional para la taxonomía de los virus (por sus siglas en inglés, ICTV), los papilomavirus pertenecen a la familia *Papillomaviridae*, caracterizados por ser virus desnudos, con un genoma de ácido desoxirribonucleico (ADN) circular, de

doble cadena, de aproximadamente 8,000 pares de bases, que cuentan con una cápside icosaédrica de 72 capsómeros con un tamaño aproximado de 45-55 nm [6].

El genoma de VPH está constituido por: **A) La Región Larga de Control (LCR)**, con una longitud de 800 a 1000 pb, es una secuencia no codificante. Contiene sitios de unión para factores de transcripción celulares, así como para las proteínas E1 y E2 que controlan la replicación y la transcripción viral. Funcionalmente, la LCR contiene un dominio regulado por la proteína E2 y donde se localiza tanto el origen de replicación viral [7], como el promotor de los genes tempranos; y otro dominio llamado CE (celular enhancer), el cual es un potenciador de la transcripción cuya activación depende de factores transcripcionales celulares [8-10] (Figura 2). **B)** La segunda, es la **región de expresión temprana (Early)**, que consiste en los genes E1, E2, E4, E5, E6 y E7. Sus productos génicos participan en la regulación de las fases vegetativas y productivas del ciclo viral, así como en la oncogénesis [8] (Figura 2). **C)** La tercera, es la **región de expresión tardía (Late),** que codifica para las proteínas estructurales L1 y L2 que forman la cápside viral [6, 7] (Figura 2).
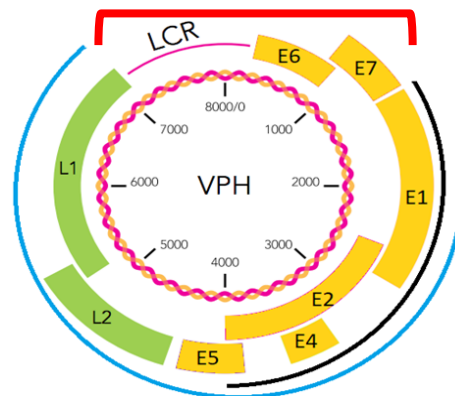
Figura 2. Organización del genoma del Virus del Papiloma Humano 18. En rosa está delimitada la región larga de control, en amarillo la región de expresión temprana y en verde la región de expresión tardía, mientras que cuando sucede el evento de integración, existe una zona donde preferencialmente sucede la ruptura marcada en negro, una región que al integrarse pierde su expresión marcada en azul y una región del genoma viral marcada con corchete rojo que al ser integrada en el genoma celular es sobre-expresada. Modificada de: The Health Professional's HPV Handbook, 2006.

Los Virus de Papiloma se clasifican en 3 niveles taxonómicos: Género, Especie y Tipo [6]. Los géneros comparten menos del 60 % de identidad en la secuencia de L1. El gen L1 es de los más conservados del genoma viral y se ha usado para identificar nuevos tipos virales que son reconocidos solo si la secuencia nucleotídica del gen difiere por más del 10 % de aquella del tipo viral conocido más cercano. Diferencias entre el 2 y 5%

define a una variante viral intratipo. Hasta la fecha se han descrito y secuenciado completamente más de 200 tipos virales y se ha identificado un número mayor mediante la amplificación de regiones subgenómicas. Las especies de un género comparten una identidad de 60 a 70 % y los tipos virales dentro de una especie comparten de 71 a 89 % de identidad [6].

Los VPH se han clasificado en virus de alto riesgo (AR) o bajo riesgo (BR), de acuerdo con su potencial oncogénico que presentan para el desarrollo de lesiones cancerosas, así como la capacidad transformante que tienen sus proteínas en estudios *in vitro* y en modelos animales (Tabla 1) [11-13].

Tabla 1: Principales VPH de alto y bajo riesgo oncogénico. De acuerdo con su potencial oncogénico, los tipos de mayor frecuencia encontrados en lesiones benignas son los tipos virales 6 y 11; mientras que los tipos 16 y 18 son los de mayor frecuencia en casos de cáncer cervical [11].

Virus de bajo riesgo (VPH-BR)	**6, 11,** 10, 3, 7, 28, 29, 32, 40, 42, 43, 44, 54, 61, 72, 81, 83, 84, 78
Virus de alto riesgo (VPH-AR)	**16, 18**, 31, 33, 35, 39, 45, 51, 52, 56, 58 y 59.

- **HISTORIA NATURAL DE LA INFECCIÓN POR VPH Y EL PAPEL DE LA PROTEÍNA E1 EN EL CICLO REPLICATIVO.**

El primer paso en ciclo viral es la infección del VPH a las células epiteliales basales. Actualmente se considera que los VPH-AR requieren de la presencia de una micro-lesión epitelial que exponga las células epiteliales basales al ingreso del virus. Modelos experimentales sugieren que se requiere el acceso de las partículas vírales a la lámina basal y de su interacción con proteoglicanos de heparán sulfato y posiblemente laminina [14]. Cambios estructurales en la cápside del virión, como el corte de la proteína L2 por furina, promueven la transferencia del virión a un receptor secundario sobre los queratinocitos basales para el ingreso del virus a la célula hospedera y la transferencia del genoma viral al núcleo [14]. La naturaleza del receptor o co-receptores aún es poco clara, sin embargo, se han propuesto al receptor a factor de crecimiento (GFR) y a la

integrina alpha-6 como posible receptor y anexina A2 entre uno de los diversos co-receptores descritos que puede utilizar VPH [14] (Figura 3).
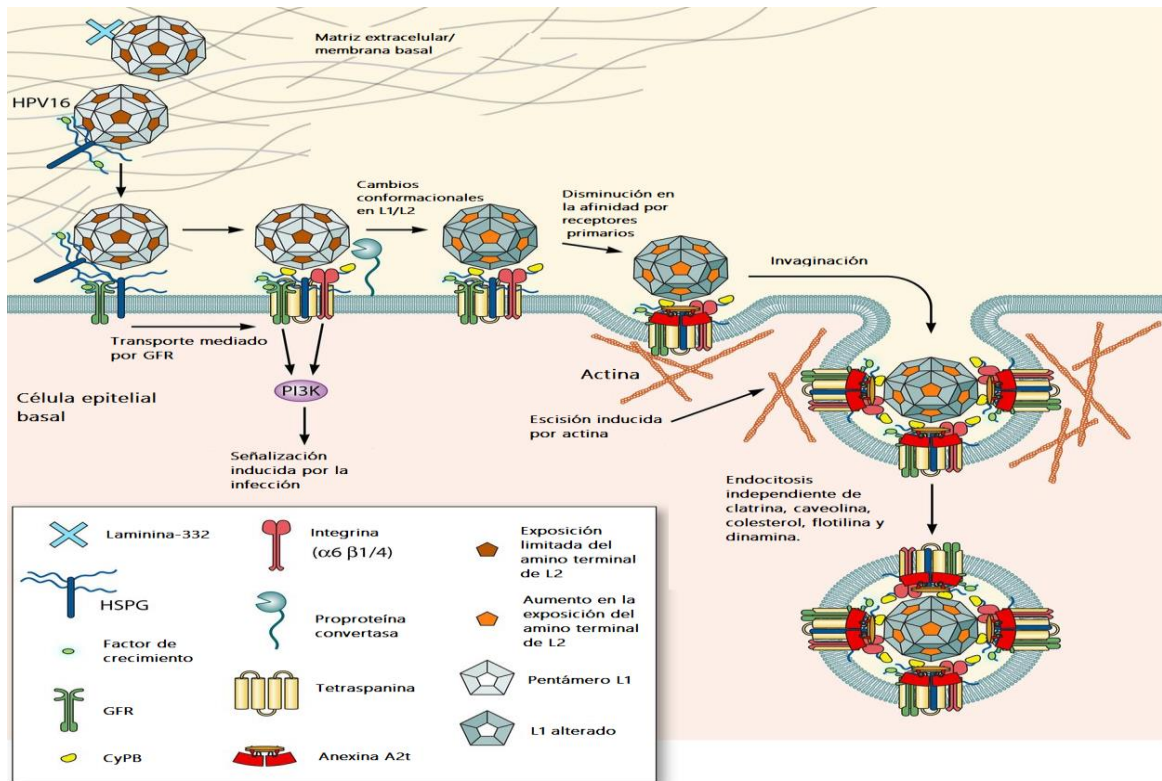
Figura 3. Mecanismo de entrada de VPH-16 a la célula huésped. El VPH-16 es capaz de unirse a los proteoglicanos de sulfato de heparina (HSPG) en la superficie de la célula epitelial o en la membrana basal o a través de laminina-332 en la matriz extracelular (MEC). El receptor del factor de crecimiento epidérmico (EGFR) y/o receptor del factor de crecimiento de queratinocitos (KGFR) pueden activarse e iniciar cascadas de señalización intracelular que incluyen la activación de la vía fosfatidilinositol 3-cianasa (PI3K). Después de unirse a los HSPG, el virión experimenta un cambio conformacional que se ve facilitado por la ciclofilina B (CyPB), que expone más aminoácidos del extremo N-terminal de L2. Posteriormente, VPH-16 se une a la integrina α6, que inicia una segunda cascada de señalización intracelular, que conlleva a cambios conformacionales en la cápside del virus lo cual facilita su unión con la proteína A2t. Después de la unión con A2t, se activa la endocitosis independiente de clatrina, caveolina, balsa lipídica, flotilina, colesterol o dinamina. (Modificada de Raff AB, *et al*, 2013) [14].

Posterior del ingreso y des-encapsulación del virus, los genomas del VPH se replican en el núcleo. Las proteínas implicadas en replicación viral son E1 y E2, las cuales son esenciales para esta fase de amplificación de episomas virales.

La proteína E1 está compuesta de tres dominios: El dominio Carboxilo terminal, el cual posee actividad helicasa/ATPasa y es el más conservado de la proteína [15]. El dominio central o de unión a ADN (DBD) y el dominio N-terminal que contiene señales de localización nuclear (NLS) los cuales son fosforilados para que la proteína E1 pueda permanecer en núcleo, y una secuencia de exporte nuclear (NES) [10, 16, 17] (Figura 4). Además, la región amino terminal de E1 contiene dos sitios (DxxDxxD) sobrelapados para el corte de caspasa 3 y 7 [17, 18]. El corte en este sitio es requerido para la amplificación del genoma viral en queratinocitos diferenciados [18]. En la siguiente figura se muestra un esquema que contempla parte de los sitios antes descritos (Figura 4).
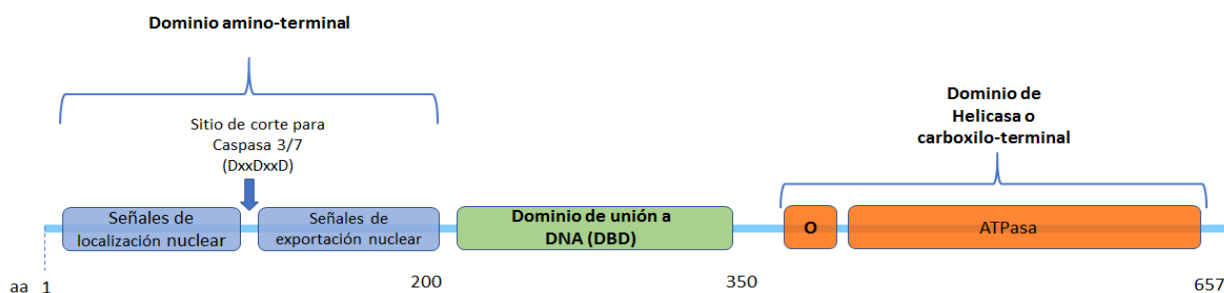
Figura 4. **Representación esquemática de la proteína E1 del VPH-18.** Se muestran los tres dominios de la proteína: El dominio N-terminal (azul), en el que se encuentran las señales de localización y exportación nuclear, así como la secuencia de corte para las caspasas 3 y 7; El dominio de unión a DNA (verde) y el dominio carboxilo terminal (naranja), donde radica la función de Helicasa/ATP y las secuencias de oligomerización (O) de la proteína.

Durante la replicación del genoma viral, la proteína viral E1 forma un complejo con la proteína viral E2 en el origen de replicación, este complejo E1-E2 es fundamental para la estabilización de la proteína E1 con el ADN [19]. En ausencia de E2, la replicación *in vitro* de genomas es muy baja en comparación cuando están presentes E1 y E2 [10, 20]. Una vez que el complejo E1-E2 está unido al ADN, E1 puede abrir la doble hélice de manera bidireccional, reclutando a su vez a la ADN polimerasa-α y a las proteínas de replicación A (RPA) [19] (Figura 5). Cabe mencionar que la proteína E1 es la única proteína de VPH con actividad enzimática, específicamente, con actividad helicasa 3'a 5' dependiente de ATP, dicha función enzimática la hace ser una de las proteínas más conservadas del VPH [15]**.**
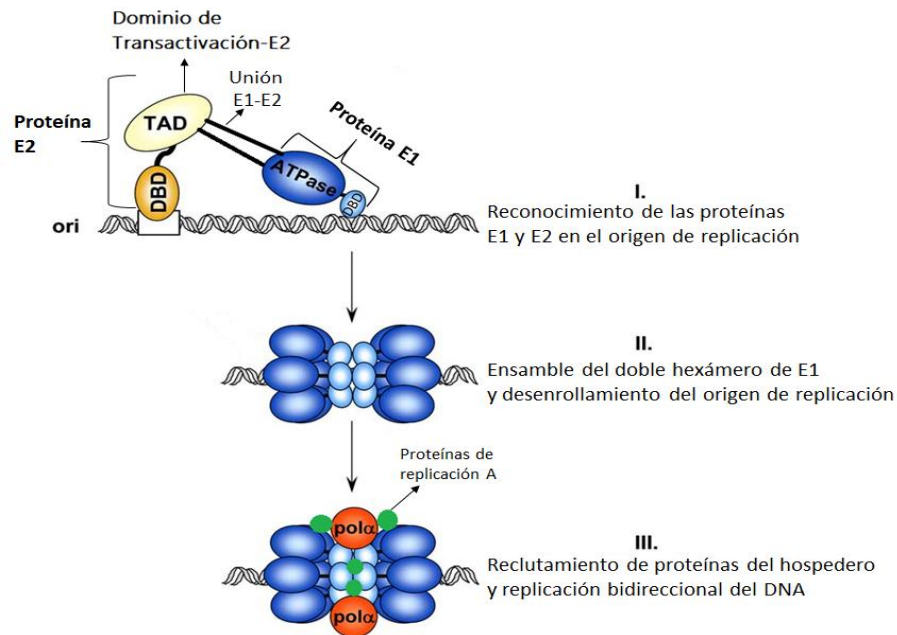
Figura 5. Esquema del inicio de la replicación del ADN de VPH. (I) La replicación se inicia mediante el reclutamiento de E1 (azul) por E2 (amarillo), al origen de replicación viral. Este paso de reclutamiento implica una interacción proteína-proteína esencial entre el TAD-E2 y el dominio helicasa de E1. (II) E2 recluta moléculas E1 adicionales y promueve el ensamblaje de un doble hexámero de E1. El ATP estimula la oligomerización de E1, la cual es necesaria para promover la actividad helicasa de E1. (III) Finalmente, E1 interactúa con los factores de replicación de la célula hospedadora, como la polimerasa α primasa (polα, naranja), así como proteínas de replicación A (verde) para promover la replicación bidireccional del genoma viral (Modificada de D´Abramo, *et al.* 2011).

Las proteínas de replicación celular que se necesitan para la replicación del ADN viral normalmente no están expresadas en abundancia en los queratinocitos en diferenciación debido a que no están en fase "S" del ciclo celular. No obstante, los VPH tienen mecanismos por los cuales favorecen que los queratinocitos entren a fase S, permitiendo un aumento de las proteínas de replicación.

La proteína viral responsable para mantener en ciclo celular a los queratinocitos en diferenciación es E7, y es llevado a cabo en parte por la inactivación de miembros de la familia pRb [21].

Durante la diferenciación, los niveles de los transcritos de los genes E1, E2, y E5 se incrementan [7]. Se ha descrito que el corte de E1 mediado por caspasas facilita la amplificación del genoma viral dependiente de diferenciación, y que la acumulación de E1 en el núcleo potencia la replicación del genoma viral [18].

Seguido de la amplificación del genoma, las proteínas L1 y L2 son producidas en la fase tardía y los viriones son ensamblados. Múltiples niveles de regulación controlan la expresión de las proteínas de la cápside, que permiten su expresión solo en los estratos celulares más diferenciados. Estos niveles incluyen la regulación dependiente de diferenciación de donadores y aceptores de splicing alternativo, regulación de estabilidad del transcrito, y el uso de codones poco comunes [7].

Finalmente, la liberación de las partículas virales se da mediante la actividad de E4, la cual desestabiliza las redes de citoqueratina al formar poros por los cuales ocurre la liberación de viriones [22], lo que contribuye a la persistencia viral. Además, este proceso de liberación no ocasiona un evento lítico en el epitelio, por lo que evita la generación de procesos inflamatorios que son indispensables en el desarrollo de una respuesta inmunológica.

La progresión de lesiones hacia cáncer microinvasor o invasor, se asocia con la integración del genoma del VPH al genoma del hospedero. En dicho proceso usualmente se pierde la integridad de la proteína E2, que es un regulador negativo de la expresión de las oncoproteínas E6 y E7. Por lo tanto, se propicia la subsecuente sobreexpresión de los oncogenes E6 y E7, cuyas proteínas llevan a la presencia de un fenotipo maligno [23].

De esta manera durante la historia natural de infección, la expresión de la proteína E1 se da principalmente en etapas tempranas de la infección y lesiones de bajo grado (NIC-1 y NIC-2). Sin embargo, recientemente se ha reportado una elevada expresión de E1 en etapas tardías como NIC-3 y cáncer *in situ* [24].

La figura 6 resume los eventos más importantes en la progresión maligna inducida por VPH de alto riesgo.
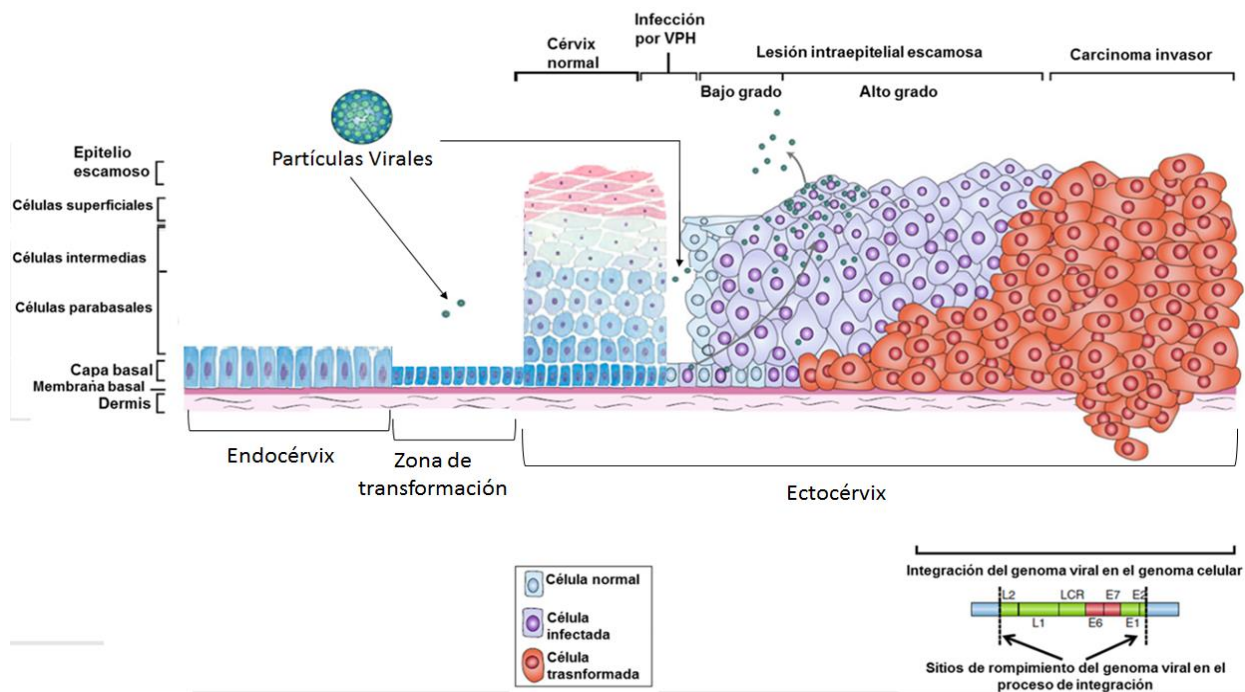
Figura 6. Progresión maligna inducida por el VPH. El VPH infecta células de la capa basal del epitelio estratificado del ectocérvix, estas células pueden ser expuestas por una micro lesión. La infección de las células en la zona de transformación se considera un riesgo adicional para la transformación celular inducida por VPH. Durante la fase productiva de la infección, se expresan los genes tempranos y el ADN viral se replica en bajo número de copias. En las capas superiores del epitelio, el genoma viral eleva su tasa de replicación, y comienzan a expresarse los genes tardíos L1, L2, así como E4. L1 y L2 encapsulan el ADN viral, con lo cual, los viriones pueden iniciar una nueva infección. Las lesiones intraepiteliales de bajo grado (LSIL) soportan la replicación viral productiva. En una minoría de mujeres infectadas, la lesión progresa a una lesión intraepitelial escamosa de alto grado (HSIL). La progresión de lesiones no tratadas a cáncer invasivo está asociada con la integración del genoma viral en los cromosomas del hospedero, en la que se presenta el rompimiento del genoma viral principalmente en la región E1-E2, dando como resultado la sobreexpresión de las oncoproteínas E6 y E7 (Modificada de Woodman CB, et al, 2007) [25].

Hasta el momento no se ha reportado un sitio único de rompimiento de DNA, así como un sitio único de integración en el genoma celular [26]. Además, no se tiene reporte de algún mecanismo específico para que esto ocurra, por lo que se considera que la integración es un evento azaroso. Sin embargo, se sabe que hay procesos como la inestabilidad genómica o el aumento de especies reactivas de oxigeno que favorecen el evento de integración [27].

Se ha reportado que la mayoría de las infecciones por VPH pueden ser eliminadas, sin embargo, aproximadamente un 15% de estas infecciones pueden evolucionar hacia una infección persistente, la cual es un factor de riesgo para el desarrollo de cáncer [28], debido a una deficiente respuesta inmunológica contra el VPH.

- **EVASIÓN DE LA RESPUESTA INMUNE POR VPH**

Durante la historia natural de infección, el VPH puede evadir el sistema inmune por diferentes mecanismos. Durante la infección de los queratinocitos de la capa basal del epitelio cervical [29, 30] y posiblemente las células troncales de este epitelio [31, 32], estas células juegan un papel importante durante el inicio de la infección ya que se convierten en un vínculo para promover una respuesta inmune adaptativa efectiva. Los queratinocitos son parte del sistema de defensa inmune innato y se han considerado como centinelas inmunes [33], capaces de inducir la expresión de citocinas de tipo Th1 y TH2 [34]. Los queratinocitos en los tractos genitales femeninos expresan varios receptores Toll-like (TLR), ubicados en la superficie de la célula (TLR-1, TLR-2, TLR-4, TLR-5 y TLR-6) o en endosomas (TLR-3 y TLR-9) [35]. Los TLR son una familia de receptores inmunológicos que reconocen patrones moleculares asociados a patógenos (PAMP), su activación inicia vías de señalización que dan como resultado respuestas inmunes innatas y adaptativas. Los TLR endosómicos juegan un papel importante contra las infecciones virales y en el reconocimiento de ácidos nucleicos virales; TLR-3 reconoce el ARN bicatenario (dsARN), TLR-7 y TLR-8 reconoce ARN monocatenario (ssARN) y el ADN rico en CpG de doble cadena es reconocido por TLR-9. La activación de estos receptores promueve la producción de citocinas y crea un ambiente proinflamatorio [36-38], en particular, la activación de TLR-9 en queratinocitos da como resultado la producción de diversas citocinas incluyendo IFN tipo 1, TNF-α, IL-8, CCL2, CCL20 y CXCL9 [39, 40].

La expresión de interferones está asociada en la regresión de lesiones por VPH. Sin embargo, en estudios con ratones transgénicos para las oncoproteínas E6/E7 de VPH-18, se mostró que estas oncoproteínas interactúan con IRF-1 e IRF-3 (Factor regulador de interferón), impidiendo la transcripción de genes como IFN-β y MCP1 en el

queratinocito [41], mientras que VPH-18/E6 puede inhibir la fosforilación de moléculas implicadas en la señalización de IFN como Tyk2 cinasa, STAT1 y STAT2 en líneas celulares de cáncer de cuello uterino [42]. Esto concuerda clínicamente en donde pacientes positivos para VPH-16 con lesiones premalignas responden al tratamiento con IFN-α de manera más eficaz cuando los niveles de transcritos de E7 son bajos [43].

Estos hallazgos enfatizan la importancia del queratinocito como iniciador de la respuesta inmune contra el VPH y como un enlace a la respuesta inmune adaptativa, y desregulación de la mayoría de las citocinas antes mencionadas es una de las principales estrategias utilizadas por VPH en la evasión de la respuesta inmune. La Figura 7 muestra las citocinas que son sobre-expresadas y sub-expresadas en el microambiente de un tejido infectado por VPH.
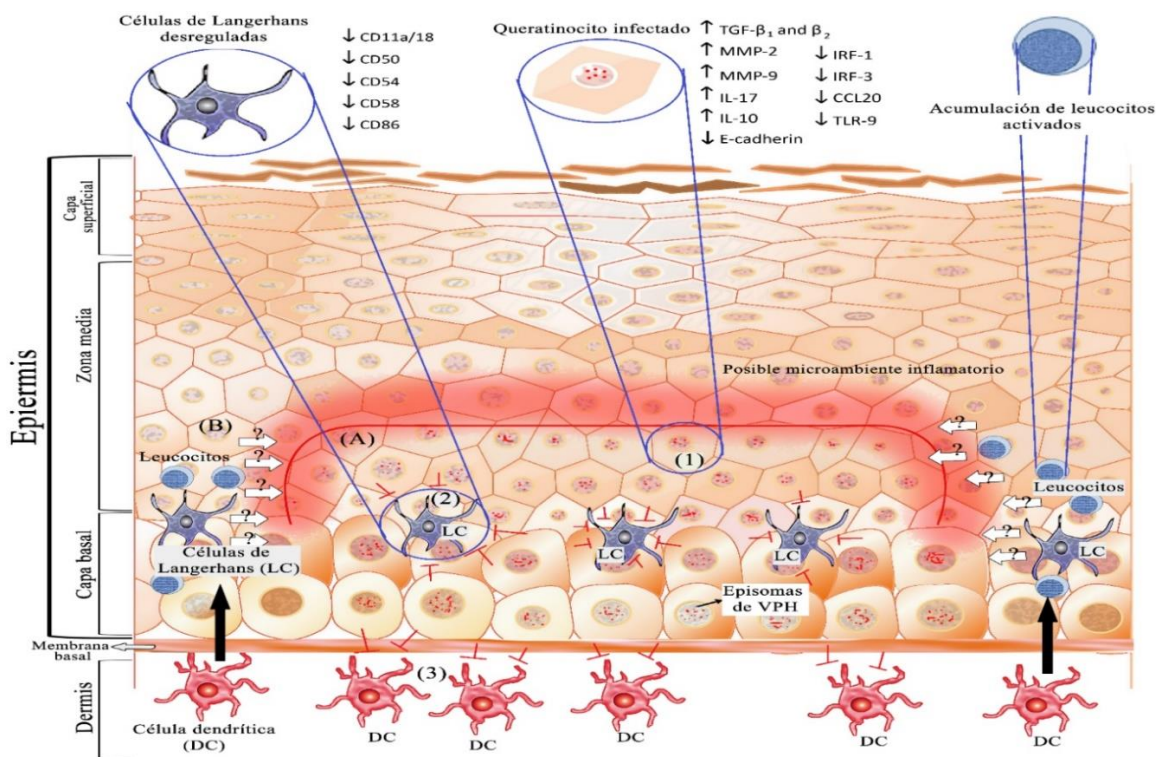
Figura 7. Representación del microambiente inmunológico en una infección por virus del papiloma humano. (A) El microambiente predominante inducido por el VPH impide que la presentación de antígeno se lleve a cabo de manera eficiente, lo que desencadena: (1) modulación de la respuesta inflamatoria de los queratinocitos mediada por citoquinas como la primera línea de defensa contra la infección; (2) la inhibición de la activación y migración de Langerhans (LC) a los nódulos linfoides; y (3) evasión de la infiltración de células dendríticas (DC) del estroma. (B) El posible microambiente proinflamatorio en los queratinocitos adyacentes a la lesión. Este microambiente se caracteriza por un aumento en la expresión de IL-10 y la presencia de linfocitos T activados. Las flechas con un signo de interrogación indican un

proceso desconocido que podría revertir el microambiente inducido por el VPH. (Tomada de Amador-Molina A, et al, 2013) [43].

La proteína E5 también participa en la evasión de la respuesta inmune, disminuyendo la expresión en membrana tanto de MHC clase I y II. Para MHC-II lo hace modificando el pH de endosomas donde sufre cortes proteolíticos esta molécula, impidiendo su maduración y posterior expresión en membrana citoplasmática. Además, es capaz de retener en retículo endoplásmico a la molécula MHC-I evitando la translocación de esta molécula en membrana [44]. Esto afectaría la respuesta de linfocitos T CD8+ y T CD4+, los cuales son indispensable para la eliminación de células infectadas por VPH.

Cambios en la respuesta inmune de la mucosa cervical, han sido implicados en el desarrollo de lesiones premalignas. En lesiones NIC I, se ha observado un predominio de células CD4+ en el estroma cervical, con radio superior de células CD4/CD8 comparado con pacientes que poseen un NIC 1 progresivo, NIC 3, y carcinoma invasor. El incremento de células T reguladoras (Tregs) y células mieloides supresoras ha sido detectado en tumores positivos a VPH. Las células Treg parecen ser atraídas por la citocina CXCL12 producidas por el tumor[45] y el ambiente inmunosupresor generado en este contexto, al parecer se da gracias a la influencia de mediadores generados por el tumor como por ejemplo IL-6 y prostaglandina 2. Aunado a lo anterior, muestras de lesiones premalignas positivas a VPH muestran una disminución en la expresión de diversas citocinas inflamatorias incluyendo IL-1 y TNF-α. Al mismo tiempo, la expresión de citocinas antinflamatorias como la IL-10 y TGF-β es incrementada en tejidos positivos a VPH. Estas alteraciones en la producción de citocinas reducen la capacidad de las células del sistema inmune para infiltrar tejidos infectados [43].

Además del papel de las células Treg, la enzima indolamina 2, 3-deoxigenasa (IDO), la cual suprime la proliferación de linfocitos T, juega un papel importante en el desarrollo de cáncer cervical. Se ha determinado que células de cáncer metastásico, cáncer microinvasivo, así como células presentadoras de antígeno (APC) expresan IDO en regiones dónde células Treg están presentes [46, 47].

Al igual que los linfocitos T CD8+, los linfocitos NK juegan un papel importante en la eliminación de células infectadas por virus y células tumorales. Linfocitos aislados de tejidos de cáncer cervical mostraron un decremento en la población de células NK

comparado con tejidos provenientes de personas sanas, así como la expresión de receptores activadores de células NK como lo son NKp30 y NKp46, están disminuidos en pacientes de cáncer cervical y mujeres con NIC 2-3. Esta disminución en su expresión se correlaciona con la baja actividad citolítica de células NK [48].

También se conocen otras poblaciones celulares del sistema inmunológico como los linfocitos T γδ por tener un rol protector contra la formación de diversos tipos de cáncer, incluyendo carcinomas de células escamosas [49, 50], no obstante, su papel en el cáncer de cuello uterino asociado a la infección de VPH aún no está del todo dilucidado. En modelos de ratón se conoce que las oncoproteínas E6 y E7 inducen una disminución de la subpoblación de linfocitos T γδ/Vγ5+, los cuales son reemplazados por la subpoblación de linfocitos T /Vγ6+ γδ^{low}CCR2$^+$CCR6$^-$, la cuales fueron asociados al desarrollo de lesiones inducidas por las oncoproteinas E6 y E7 de VPH-16 [51].

- **USO DE ADYUVANTES COMO POTENCIADORES DE LA RESPUESTA INMUNOLÓGICA.**

Los adyuvantes son sustancias o preparados químicos que activan la respuesta inmune innata e inflamación, en parte por la inducción de señales co-estimulatorias en células presentadoras de antígeno, las cuales son críticas para la activación de linfocitos T [52]. El uso de adyuvantes es ampliamente usado en el diseño de vacunas y en la caracterización inmunológica contra patógenos. Sin embargo, algunos adyuvantes ayudan a promover preferencialmente una respuesta inmune humoral, mientras que otros promueven preferencialmente una respuesta celular por linfocitos T CD8+.

Particularmente, el α-Galactosilceramida (α-GalCer) que es un glucolípido sintético, originalmente extraído de esponjas marinas, constituido de una cadena alquil, una cadena de esfingosina y una galactosa unidas con enlaces glucosídicos α (Figura 8) [53], capaz de activar directamente a los linfocitos iNKT y promover indirectamente una fuerte respuesta de linfocitos T CD8+.

α-Galactosylceramide (αGalCer)
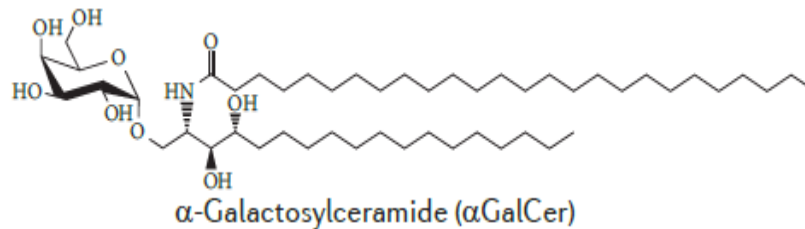
Figura 8. Estructura del α-Galactosilceramida (α-GalCer). El α-GalCer está compuesto de una cadena de esfingosina y una cadena alquil unidos a una galactosa. Modificada de Hayakawa, et al. 2004.

El α-GalCer es un antígeno presentado exclusivamente a las células iNKT (Invariant Natural Killer T cells por sus siglas en ingles). Las células iNKT o de tipo 1, son un grupo de linfocitos T definidos como células T restringidas a CD1d que expresan un receptor de antígeno de linfocitos T αβ semi-invariante (TCR) y antígenos de superficie típicamente asociados con células asesinas naturales como CD161 en humanos [54, 55]. El TCR encontrado en células NKT tipo 1 reconoce antígenos de glucolípidos presentados por la glucoproteína CD1d relacionada con MHC de clase I, que se expresan abundantemente en células presentadoras de antígeno y otros tipos de células. Hay dos maneras en que las células iNKT se activan: directamente, mediante la participación del TCR invariable con antígenos de glucolípidos y moléculas CD1d expresada en células dendríticas, e indirectamente a través de células presentadoras de antígeno activadas. Después de la estimulación, las células iNKT secretan rápidamente grandes cantidades de diversas citocinas, incluyendo IFN-γ, TNF, IL-4, IL-10 e IL-3, entre otros [56, 57], las cuales tienen repercusión en diferentes procesos inmunológicos como la activación y la generación de memoria de linfocitos T CD8+ (Figura 9) [43].
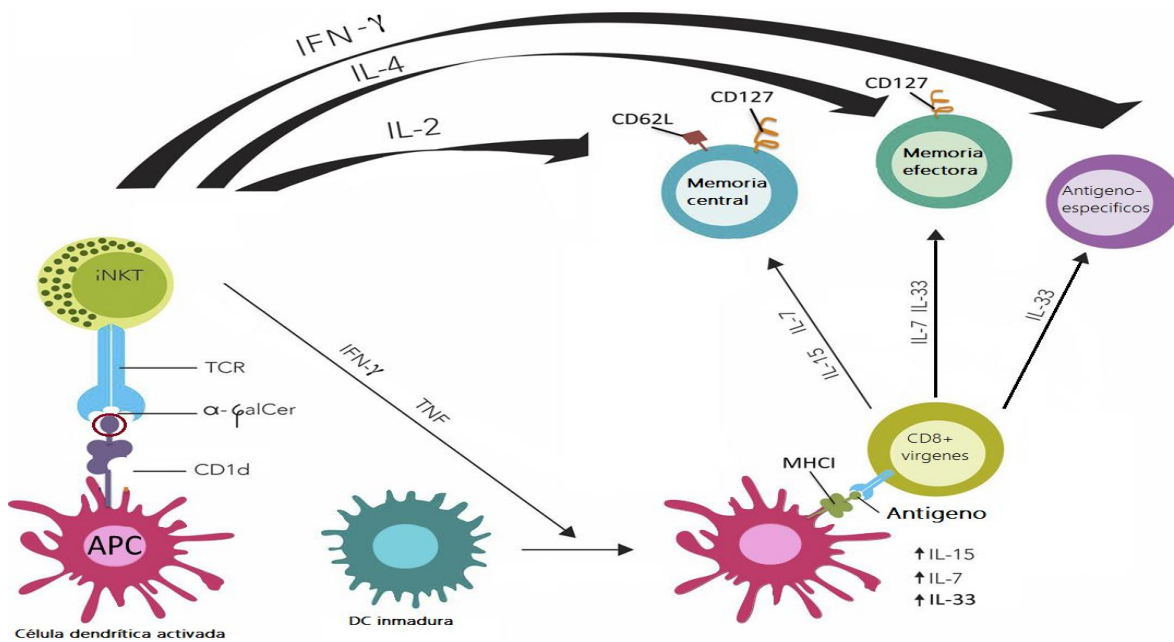
Figura 9. Presentación antigénica de α-GalCer y activación de linfocitos iNKT. Las células Dendríticas (rosa) son capaces de presentar glucolípidos (círculo rojo) a través de la molécula CD1d (morado). Estos glucolípidos son reconocidos por un receptor de células T invariantes (azul), el cual está en la membrana de células iNKT (verde y amarillo). Al ser activadas por la presentación del antígeno glucolipídico, estas liberan grandes cantidades de citocinas que están involucradas en procesos tales como la activación y generación de fenotipos de memoria de linfocitos T CD8+ (memoria central: CD62L$^+$/CD127$^+$ y memoria efectora: CD62L$^-$/CD127$^+$), así como la maduración de células dendríticas.

El α-GalCer es el glucolípido que más estimula a las células iNKT [43] en comparación con otros glucolípidos, y cuando es coadministrado con antígenos proteicos promueve la generación de linfocitos T CD4$^+$ y CD8$^+$ antígeno-específicas [58]. Dicho efecto de promover preferencialmente una respuesta de linfocitos T se ha comparado con otros adyuvantes, como IFN-α, poly (I:C), agonistas de TLR-9, adyuvante incompleto de Freund y α-GalCer es capaz de promover hasta 5 veces más el porcentaje de linfocitos T CD8+ antígeno-específico sobre cualquier adyuvante antes mencionado [59]. Además, α-GalCer es capaz de aumentar la presentación cruzada en células dendríticas, mejorando así la respuesta de linfocitos T CD8+ [60].

Cabe señalar que los adyuvantes basados en sales de aluminio los cuales se emplean en las vacunas contra VPH generan preferencialmente una respuesta inmune mediada por anticuerpos [61]. Sin embargo, estos adyuvantes se han probado en modelos animales para evaluar la respuesta de linfocitos T CD8+ contra las proteínas virales E6

y/o E7, mostrando que generan una pobre respuesta de linfocitos T CD8+ comparado con el uso de vectores virales [62, 63].

- **CARACTERIZACIÓN DE LA RESPUESTA INMUNE CONTRA PROTEINAS DE VPH; VACUNAS PROFILACTICAS Y TERAPEUTICAS.**

Diversos estudios se han abocado a caracterizar la inmunogenicidad de proteínas del VPH, tales como L1, L2, E6, E7 y E2 [64, 65]. Estudios de la inmunogenicidad de las proteínas que conforman la cápside (L1 y L2) ayudaron al desarrollo de las actuales vacunas. En el mercado existen 3 vacunas que protegen de manera profiláctica y están diseñadas para promover una respuesta humoral contra epítopos de la proteína L1. Su protección es dirigida contra 2, 4 o 9 genotipos de VPH como se muestra en la figura 10 [64]. Dicha protección se produce por el uso de 2 y hasta 9 diferentes proteínas L1 dependiendo la vacuna. La protección que estas confieren contra otros tipos virales no incluidos en las vacunas es limitada [66].
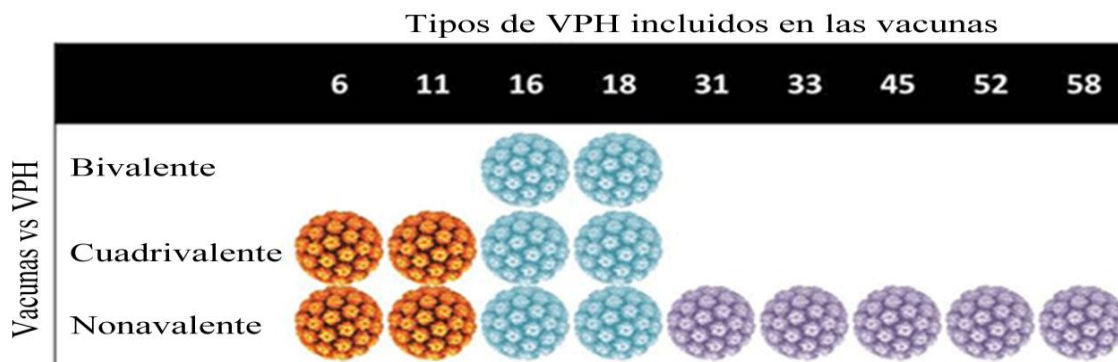
Figura 10. Vacunas contra VPH actualmente en el mercado. Actualmente existen 3 vacunas contra comerciales contra el VPH. La vacuna bivalente contra los tipos 16 y 18 de nombre comercial Cervarix la cual es fabricada por GlaxoSmithKline. La cuadrivalente contra los tipos 6, 11, 16, 18 y la nonavalente que adicionalmente protege contra los tipos 31, 33, 45, 52 y 58, ambas fabricadas por Merck y de nombre comercial Gardasil y Gardasil9 respectivamente. (Tomada de: CDC 2016: You are the key to HPV cancer prevention)

A pesar de que las actuales vacunas profilácticas son eficaces en prevenir infecciones por VPH, estas presentan algunas desventajas como no proteger contra infecciones ya establecidas, por lo que las opciones contra lesiones por VPH se limitan a la escisión

quirúrgica. Debido a que el repertorio de opciones terapéuticas es escaso, actualmente hay un gran número de vacunas terapéuticas en desarrollo en fase I y II, las cuales en su mayoría emplean a las oncoproteínas E6 y/o E7 [65]. Cabe resaltar que dichas oncoproteínas no poseen una gran homología entre los VPH.

Debido a esto, es importante caracterizar la respuesta inmunológica contra nuevos blancos terapéuticos que puedan generar una mejor respuesta inmunológica y sobre todo de amplio espectro. En el caso particular de la proteína E1, tiene diversas características que lo pueden hacer un potencial blanco inmunológico de amplio espectro, como ser la proteína más conservada entre los genes de expresión temprana de VPH. Aunado a esto, se tienen reportes en modelos animales que señalan que la inmunogenicidad de la proteína E1 puede ser mejor en comparación con otras proteínas de expresión temprana. Moore y colaboradores, demostraron que la inmunización de E1 de COPV (Canine Oral Papilloma Virus) previene la formación de papilomas y/o lesiones producidas después de una infección con partículas de COPV en el 100% de sus especímenes, en caso contrario la inmunización con E2 o E7 no protege al 100% la formación de papilomas [67].

También se ha demostrado que la inmunización en ratones con un vector que codifica para la proteína E1 de VPH-16 es capaz de inducir una respuesta de linfocitos T CD8+ E1-antígeno específicos [68]. Estos datos son similares con los de Ragonnaud E, et al., en donde la vacunación con E1 codificada en un vector adenoviral promueve una respuesta inmunológica de linfocitos T antígeno-específica contra virus del papiloma de macaca fascicularis (MfPV), en un modelo de primates [69].

Tanto para el desarrollo de vacunas profilácticas como terapéuticas, los adyuvantes son indispensables para promover una fuerte respuesta inmunológica innata que permita la generación de una fuerte respuesta adaptativa. El uso de vectores virales también se ha descrito como potenciador de la respuesta inmune innata.

- **JUSTIFICACIÓN:**

En la actualidad existen escasas opciones terapéuticas para el tratamiento de infecciones o lesiones producidas por VPH. Algunos estudios de inmunoterapias en fase

I o II que ofrecen protección contra infecciones ya establecidas utilizan a las proteínas E6 y/o E7; las cuales poseen escasa homología entre los VPH. Además, el uso de dichas proteínas en modelos animales muestra una respuesta inmunológica menos eficiente en comparación con proteínas como E2 y E1.

Dado que E1 es la proteína de expresión temprana con más homología, es de interés determinar su importancia como blanco terapéutico de amplio espectro contra infecciones o lesiones de bajo grado producidas por VPH.

- **HIPÓTESIS:**

La proteína E1 generará una respuesta inmune de linfocitos T CD8+ citotóxicos específicos en ratones, potenciada por el adyuvante α-GalCer, que será capaz de eliminar células que expresen antígenos de E1.

- **OBJETIVO GENERAL:**

Determinar si la respuesta inmune contra E1 de VPH-18 potenciada por α-GalCer, promueve la eliminación de células tumorales que expresen la proteína E1.

- **OBJETIVOS PARTICULARES:**

1. Obtención de una línea celular derivada de B16-F0 que exprese la proteína E1 de VPH-18.
2. Determinación de los péptidos inmunogénicos de la proteína E1 de VPH-18
3. Determinar el efecto de la inmunización de la proteína E1, E1+α-GalCer ó α-GalCer sobre el crecimiento tumoral en los modelos profiláctico y terapéutico.
4. Evaluar actividad citotóxica de linfocitos T CD8+ y NK en ratones con reto tumoral.
5. Determinación de la reacción cruzada de linfocitos T CD8+ contra E1-carboxilo terminal de los tipos virales 6, 11, 16, 31, 33 y 53.

MATERIALES Y METODOS

- RATONES Y LINEA CELULAR

Se usaron ratones hembra C57BL/6 provenientes del Instituto Nacional de Ciencias Médicas y Nutrición Salvador Zubirán, México. Todos los animales se mantuvieron en un ambiente libre de patógenos y se alimentaron a libre demanda. Los Comités de Ética de la Universidad Nacional Autónoma de México y del Instituto Nacional de Cancerología, México, aprobaron los procedimientos de cuidado y uso de animales (PAPIIT-IN221810), (017/001/IBI), (CEI/1076/17). Se siguieron en consecuencia todas las reglamentaciones institucionales aplicables relacionadas con el uso ético de los animales. La línea celular B16-F0 derivada de melanoma de ratón B16-F0 (ATCC® CRL-6322 ™) se cultivó en medio Eagle modificado por Dulbecco-F12 suplementado con 10% de SFB.

- OPTIMIZACIÓN DE CODONES DEL GEN E1 Y CONSTRUCCIÓN DE PLASMIDOS

Se optimizaron los codones del gen E1 de VPH-18 variante referencia [10], para mejorar su expresión en células de ratón, de acuerdo con lo reportado con Moore RA, et al, 2002 [67] . La compañía "GenScript" realizó la optimización de codones del gen E1 de VPH-18 y la introdujo en el plásmido de preservación PUC19. La secuencia optimizada de codones se usó para amplificar la secuencia de longitud completa (E1-FL) y tres fragmentos E1 que codifican para: E1-N-terminal, dominio de unión a ADN E1 y E1$_{244-550}$; los plásmidos obtenidos fueron llamados pE1-FL, pE1-NT, pE1-DBD y pE1$_{244-550}$ respectivamente. La región E1$_{244-550}$ contiene parte del dominio de unión al ADN y el dominio C-terminal. Los productos de PCR se amplificaron y se clonaron en el plásmido pcDNA 3.3 Topo (Invitrogen) con una secuencia de Kozak y una secuencia de hemaglutinina de influenza humana (HA) en su carboxilo terminal para la identificación de la proteína (Figura 11).

Los dominios carboxilo terminal de los genes E1 de VPH-6, -11, -16, -31, -33 y -53 fueron amplificados por PCR de los plásmidos pBR322-VPH6, pBR322-VPH11, pBR322-

VPH16, pT712-VPH31, pLink-VPH33 y pEMBL-VPH53 (Donados por el Dr. Alejandro García Carrancá). Dichos plásmidos contienen el genoma completo de los tipos de VPH mencionados. Los productos de PCR fueron clonados en el vector de expresión en células eucariotas pcDNA 3.3 topo (Invitrogen) junto con la secuencia Kozak y un marcaje de HA en su carboxilo terminal para la identificación de la proteína. Los plásmidos obtenidos fueron llamados pE1CT-VPH6HA, pE1CT-VPH11HA, pE1CT-VPH16HA, pE1CT-VPH31HA, pE1CT-VPH33HA y pE1CT-VPH53HA.

- PREDICCIÓN DE PÉPTIDOS INMUNOGÉNICOS PARA MHC-I Y ALINEAMIENTO DE SECUENCIAS MÚLTIPLES

El software "Rankpep" fue utilizado para predecir las afinidades de unión de péptidos de E1-VPH18 con los haplotipos MHC-I de ratón H2-D^b y H2-K^b, e identificar los dominios de la proteína que contengan un mayor número de probables péptidos inmunogénicos. Los péptidos inmunogénicos de 8 a 11 aminoácidos de longitud obtenidos del análisis por "Rankpep" fueron alienados con las secuencias E1 carboxilo-terminal de los VPH-6, 11, 16, 31, 33 y 53 usando el software "Clustal Omega". Dicho alineamiento se hizo para determinar los péptidos inmunogénicos más conservados entre los dominios E1-carboxilo terminal de estos tipos virales.

- TRANSFECCION Y SEPARACIÓN DE CÉLULAS POR CITOMETRIA (SORTING)

La línea celular B16-F0 derivada de melanoma de ratón (ATCC) fueron cultivadas en medio DMEM-F12 suplementado con suero bovino fetal al 10%. Las células B16-F0 (6 X10^5) fueron sembradas en placas de 60mm^2 y 24 horas después fueron transfectadas usando lipofectamine 2000 (invtrogen).Se realizaron co-transfecciones del plásmido que contiene el gen de la proteína verde fluorescente (GFP) más alguno de los plásmidos con secuencias E1 (pE1-FL, pE1-NT, pE1-DBD o pE1$_{244\text{-}550}$). Las células transfectadas se analizaron mediante citometría de flujo para la expresión de GFP y E1.

Posteriormente, las células con GFP^{hi} fueron separadas por citometría de flujo usando el equipo BD FACSJazz.

- ANALISIS DE LA EXPRESIÓN DE PROTEINAS POR WESTERN BLOT

Los extractos de células B16-F0 que expresan E1$_{244-550}$ previamente separadas por citometría (B16-F0/E1$_{244-550}$HA^{hi}) y de células transfectadas con pcDNA3.1/His (vector vacío), se corrieron en un gel SDS-PAGE al 10% y se transfirieron a membranas de nitrocelulosa, que luego fueron incubadas con anticuerpo policlonal de conejo anti-HA (Santa Cruz Biotechnology catálogo # sc-805), seguido de una incubación con un anticuerpo anti-conejo acoplado a peroxidasa de rábano (Santa Cruz Biotechnology catálogo # sc-2030). Se utilizó β-actina como control de carga y se detectó con el anticuerpo monoclonal de ratón sc-47778 (Santa Cruz Biotechnology) seguido de proteína de unión kappa IgG de ratón conjugada con peroxidasa de rábano (Santa Cruz Biotechnology, sc-516102). Las proteínas E1 fueron reveladas con el reactivo de quimioluminiscencia "enhanced chemiluminescence" (Amersham), realizadas tres veces para asegurar la reproducibilidad.

De la misma manera fueron evaluados los extractos proteicos de células B16-F0 transfectadas transitoriamente con pE1CT-VPH18HA, pE1CT-VPH6HA, pE1CT-VPH11HA, pE1CT-VPH16HA, pE1CT-VPH31HA, pE1CT-VPH33HA, pE1CT-VPH53HA o con vector vacío pcDNA3.1/His. Los ensayos de western blot se realizaron tres veces de manera independiente para asegurar su reproducibilidad.

- EXPRESIÓN DE LA SECUENCIA E1$_{244-550}$HA EN TUMORES

Para evaluar la expresión de E1$_{244-550}$HA en tumores, células B16-F0/E1$_{244-550}$HA^{hi} (7.5 X 10^5) previamente separadas por citometría fueron inoculadas vía subcutánea (s.c.) en el flanco izquierdo de ratones C57BL/6 sin tratamiento. Los ratones inoculados fueron sacrificados a diferentes días post-inoculación con la finalidad de obtener tumores con diferentes tiempos de expresión de la proteína E1$_{244-550}$HA, esto de acuerdo con las regulaciones para el uso de animales de laboratorio: "Animal Research Advisory

Committee (ARAC-NIH)". Los extractos proteicos de los tumores fueron analizados por western blot para determinar la expresión de $E1_{244-550}HA$ en este tejido.

- PROTEÍNA RECOMBINANTE $E1_{202-654}$

La producción y purificación del Inmunógeno *$E1_{202-654}$* fue realizada en cultivos bacterianos. La síntesis del Inmunógeno comprende los dominios de unión a ADN + carboxilo terminal (aminoácidos 202 al 654), más una etiqueta de 6 histidinas agregada en el carboxilo terminal (Figura 11). En dichos dominios residen la mayor cantidad de péptidos inmunogénicos de la proteína. La síntesis de este inmunógeno fue realizada por la compañía Genscript con una pureza >85%.
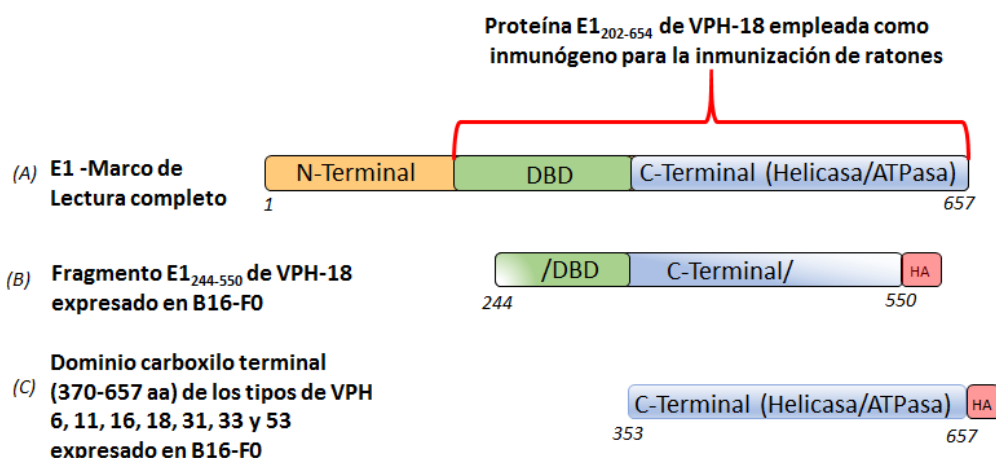
Figura 11. Dominios de la proteína E1 que fueron empleados para la caracterización de la respuesta inmunológica de linfocitos T CD8+. Región 202-654 que está delimitada en corchete rojo comprende los dominios DBD y CT, esta región fue utilizada como inmunógeno. (B) Región 244-550 corresponde a la secuencia de E1 de VPH-18, la cual fue clonada en un plásmido pCDNA para su expresión en células B16-F0 y (C) la región 370-657 corresponde al dominio CT de los tipos virales 6, 11, 16, 18, 31, 33 y 53, las cuales fueron clonadas en el plásmido pCDNA para su expresión en células B16-F0. La línea celular que expresa *$E1_{244-550}$* (B) fue utilizada para los protocolos de inmunización profiláctica y terapéutica, mientras que la línea celular que expresa el dominio más conservado (C), fue utilizada para evaluar reacción cruzada.

- PROTOCOLOS DE INMUNIZACIÓN PROFILÁCTICA, TERAPÉUTICA Y DE REACCIÓN CRUZADA

Para el protocolo profiláctico, se distribuyeron ratones hembra C57BL/6 de siete a ocho semanas de edad en cuatro grupos de seis ratones cada uno. Grupo P1: inmunizados vía s.c. en el flanco izquierdo con 4 µg de $E1_{202-654}$ recombinante; Grupo P2 inmunizados vía s.c. con 4 µg de $E1_{202-654}$ recombinante más 3 µg de α-GalCer; Grupo P3: inoculados vía s.c. con 3 µg de α-GalCer; y Grupo P4: inoculados vía s.c. con 70 µl de PBS. Catorce días después, se administró una segunda dosis idéntica s.c. a cada grupo de ratones (Figura 12A). La dosis empleada para la inmunización con la proteína recombinante $E1_{202-654}$ se eligió mediante una curva dosis-respuesta en donde se determinó el número de CTL que respondían ante E1. La dosis de α-GalCer administrada s.c. ha sido reportada previamente [59]. Para examinar el efecto de estos tratamientos sobre el crecimiento tumoral, se inocularon 1.8×10^6 células B16-F0/$E1_{244-550}HA^{hi}$ en el flanco izquierdo en cada uno de los ratones cinco días después de la administración de la segunda dosis. El crecimiento tumoral se midió cada tres días usando un calibrador digital y el volumen estimado se determinó con la fórmula; volumen = (largo x ancho^2)/2, como previamente se ha descrito [70]. Los ratones se sacrificaron cuando el tamaño de la masa tumoral alcanzó 20 mm en cualquier dimensión, o hasta un máximo de 21 días después de la inoculación (Figura 12A). El volumen exacto de las masas se determinó *ex vivo* por la formula previamente descrita y se reportó en mm^3 [71].

Para el protocolo terapéutico, se inocularon 24 ratones C57BL/6 hembra de siete a ocho semanas de edad con 1.8×10^6 células B16-F0/$E1_{244-550}HA^{hi}$. Cinco días después de la inoculación de células, cuando todos los ratones tenían tumores palpables, se distribuyeron en cuatro grupos de seis ratones cada uno al igual que en el modelo profiláctico y se inocularon con las mismas dosis de antígeno y adyuvantes descritas previamente. Los grupos fueron nombrados: T1, T2, T3 y T4 (Figura 12B). El crecimiento tumoral se midió cada tres días y el volumen estimado se determinó como se menciona anteriormente. Los ratones fueron sacrificados y se determinó el volumen exacto de los tumores de la misma manera que en el modelo profiláctico.

Para el protocolo de reacción cruzada, se inmunizaron ratones hembra de siete a ocho semanas de edad, distribuidos en grupos de cuatro ratones cada uno; grupo C1: inmunizado s.c. con $E1_{202-654}$ recombinante; grupo C2: inmunizado s.c. con $E1_{202-654}$ + α-GalCer; grupo C3: inoculado s.c. con α-GalCer; y grupo C4: inoculado s.c. con PBS. Este modelo se realizó tres veces con cuatro ratones por grupo cada vez (Figura 12C).

Una vez sacrificados los ratones, se extirparon los bazos para la obtención de linfocitos T CD8+ y NK, para la determinación de actividad citotóxica contra células tumorales, como se describe más adelante en la sección de materiales y métodos.
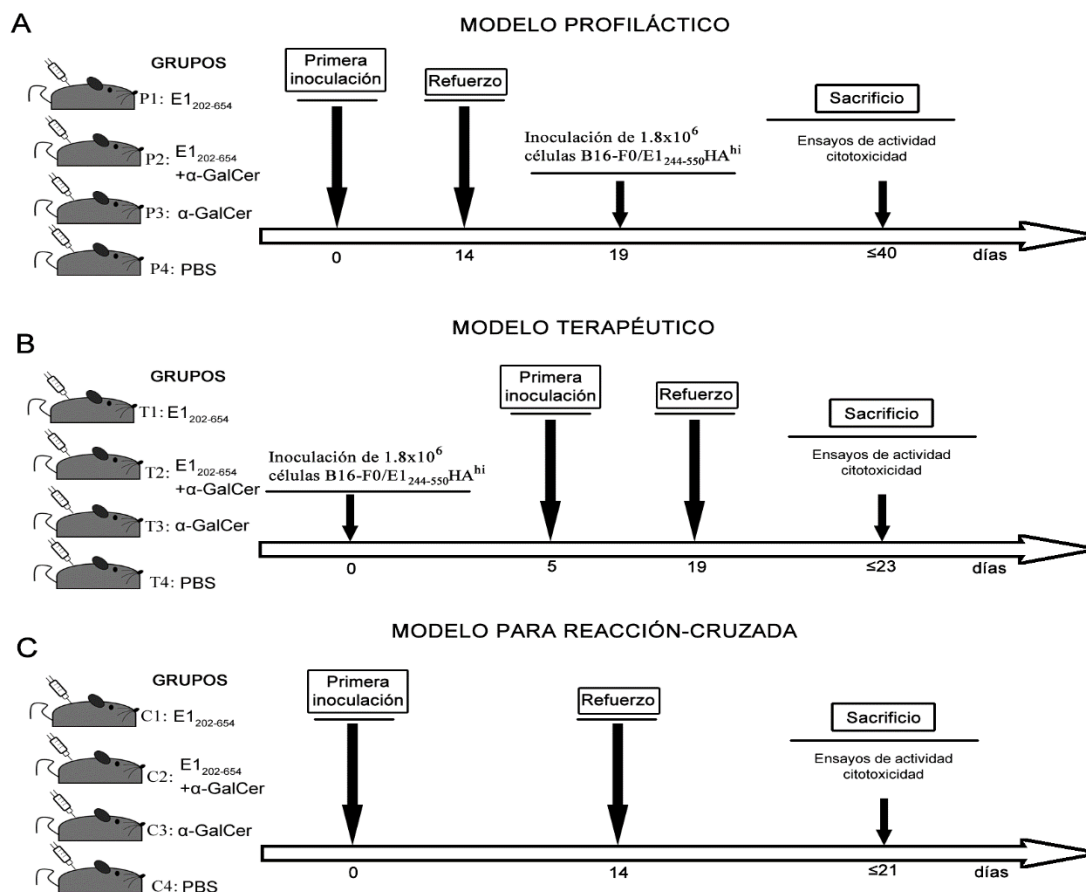
Figura 12. Protocolos de inmunización. (A) Para la inmunización profiláctica, se usaron seis ratones por grupo. Fueron inoculados y un refuerzo fue aplicado dos semanas después de la inoculación inicial. Cinco días más tarde, todos los ratones fueron inoculados con células B16-F0/E1$_{244-550}$HA^{hi}. Los ratones se sacrificaron hasta un máximo de 21 días después de la inoculación y se extirpó el bazo para realizar ensayos de actividad citotóxica. (B) Para la inmunización terapéutica, se inocularon 24 ratones con células B16-F0/E1$_{244-550}$HA^{hi}. Cinco días después de la inoculación cuando todos los ratones desarrollaron tumores detectables, se distribuyeron aleatoriamente en cuatro grupos de seis ratones cada uno y se inocularon

como se especificó previamente. Los ratones se sacrificaron hasta un máximo de 23 días después de la inoculación y se extirpó el bazo para realizar ensayos directos de actividad citotóxica *ex vivo*. (C) Para determinar la reacción cruzada, se distribuyeron ratones en grupos de cuatro especímenes cada uno, inmunizados a las mismas dosis y en los mismos intervalos que en los protocolos anteriores, sin realizar un reto tumoral. Este modelo se realizó tres veces con cuatro ratones por grupo cada vez.

- OBTENCIÓN DE ESPLENOCITOS DE RATÓN Y PURIFICACIÓN DE LINFOCITOS NK Y T CD8+

Los bazos de ratón extirpados fueron colocados en una malla de nylon de 70 µm, (Corning Life Sciences). La malla fue anexada a un tubo cónico de 50 mL y los bazos fueron macerados. Los esplenocitos colectados dentro del tubo fueron lavados con PBS y centrifugados a 1,600 rpm por 5 minutos. El botón celular fue incubado con solución de lisis (Becton Dickinson Pharm Lyse™) por dos minutos a 37°C, posteriormente se detuvo la reacción diluyendo la solución de lisis con 40 mL de PBS y se centrifugó a 1,600 rpm por 5 minutos.

Los linfocitos T CD8+ y NK fueron aislados de esplenocitos totales con los kits de purificación: "CD8α^+ T Cell Isolation Kit II" y "NK Cell Isolation Kit (Miltenyi Biotec)" respectivamente, siguiendo las instrucciones del fabricante. La viabilidad de los esplenocitos, así como la de linfocitos NK y T CD8+ se determinó por conteo celular con azul de tripano en el contador celular automatizado TC20 (BIORAD). Los linfocitos T CD8+ fueron incubados con los anticuerpos CD8+/PE y CD3+/Alexa Fluor488 y los linfocitos NK fueron incubados con NK1.1/Alexa Fluor648 y CD3+/Alexa Fluor488 para determinar la pureza por citometría de flujo tanto de linfocitos T CD8+ como de NK.

- ENSAYO DE ACTIVIDAD CITOTÓXICA DE LINFOCITOS T CD8+ y NK

Células B16-F0 (4×10^4) transfectadas con pE1$_{244-550}$HA fueron co-cultivadas en placas de 24 pozos con 4×10^5 linfocitos T CD8+ provenientes de ratones pre-inmunizados.

Para determinar la actividad citotóxica de NK, se co-cultivaron 1×10^4 células B16-F0/E1$_{244-550}$ con 1×10^5 células NK.

Para los ensayos de reactividad cruzada, las células B16-F0 transfectadas con pE1CT-VPH6HA, pE1CT-VPH11HA, pE1CT-VPH16HA, pE1CT-VPH31HA, pE1CT-VPH33HA, pE1CT-VPH53HA o pE1CT-VPH18HA se co-cultivaron con células CD8 + T de ratones pre-inmunizados.

Los anticuerpos conjugados con el fluoróforo Alexa fluor-488 diseñados para reconocer las proteínas de la membrana granular CD107a y CD107b fueron añadidos a los co-cultivos de linfocitos NK y T CD8+. Como control positivo de actividad citotóxica, linfocitos T CD8+ y NK de ratones NO-inmunizados fueron estimulados con phorbol-12-myristate-13-acetate (PMA, 300 ng/ml, Sigma Chem.) y Ionomycin, 1500 ng/ml (Sigma Chem.). Los co-cultivos fueron incubados por 4 horas y la molécula monensina inhibidora del transporte intracelular de proteínas fue añadida al co-cultivo las últimas 2 horas. Los linfocitos T CD8+ y NK de estos co-cultivos fueron lavados y fijados con paraformaldehido al 1%. Controles de isotipos fueron incluidos para todos los experimentos.

- CITOMETRÍA DE FLUJO

Las muestras de los ensayos de actividad citotóxica fueron adquiridas en el citómetro de flujo FACSAria II (Becton Dickinson) usando el software FACS Diva 8.0.1 y analizadas en el software FlowJo versión 10.2, y fueron adquiridos 50,000 eventos para linfocitos T CD8+ y 10,000 para NK.

Para la determinación de la expresión de GFP y E1$_{244-550}$HA en células B16-F0 se realizó en el citómetro de flujo FACSAria II, mientras que la separación de células B16-F0 con alta expresión de GFP se realizó en el citómetro BD FACSJazz.

Los paneles de anticuerpos con fluoróforos conjugados empleados para citometría de flujo fueron los siguientes:

- Determinación de pureza de linfocitos T CD8+ esplénicos: PerCP anti-CD8a, Alexa Fluor 488®-CD3
- Determinación de pureza de linfocitos NK esplénicos: Alexa Fluor 648®-NK 1.1, Alexa Fluor 488®-CD3
- Ensayo de actividad citotóxica: Alexa Fluor 488®-CD107a, Alexa Fluor 488® (AF488)-CD107b.

> Separación de células con alta expresión de GFP/HA: Alexa Fluor 648®-HA, GFP.

- ANÁLISIS ESTADÍSTICO

El análisis estadístico fue determinado con ANOVA de una cola y con una prueba de Tukey's post-análisis, usando el software GraphPad Prism software. Las barras de error representan el error estándar de la media (SEM) y los valores de $P<0.05$ fueron considerados estadísticamente significativos.

RESULTADOS

- PREDICCIÓN DE PÉPTIDOS INMUNOGÉNICOS PARA MHC-I Y ALINEAMIENTO MÚLTIPLE DE SECUENCIAS

La proteína E1 fue analizada en el software Rankpep para predecir péptidos de unión al MHC clase I del presente modelo animal. Para dicho análisis se tomaron en cuenta los dos haplotipos del MHC-I descritos para la cepa de ratón C57BL/6; $H2K^b$ y $H2D^b$, así como el tamaño del péptido que puede presentar cada uno de estos haplotipos. El análisis mostró que la mayoría de los péptidos inmunogénicos residen en el dominio carboxilo terminal el cual es el más conservado, seguidos del dominio de unión a ADN, mientras que el domino amino terminal de la proteína, el cual es el menos conservado, presenta menos péptidos inmunogénicos (Tabla 2).

Tabla 2. Número de péptidos de E1 con posible afinidad a haplotipos de ratón MHC-I: $H2K^b$ y $H2D^b$.

Dominio E1	Número de péptidos potenciales para MHC-I	MHC- I	RANKPEP (% OPT)[a]
N-terminal	30/120	$H2\text{-}D^b$ and $H2\text{-}K^b$	15.34-42.02%
DBD y C-terminal	90/120	$H2\text{-}D^b$ and $H2\text{-}K^b$	15.18-43.98%
Secuencia $E1_{244\text{-}550}$	62/120	$H2\text{-}D^b$ and $H2\text{-}K^b$	15.47-43.98%

[a] Puntaje del péptido predicho en relación con la secuencia consenso. La secuencia consenso es aquella que produce la puntuación máxima o la puntuación óptima con el perfil seleccionado en RANKPEP.

La predicción de péptidos inmunogénicos de la proteína E1 de marco completo, mostró que la mayoría de los péptidos inmunogénicos están localizados en el dominio carboxilo-terminal y de unión a ADN.

Después de obtener una gran variedad de péptidos predichos, se alineó en el servidor de Clustal Omega el dominio más conservados de E1 (Carboxilo terminal) de los tipos VPH 6, 11, 18, 16, 31, 33 y 53. Posteriormente, se buscaron los péptidos inmunogénicos predichos en el dominio CT para encontrar aquellos que son conservados entre los tipos virales antes mencionados (Tabla 3). El análisis mostró que al menos 15 péptidos se conservan entre los siete tipos de VPH. Además, E1CT-VPH53 y el E1CT-VPH18 comparten 20 péptidos inmunogénicos idénticos o altamente homólogos (Tabla 4).

Tabla 3. Predicción de péptidos inmunogénicos conservados en el dominio E1-carboxilo terminal de diferentes tipos de VPH, que se unen a las proteínas murinas MHC de clase I.

	Péptidos para MHC-I H2Dᵇ 10 aa	Péptidos para MHC-I H2Dᵇ y H2Kᵇ 9 aa	Péptidos para MHC-I H2Dᵇ 8 aa	Péptidos para MHC-I H2Dᵇ 8 aa	Péptidos para MHC-I H2Dᵇ y H2Kᵇ 9 aa	Péptidos para MHC-I H2Dᵇ 10 aa	Péptidos para MHC-I H2Kᵇ 9 aa	Péptidos para MHC-I H2Dᵇ 8 aa
E1–CT/VPH18	KCPPILLTTN	NTGKSYFGM	PANTGKSY	KNGNPVYE	DSNSNAAAF	CGPANTGKSY	VQFLRYQQI	KNWKCFFE
E1–CT/VPH6	KCPPLLVTSN	DTGKSYFCM	PDDTGKSY	RNGNAVYE	DFDSNARAF	VGPPDTGKSY	VQFLRHQNI	ANWKCFFE
E1–CT/VPH11	KCPPLLVTSN	DTGKSCFCM	PDDTGKSC	RNGNAVYE	DFDSNARAF	VGPPDTGKSC	VQFLRHQNI	ANWKCFFE
E1–CT/VPH16	KCPPLLITSN	NTGKSLFGM	AANTGKSL	KNGNPVYE	DTNSNASAF	YGAANTGKSL	VMFLRYQGV	KNWKSFFS
E1–CT/VPH31	KCPPLLITSN	NTGKSYFGM	APNTGKSY	KNGNPVYE	DSDSNACAF	HGAPNTGKSY	VKFLRYQQI	KNWKSFFS
E1–CT/VPH33	KCPPLLLTSN	NTGKSYFGM	PANTGKSY	ENGNPVYA	DSNSNAAAF	CGPANTGKSY	VQLLRYQNI	ENWKSFFS
E1–CT/VPH53	KCPPVLITTN	NTGKSCFAM	PPNTGKSC	VNGNPVYQ	DVDSNAQAF	YGPPNTGKSC	VQFLRYQGV	ANWKCFFE

Tabla 3. Predicción de péptidos inmunogénicos conservados en el dominio E1-carboxilo terminal de diferentes tipos de VPH, que se unen a las proteínas murinas MHC de clase I **(Continuación).**

	Péptidos para MHC-I H2D^b 8 aa	Péptidos para MHC-I H2K^b 9 aa	Péptidos para MHC-I H2K^b 8 aa	Péptidos para MHC-I H2K^b 8 aa	Péptidos para MHC-I H2K^b 8 aa	Péptidos para MHC-I H2D^b 9 aa	Péptidos para MHC-I H2K^b 8 aa
E1–CT/VPH18	WKCFFERT	CKHYRRAQK	KHYRRAQK	RTWSRLDL	NSTSHFWL	GTPKKNCLV	SHFWLEPL
E1–CT/VPH6	WKCFFERL	CRHYKRAQQ	RHYKHAEM	RLSSSLDI	NSSSHFWL	GTPKKNCIA	SHFWLQPL
E1–CT/VPH11	WKCFFERL	CRHYKKAEK	RHYKHAEM	RLSSSLDI	NSCSHFWL	GTPKKNCIA	SHFWLQPL
E1–CT/VPH16	WKSFFSRT	CRHYKRAEK	RHYKRAEK	RTWSRLSL	NSKSHFWL	GIPKKNCIL	SHFWLQPL
E1–CT/VPH31	WKSFFSRT	CRHYKRAEK	RHYKRAEK	RTWCRLNL	NSKSHFWL	GVPKKNCIL	SHFWLQPL
E1–CT/VPH33	WKSFFSRT	CRHYKHAEM	RHYKRAEK	RTWCKLDL	NSKSHFWL	GIPKKSCML	SHFWLQPL
E1–CT/VPH53	WKCFFERT	CRHYKHAEM	RHYKRAQQ	RTWSRLDL	NSHSHFWL	GTPKHNCLV	SHFWLEPL

■ Indica un residuo completamente conservado con respecto a la secuencia de E1-VPH18.

■ Indica residuos con propiedades muy similares con respecto a la secuencia de E1-VPH18.

■ Residuo no conservado con respecto a la secuencia E1-VPH18.

Tabla 4. Predicción de péptidos conservados en el dominio carboxilo terminal de E1-VPH18 y E1-VPH53, que se unen a las proteínas murinas MHC de clase I.

VPH-18 / VPH-53 MHC-I y tamaño del péptido		VPH-18 / VPH-53 MHC-I y tamaño del péptido	
CKHYRRAQK/ CRHYKRAQQ	H2K^b; 9- residuos		
WKCFFERT/ WKCFFERT	H2K^D; 8- residuos	NGNPVYEI/ NGNPVYQL	H2D^D; 8- residuos
GTPKKNCLV/ GTPKHNCLV	H2D^D; 9- residuos	PKKNCLVF/ PKHNCLVI	H2D^D; 8- residuos
SHFWLEPL/ SHFWLQPL	H2K^D; 8- residuos	GDWRPIVQ/ GDWKPIVQ	H2D^D; 8- residuos
KCPPILLTTN/ KCPPVLITTN	H2D^D; 10- residuos	IQLKCPPI/ VQIKCPPV	H2D^D; 8- residuos
CSKIDEGGDWR/ CSKVDDGGDWK	H2D^D; 11- residuos	WAFDNELTDE/ WAFDNDVTDD	H2D^D;10- residuos
LKGTPKKNCLV/ LQGTPKHNCLV	H2D^D; 11- residuos	KHYRRAQK/ RHYKRAQQ	H2K^D; 8- residuos
LKGTPKKNCL/ LQGTPKHNCL	H2D^D; 10- residuos	RTWSRLDL/ RTWSRLDL	H2K^D; 8- residuos
SKIDEGGDWR/ SKVDDGGDWK	H2D^D; 10- residuos	KGTPKKNCL/ QGTPKHNCL	H2K^D; 9- residuos
PIVQFLRYQ/ PIVQFLRYQ	H2K^D; 9- residuos	LDGNPISI/ LDGNPISI	H2K^D; 8- residuos

■ Indica un residuo completamente conservado con respecto a la secuencia de E1-VPH18.

■ Indica residuos con propiedades muy similares con respecto a la secuencia de E1-VPH18.

■ Residuo no conservado con respecto a la secuencia E1-VPH18.

- EXPRESIÓN DE LA SECUENCIA OPTIMIZADA *E1$_{244-550}$HA* Y E1CT EN CÉLULAS B16-F0

Para obtener una eficiente expresión del gen E1 en células de ratón B16-F0, se optimizaron los codones de su marco de lectura. Dicha expresión solo fue observada en células transfectadas con el plásmido que contiene el gen E1 optimizado y no con el gen E1 VPH referencia (Figura 13).
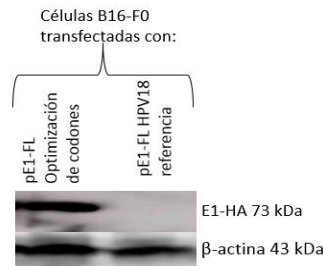
Figura 13. Expresión de la proteína E1 en células B16-F0. Células B16-F0 fueron transfectadas con pE1-FL que contiene optimización de codones y con pE1-FL VPH-18 referencia, el cual no tiene optimización de codones. La expresión de E1-FL se observa solo en el carril izquierdo que se cargó con el extracto proteico de células B16-F0 que fueron transfectadas con pE1-FL optimización de codones.

La optimización de codones del gen E1 para un modelo de perro ya se había reportado previamente [67].

Para generar líneas de expresión estables del gen E1 y/o fragmentos de dicho gen, cinco diferentes plásmidos que codifican para fragmentos optimizados del gen E1 fueron transfectados en células B16-F0 (E1-FL, E1-NT, E1-DBD, E1-CT y E1$_{244-550}$). Aunque ninguna de las construcciones previamente mencionadas pudo generar una línea de expresión estable, la secuencia E1$_{244-550}$ se expresó eficientemente en una transfección transitoria, lográndose detectar hasta por 17 días (Figura 14).
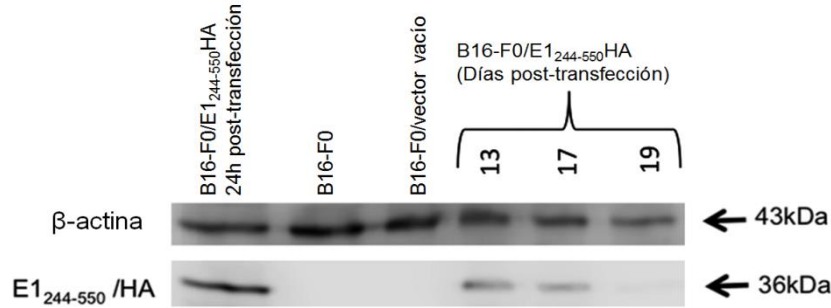
Figura 14. Expresión de la secuencia optimizada E1$_{244-550}$HA. Las células B16-F0 se transfectaron con pE1$_{244-550}$HA. La proteína E1$_{244-550}$HA se detectó a diferentes días post-transfección (13, 17 y 19 días) a través de western blot, utilizando un anticuerpo anti-HA. Las proteínas extraídas de células B16-F0 sin transfectar o transfectadas con el vector vacío se usaron como controles negativos, mientras que el extracto proteico de células B16-F0-24h post-transfección con el plásmido pE1$_{244-550}$/HA fue usado como control positivo.

Posteriormente, se determinó por citometría de flujo que aproximadamente un 18% de las células transfectadas tienen una alta expresión de E1$_{244-550}$HA de acuerdo con la intensidad media de fluorescencia, por lo que fueron nombradas B16-F0/E1$_{244-550}$HA^{hi} (Figura 15).
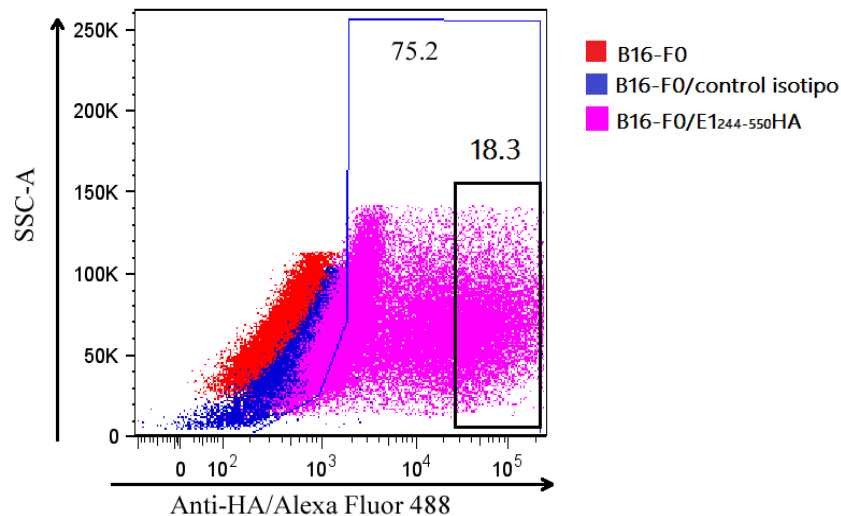
Figura 15. Eficiencia de transfección. Las células B16-F0 se transfectaron con pE1$_{244-550}$/HA y 24 horas después, las células fueron lavadas, permeabilizadas y se teñidas con el anticuerpo anti-HA/Alexa Fluor488. Se incluyó un control de isotipo para determinar el pegado inespecífico del anticuerpo anti-HA. La marca de HA intracelular se midió con Alexa Fluor 488 anti-HA.11. La eficiencia de transfección fue del 75% y la población E1$_{244-550}$HA^{hi} fue del 18%.

Adicionalmente, se analizaron por citometría de flujo las células transfectadas con pGFP+pE1$_{244-550}$HA para la expresión de GFP y E1$_{244-550}$HA. El análisis mostró que las células con E1$_{244-550}$HA^{hi} también mostraban alta expresión de GFP (GFP^{hi}) (Figura 16A). De esta manera, las células GFP^{hi} fueron separadas por del resto de la población celular mediante citometría de flujo (Cell sorting), obteniéndose una población enriquecida del 96% (Figura 16B). Como pE1$_{244-550}$HA produjo una expresión más alta y más consistente que los otros plásmidos que expresan E1, este plásmido se usó para los experimentos posteriormente descritos.
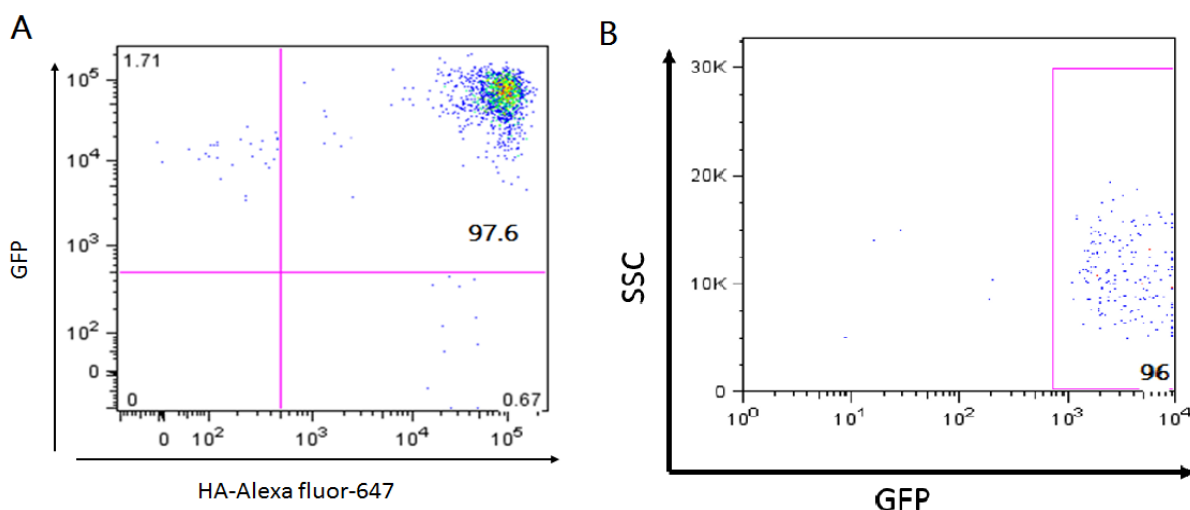
Figura 16. Células B16-F0 transfectadas con pE1$_{244-550}$HA y pGFP muestran tanto una alta expresión de GFP como de E1$_{244-550}$HA. A) Células B16-F0 se transfectaron con el plásmido GFP y pE1$_{244-550}$/HA. Después de 24 horas, fueron lavadas, permeabilizadas y teñidas con el anticuerpo anti-HA/Alexa Fluor647. Se incluyó un control de isotipo para determinar el pegado inespecífico del anticuerpo anti-HA. Se determinó simultáneamente la expresión de ambas proteínas identificándose una población celular que tuviera alta expresión de ambas proteínas y se observó que el 97% de células que tienen E1$_{244-550}$HA^{hi} y GFP^{hi}. **B) Separación de células B16-F0/E1$_{244-550}$HA^{hi}/GFP^{hi}.** La población celular con alta expresión de GFP se aisló por citometría de flujo obteniendo una población enriquecida del 96% de células GFP^{hi}.

De la misma manera que las células B16-F0/E1$_{244-550}$HA, también se analizó la expresión curso-temporal de E1$_{244-550}$HA en las células B16-F0/E1$_{244-550}$HA^{hi} previamente separadas por citometría, y en comparación con las células sin separación por citometría (Figura 14), la expresión de E1$_{244-550}$HA fue detectada hasta 27 días post-transfección (Figura 17). Las células B16-F0/E1$_{244-550}$HA^{hi} fueron utilizadas para producir tumores en ratones C57BL/6.
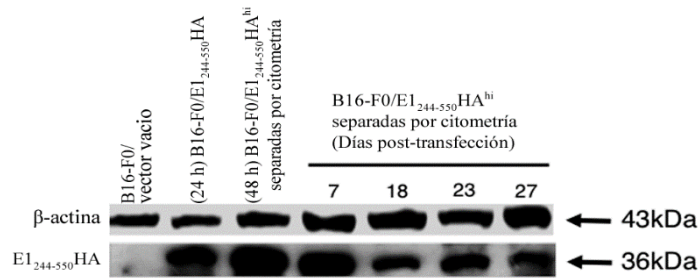
Figura 17. Expresión de la secuencia optimizada E1$_{244-550}$HA en células separadas por citometría. Células B16-F0 que expresan E1$_{244-550}$HA y previamente separadas por citometría fueron analizadas a diferentes días post-transfección (7, 18, 23 y 27 días) mediante western blot, usando un anticuerpo anti-HA. Se usó un extracto de células B16-F0 transfectadas con el vector vacío como control negativo. Se usaron extractos de células B16-F0 sin separación por citometría transfectadas con pE1$_{244-550}$HA (24 horas post-transfección) y de células B16-F0 separadas por citometría transfectadas con pE1$_{244-550}$HA (48 horas post-transfección) como controles positivos.

Con la finalidad de evaluar si existe reacción cruzada contra otros tipos de VPH, se determinó la expresión del dominio de E1 con más homología entre los VPH. El dominio E1-carboxilo terminal de VPH 6, 11, 16, 18, 31, 33 y 53 fue detectado 24 h post-transfección (Figura 18). Los extractos de células B16-F0 transfectadas con vector vacío se usaron como control negativo. Las células B16-F0 que expresan los diferentes tipos de E1-CT se usaron como blanco inmunológico para determinar la reactividad cruzada de linfocitos T CD8 +.
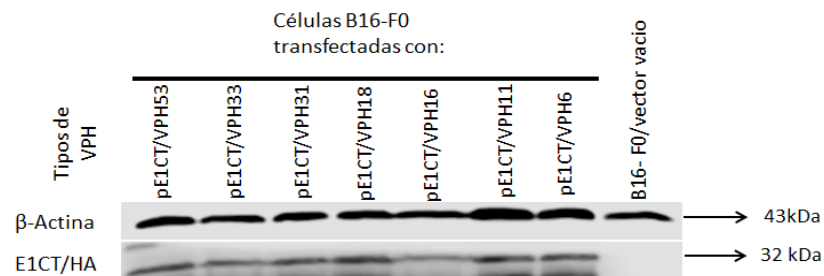
Figura 18. Expresión del dominio E1 carboxilo terminal de diferentes VPH. Las células B16-F0 se transfectaron con pE1CT-VPH6HA, pE1CT-VPH11HA, pE1CT-VPH16HA, pE1CT-VPH31HA, pE1CT-VPH33HA, pE1CT-VPH53HA y pE1CT-VPH18HA. Los dominios carboxilo terminales se detectaron a un peso de 32 kDa 24 horas después de la transfección mediante western blot, usando un anticuerpo anti-HA. La proteína extraída de B16-F0 transfectada con vector vacío se usó como control negativo.

- DETECCIÓN DE $E1_{244-550}HA$ EN TUMORES DE RATÓN

La expresión de la proteína $E1_{244-550}HA$ fue evaluada en tumores de ratón generados a partir de la inoculación de 7.5×10^5 células $B16\text{-}F0/E1_{244-550}HA^{hi}$. La expresión de la proteína $E1_{244-550}HA$ se identificó claramente en lisados tumorales, hasta 25 días después de la inoculación en ratones (Figura 19). Por lo tanto, la expresión *in vivo* de $E1_{244-550}HA$ hace a estas células blancos inmunológicos potenciales para ser reconocidos por los linfocitos T CD8+ antígeno-específicos.
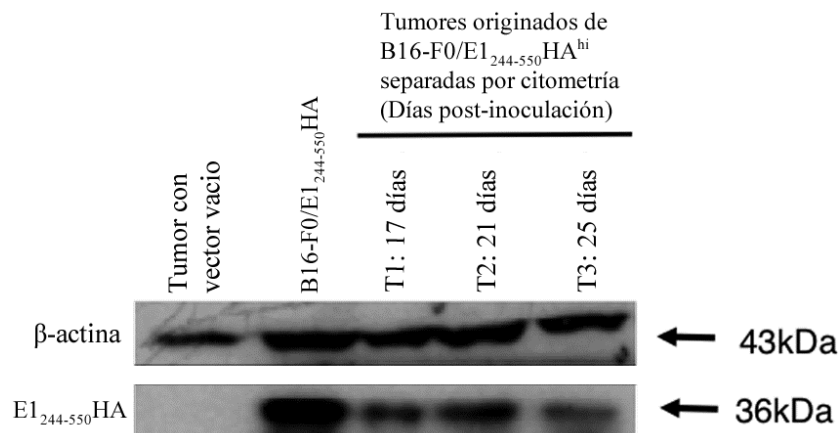
Figura 19. Detección de $E1_{244-550}HA$ en tumores originados a partir de células $B16\text{-}F0/E1_{244-550}HA^{hi}$ separadas por citometría. Ratones sin tratamiento se inocularon con células $B16\text{-}F0/E1_{244-550}HA^{hi}$ y la expresión de $E1_{244-550}HA$ se analizó en extractos tumorales (Tumores 1, 2 y 3) cosechados a diferentes días después de la inoculación (17, 21 y 25 días). El extracto de células $B16\text{-}F0/E1_{244-550}HA$ cosechado 24 horas después de la transfección fue usado como control positivo. Se usaron extractos de un tumor originado de $B16\text{-}F0$/vector vacío como control negativo.

- INMUNIZACIÓN DE $E1_{202-654}$ + α-GALCER PROTEGE CONTRA CÉLULAS TUMORALES QUE EXPRESAN LA PROTEÍNA E1

Con el fin de determinar si la respuesta inmune antígeno-específica afecta la formación y el crecimiento de tumores, se examinó la eficacia protectora de la inmunización con $E1_{202-654}$+α-GalCer en un modelo de tumor de ratón. Para esto, ratones C57BL/6 fueron inoculados con diferentes tratamientos, tal como se describe en Materiales y Métodos (Figura 12). Posteriormente al día 19, se inocularon células $B16\text{-}F0/E1_{244-550}HA^{hi}$, y el crecimiento tumoral fue monitoreado y medido cada tercer día en los cuatro grupos de

ratones. En las Figuras 20A, B, C y D, se observó una inhibición del crecimiento tumoral en los grupos P2 y P3. La Figura 20E muestra que después de ser sacrificados los ratones, la media del tamaño tumoral es significativamente menor en el grupo inmunizado con $E1_{202-654}$+α-GalCer con respecto a los grupos inoculados con PBS, α-GalCer o $E1_{202-654}$. Además, cuatro de seis ratones no mostraron ningún crecimiento tumoral después de finalizar el protocolo profiláctico. La media del crecimiento tumoral en ratones inoculados con α-GalCer también fue significativamente menor que los inoculados con PBS. Adicionalmente el panel E, muestra un ejemplo de los tumores extirpados de cada uno de los grupos antes mencionados.
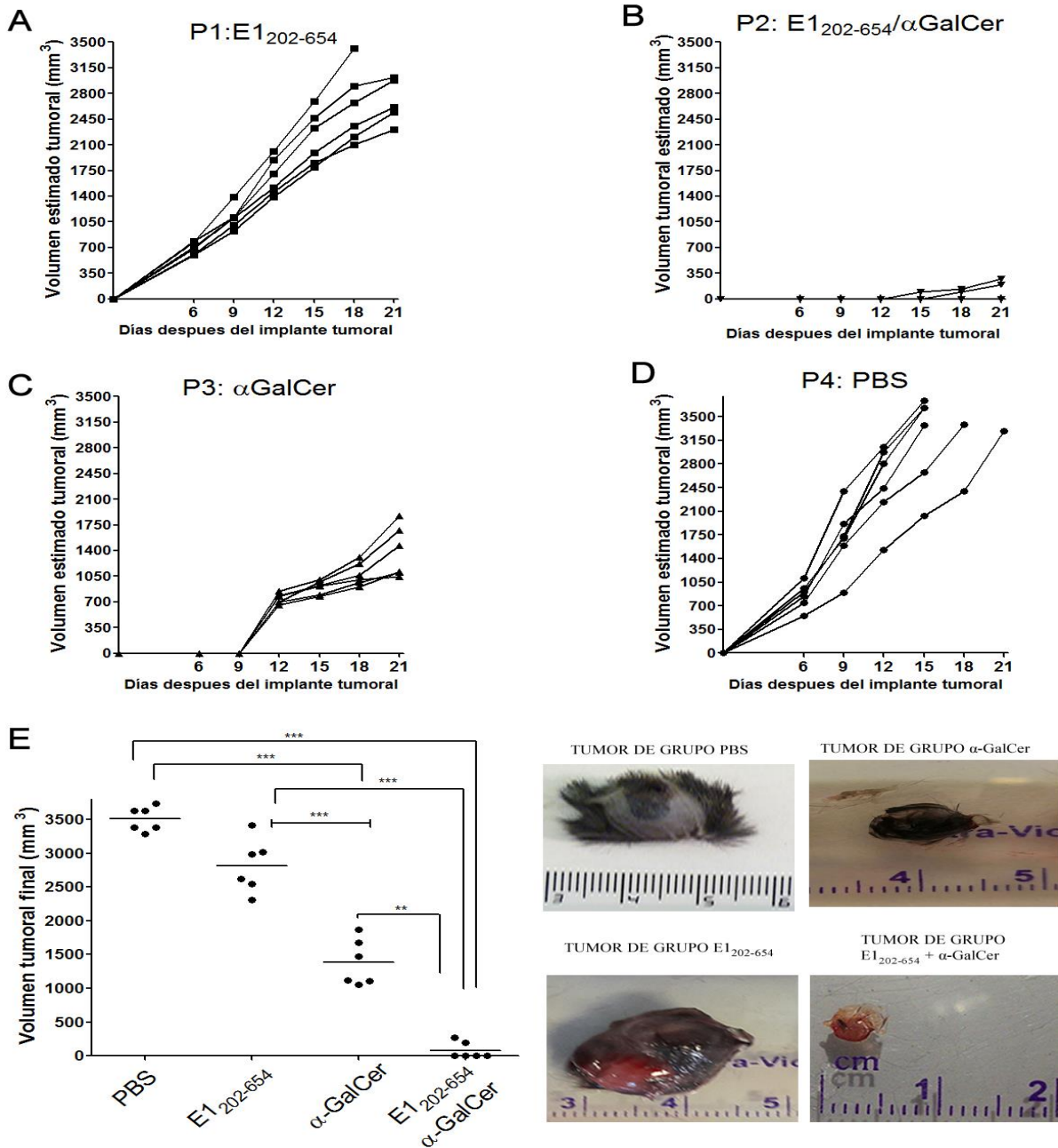
Figura 20. Efecto de las inmunizaciones profilácticas sobre el crecimiento tumoral. Cada grupo de ratones se inoculó con células B16-F0/E1$_{244-550}$HA^{hi} y se monitoreó el crecimiento tumoral a lo largo del tiempo para los grupos (A) P1, (B) P2, (C) P3 y (D) P4. El tamaño del tumor se midió como se describe en "Materiales y métodos" y su volumen estimado se graficó a lo largo del tiempo. (E) Efecto de las inmunizaciones en el crecimiento tumoral. Una vez que los ratones se sacrificaron, los tumores se extirparon y sus tamaños se determinaron por la ecuación previamente descrita y se reportaron en mm^3. El tamaño del tumor se trazó para cada ratón y la media se representa para cada grupo. La significancia estadística con ** $P < 0.01$ y *** $P < 0.0001$ por análisis multiparamétrico ANOVA de una vía y prueba de comparación múltiple de Tukey está representada en la gráfica.

40

- E1$_{202-654}$+α-GALCER INHIBE EL CRECIMIENTO DE LOS TUMORES YA ESTABLECIDOS

Para analizar si la inoculación de E1$_{202-654}$+α-GalCer confiere protección a animales con tumores establecidos derivados de células B16-F0/E1$_{244-550}$HA^{hi}, cuatro grupos de ratones se inocularon con estas células y cinco días después se inmunizaron de acuerdo con el protocolo descrito en Materiales y Métodos (Figura 12B). El crecimiento tumoral se monitoreó hasta 23 días después de la implantación de las células tumorales. Se observó que la vacunación con E1$_{202-654}$ + α-GalCer (Figura 21B) afecta el crecimiento tumoral, en comparación con los otros tratamientos (Figura 21A, C y D), esto indica que este tratamiento es capaz de reducir la masa tumoral, cuando el crecimiento del tumor ya ha comenzado. Adicionalmente se observó que la media del tamaño tumoral en ratones inoculados exclusivamente con α-GalCer fue significativamente menor (3,46 cm^3) que el de ratones inoculados con PBS (6,55 cm^3) (Figura 21E). El panel E, muestra un ejemplo representativo de los tumores extirpados de cada uno de los grupos antes mencionados.
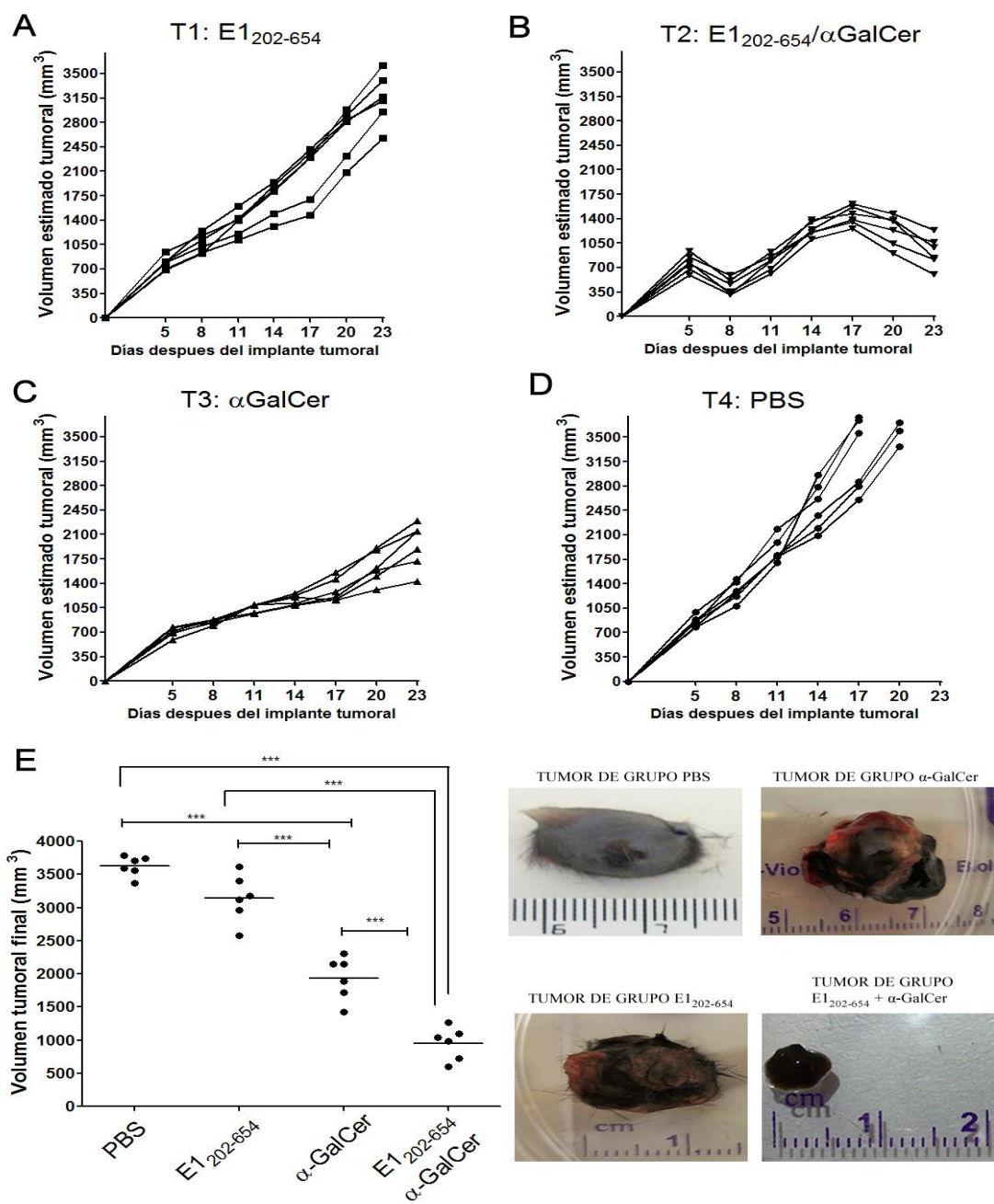
Figura 21. Efecto de las inmunizaciones terapéuticas sobre el crecimiento tumoral. Cada grupo de ratones se inoculó con células B16-F0/E1$_{244-550}$HA^{hi} y se monitoreó el crecimiento tumoral a lo largo del tiempo para los grupos (A) T1, (B) T2, (C) T3 y (D) T4. El tamaño del tumor se midió como se describe en "Materiales y métodos" y su volumen estimado se graficó a lo largo del tiempo. (E) Efecto de las inmunizaciones en tumores establecidos. Una vez que los ratones se sacrificaron, los tumores se extirparon y sus tamaños se determinaron por la ecuación previamente descrita y se reportaron en mm^3. El tamaño del tumor se graficó para cada ratón y la media se representa para cada grupo. La significancia estadística con *** P <0.0001 por análisis multiparamétrico ANOVA de una vía y prueba de comparación múltiple de Tukey está representada en la gráfica.

42

- INMUNIZACIÓN CON E1$_{202\text{-}654}$ + α-GALCER PROMUEVE UNA RESPUESTA ANTÍGENO-ESPECÍFICA EN LINFOCITOS TCD8 + TANTO EN EL MODELO PROFILÁCTICO COMO TERAPÉUTICO

La exocitosis de gránulos citotóxicos contenidos en linfocitos T CD8+, conlleva a la aparición de moléculas CD107a y CD107b en la membrana celular [72]. Las moléculas CD107a/b han sido usadas como marcadores de actividad citotóxica tanto en células NK y CD8+ de humano y ratón [72-75].

De esta manera, se examinó el curso temporal de la aparición de los marcadores de actividad citotóxica CD107a/b en la membrana de linfocitos T CD8 + esplénicos y se determinó que el tiempo a 4 horas es donde se presenta mayor expresión de los marcadores CD107a/b (Figura 22).

Aunque determinamos otros marcadores de actividad citotóxica como la pérdida intracelular de perforina y granzima A, su detección no fue la ideal en linfocitos T CD8+ de ratón. La molécula perforina fue indetectable, lo cual fue concordante con lo reportado por la casa comercial Affymetrix eBioscience (número de catálogo 179392); En cuanto a la pérdida intracelular de granzima A, la cinética de la desgranulación en los ensayos osciló entre valores altos y bajos de detección intracelular. Por lo tanto, decidimos evaluar exclusivamente la expresión superficial de CD107a y CD107b.
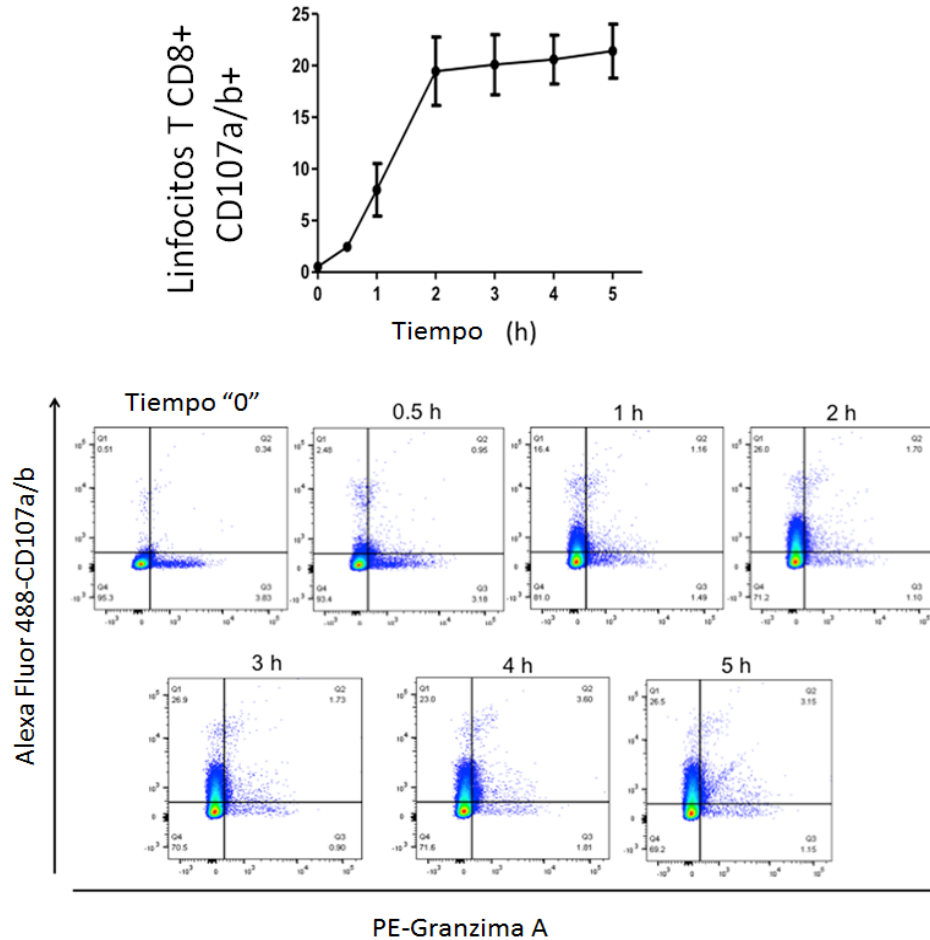
Figura 22. Adquisición de los marcadores CD107a/b en superficie celular de linfocitos T CD8+. Se midió la aparición de CD107a/b en membrana celular como marcador de actividad citotóxica de linfocitos T CD8+. Los linfocitos T CD8+ de bazo fueron estimuladas con Ionomicina (1500 ng/ml) y PMA (300 ng/ml) hasta por 4 h en presencia de anti-CD107a/b-Alexa Fluor 488. El aumento de la superficie celular CD107a/b indica actividad citotóxica de linfocitos T CD8+. En los paneles de abajo se muestran ejemplos representativos de la curva de actividad citotóxica, en donde se observa que conforme se incuban por tiempos prolongados, la expresión en superficie de CD107a/b va aumentando.

Para examinar la actividad citotóxica E1-específica en los modelos profiláctico y terapéutico, se co-cultivaron linfocitos T CD8 + de cada ratón con células B16-F0 y B16-F0/E1$_{244-550}$ como blancos inmunológicos. Se observó que en linfocitos T CD8 + de ratones inmunizados con E1$_{202-654}$ + α-GalCer co-cultivados con células B16-F0/E1$_{244-550}$, hubo un aumento notable en la expresión superficial de CD107a/b, indicando una

44

actividad citotóxica E1-específica de los linfocitos T CD8 + (Figura 23 A y B), lo cual se correlacionó con la inhibición del crecimiento tumoral en ambos protocolos.
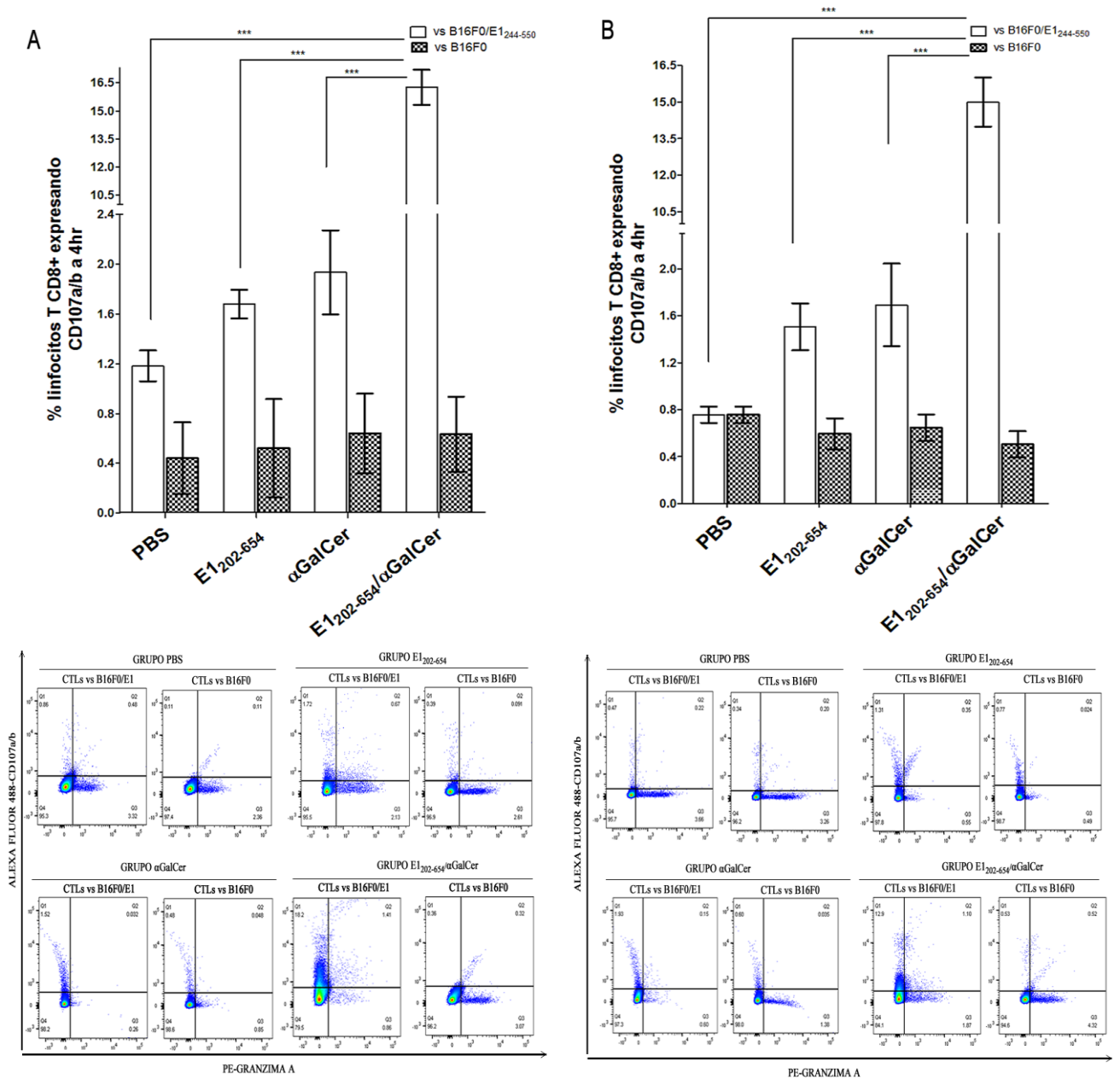
Figura 23. Respuesta citotóxica de linfocitos T CD8+ específicas. La expresión de CD107a/b en la superficie celular se midió en linfocitos T CD8 + esplénicas de ratones inoculados con E1$_{202-654}$+α-GalCer (n = 6), PBS (n = 6), E1$_{202-654}$ (n = 6) y α-GalCer (n= 6) co-cultivadas con células B16-F0 (barras vacías) o células transfectadas B16-F0/E1$_{244-550}$ (barras cuadriculadas) hasta por 4 horas en presencia de anti-CD107a/b-Alexa Fluor-488, para comparar si los linfocitos T CD8+ tienen una actividad E1-específica. La actividad citotóxica de los linfocitos T CD8+ fue determinada tanto para el modelo **A) profiláctico,** como

B) terapéutico. Los paneles inferiores en **A y B** muestran imágenes representativas de citometría de flujo de ensayos de actividad citotóxica. La significancia estadística con *** $P < 0.0001$ por análisis multiparamétrico ANOVA de una vía y prueba de comparación múltiple de Tukey se representa en el gráfico.

En los protocolos profiláctico (Figura 23A) y terapéutico (Figura 23B), los grupos inoculados con PBS, E1 y α-GalCer no mostraron una respuesta E1-específica de linfocitos T CD8+ en ambos protocolos. En base a estos ensayos de actividad citotóxica, la inhibición del crecimiento tumoral observada en los ratones tratados con α-GalCer no es dependiente de linfocitos T CD8+, tanto en los protocolos profiláctico como terapéutico.

- α-GALCER PROMUEVE UNA RESPUESTA DE LINFOCITOS NK TANTO EN LOS MODELOS PROFILÁCTICO COMO TERAPÉUTICO

Debido a que la respuesta de las células NK se ha asociado con un efecto antitumoral [76, 77], y α-GalCer es un adyuvante capaz de incrementar las poblaciones de células NK [78], se procedió a examinar el papel de las células NK en la inhibición del crecimiento tumoral de los modelos profiláctico y terapéutico. Al igual que en los linfocitos T CD8+, se determinó el curso temporal de las moléculas CD107a/b en linfocitos NK esplénicas y se determinó que el tiempo entre 3 y 4 horas fue donde se presentó la mayor expresión de CD107a/b (Figura 24).
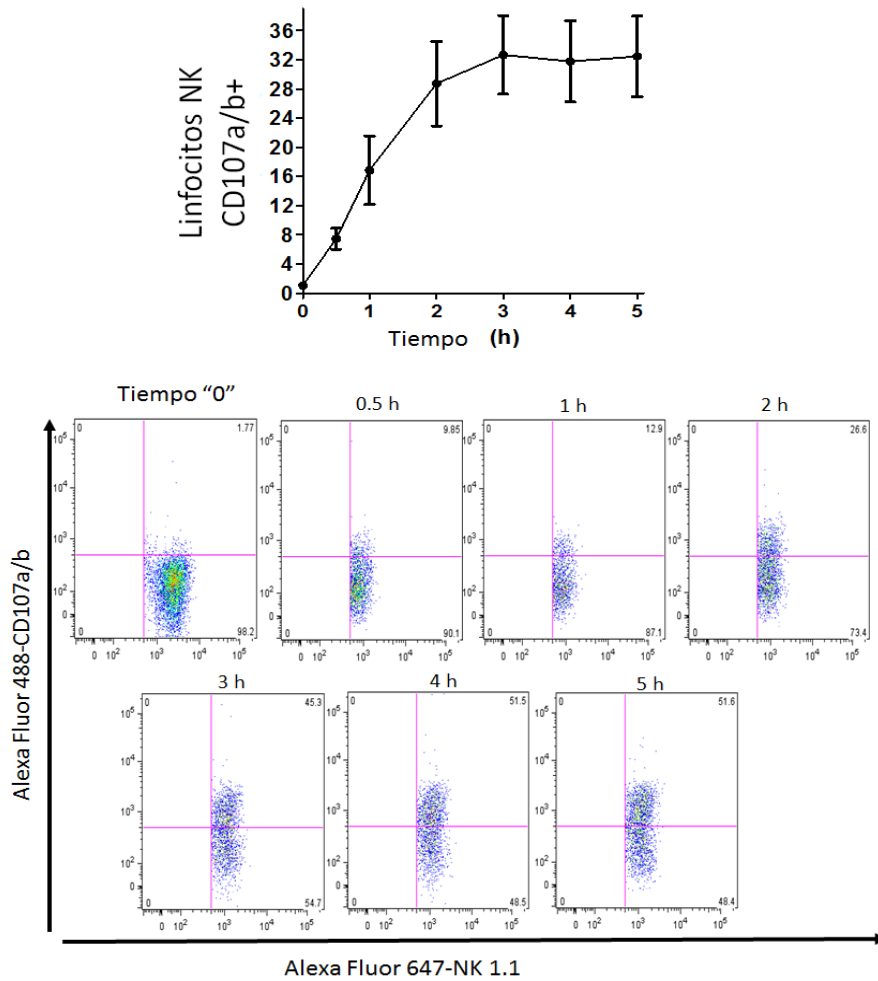
Figura 24. Adquisición de los marcadores CD107a/b en superficie celular. Se midió la aparición de CD107a/b en membrana celular como marcador de actividad citotóxica de células NK. Células NK de bazo fueron estimuladas con Ionomicina (1500 ng/ml) y PMA (300 ng/ml) hasta por 4 h en presencia de anti-CD107a/b-Alexa Fluor 488. El aumento de la superficie celular CD107a/b indica actividad citotóxica de células NK. En los paneles de abajo se muestran ejemplos representativos de la curva de actividad citotóxica, en donde se observa que conforme se incuban por tiempos prolongados, la expresión en superficie de CD107a/b va aumentando.

Para examinar la actividad citotóxica de NK en los protocolos profiláctico y terapéutico, se realizaron co-cultivos de células NK con células B16-F0/E1$_{244-550}$. En ambos protocolos, los linfocitos NK de ratones inoculados con α-GalCer mostraron la actividad citotóxica más fuerte en comparación con todos los grupos (Figura 25A y B). Sin embargo, la inoculación de E1$_{202-654}$+α-GalCer en ambos protocolos también indujo

actividad citotóxica NK significativa en comparación con los grupos de ratones inoculados con PBS ó E1$_{202-654}$ (Figura 25A y B). Además, los ratones inmunizados con E1$_{202-654}$ de los protocolos profiláctico y terapéutico no mostraron una actividad citotóxica de NK diferencialmente significativa en comparación con el grupo inoculado con PBS. Estos resultados indican que, además de las respuestas citotóxicas de linfocitos T CD8+ específicas de tumor, las células NK pueden proporcionar una actividad antitumoral adicional que contribuye al potencial terapéutico y profiláctico de la inmunización con E1+α-GalCer.
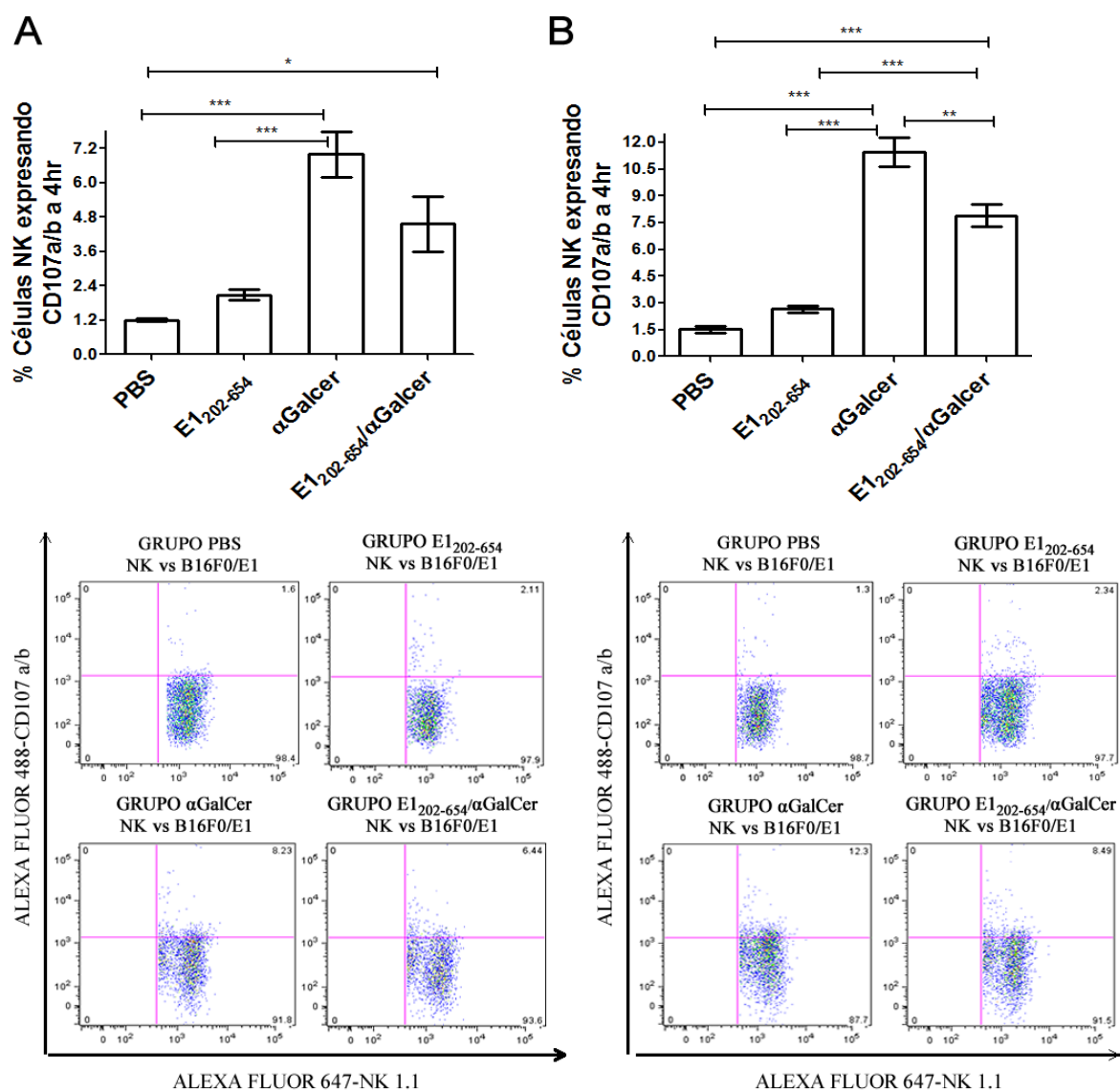
Figura 25. Expresión de CD107a/b en la superficie celular de NK como marcador de citotoxicidad. Las células NK esplénicas de ratones inoculados con E1$_{202-654}$+α-GalCer (n = 6), PBS (n = 6), E1$_{202-654}$ (n = 6) y α-GalCer (n = 6) se co-cultivaron con B16 -F0/E1$_{244-550}$HA hasta por 4 h en presencia de anti-

CD107a/b-Alexa Fluor 488. Se evaluó la actividad citotóxica de linfocitos NK contra células tumorales B16-F0/E1$_{244-550}$HA tanto en un modelo **A) profiláctico,** como **B) terapéutico**. Los paneles inferiores en **A y B** muestran imágenes representativas de citometría de flujo de ensayos de actividad citotóxica. La significancia estadística con *P <0.05, **P <0.01 y ***P <0.0001 por un análisis multiparamétrico ANOVA de una vía y prueba de comparación múltiple de Tukey está representada en el gráfico.

- REACTIVIDAD CRUZADA CONTRA E1 DE OTROS VPH

Para determinar si los linfocitos T CD8+ de ratones inmunizados con VPH18-E1$_{202-654}$ podrían tener actividad citotóxica contra otros tipos de E1-VPH, se co-cultivaron linfocitos T CD8+ esplénicas de estos ratones con células B16-F0 que expresan los dominios E1-carboxilo terminal de VPH-6, 11, 16, 18, 31, 33 ó 53, los cuales previamente mediante análisis *in-silico* se determinó que comparten potenciales péptidos inmunogénicos. Las células B16-F0 no transfectadas se usaron como control negativo. Los co-cultivos se monitorearon hasta por 4 h, momento en el que alcanzaron la expresión de superficie celular CD107a/b más alta, por lo tanto, se grafica la expresión CD107a/b a este tiempo. Se detectó un aumento significativo de CD107a/b en los co-cultivos de linfocitos T CD8+ de ratones inmunizados con VPH18-E1$_{202-654}$+α-GalCer co-cultivadas con células B16-F0 que expresan E1-Carboxilo terminal de los tipos de VPH-53, 33, 16, 31 y 11, en relación con el control negativo (Figura 26A). La mayor expresión de CD107a/b en la superficie celular se obtuvo en co-cultivos de células que expresan E1CT-VPH53, y el más bajo se obtuvo para E1CT-VPH11. No se detectó expresión de CD107a/b en linfocitos T CD8+ esplénicas cuando se co-cultivaron con células que expresan E1CT-VPH6. Estos datos indican que los linfocitos T CD8+ de ratones inmunizados con VPH18-E1$_{202-654}$+α-GalCer también pueden mostrar actividad citotóxica contra células que expresan E1CT-VPH53, E1CT-VPH33, E1CT-VPH16, E1CT-VPH31 y E1CT-VPH11.

Los linfocitos T esplénicos CD8+ de ratones inyectados solo con PBS (Figura 26B), α-GalCer (Figura 26C) o inmunizados exclusivamente con proteína VPH18-E1$_{202-654}$ (Figura 26D) no mostraron actividad citotóxica cruzada en contra de algún dominio E1-carboxilo terminal.

A

B

C

D
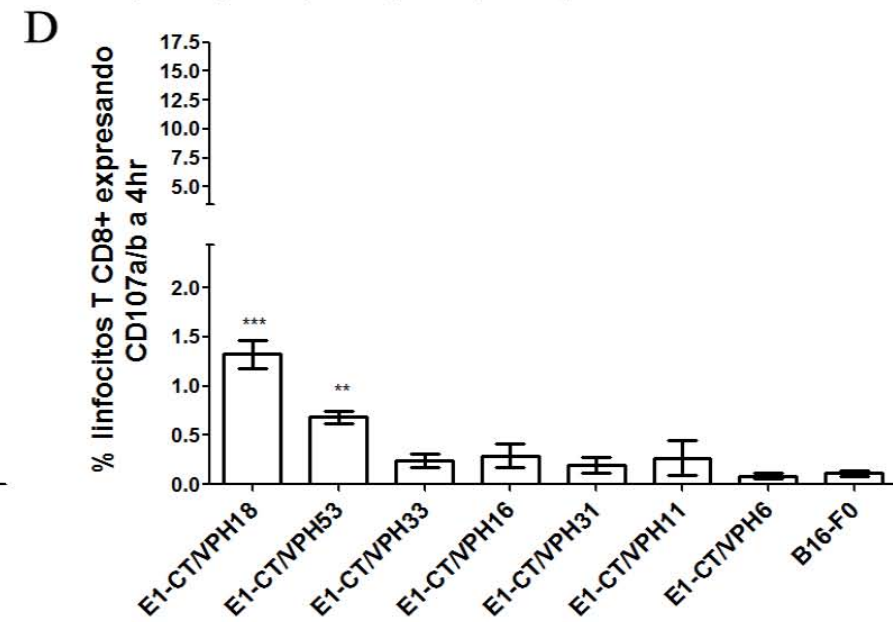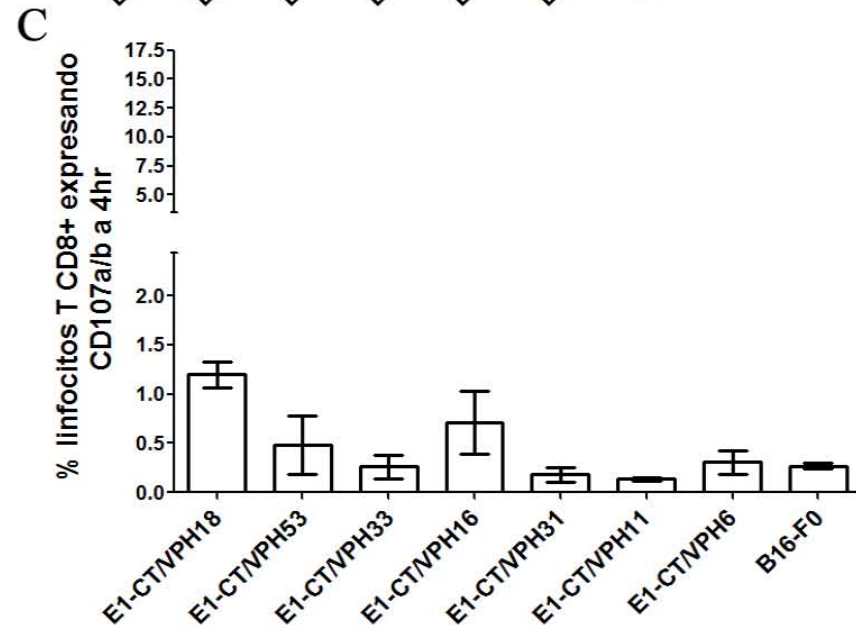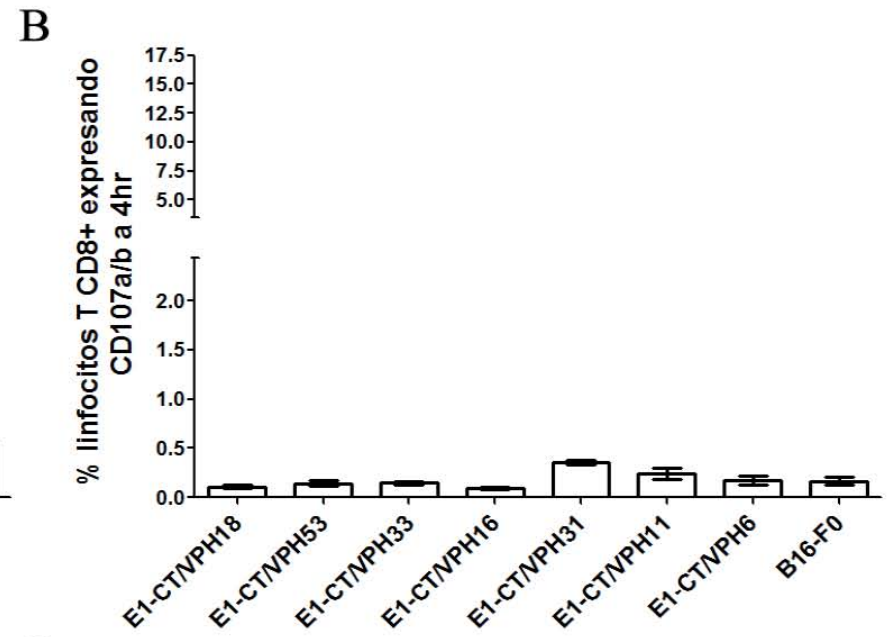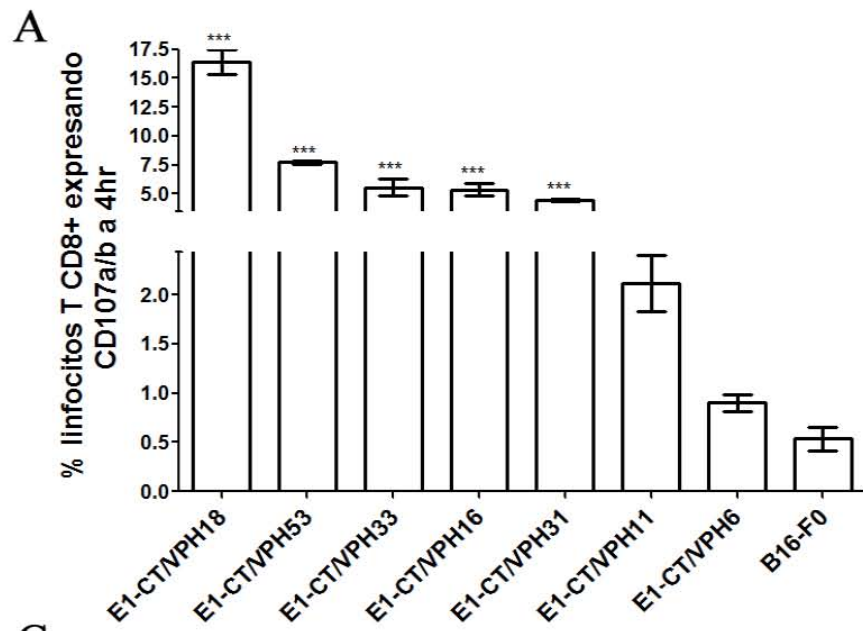
Figura 26. Reactividad cruzada de linfocitos T CD8+ contra células B16-F0 que expresan E1-CT de varios tipos de VPH. La adquisición de CD107a/b en superficie celular se midió como marcador de actividad citotóxica de linfocitos T CD8+. Los linfocitos T CD8+ esplénicos de ratones inmunizados o inoculados con: **(A)** proteína VPH18-E1$_{202-654}$ más α-GalCer, **(B)** PBS, **(C)** α-GalCer o **(D)** E1$_{202-654}$, se co-cultivaron hasta a por 4 h con B16-F0E1-CT/VPH18HA, B16-F0E1-CT/VPH53HA, B16-F0E1-CT/VPH33HA, B16-F0E1-CT/VPH16HA, B16-F0E1-CT/VPH31HA, B16-F0E1-CT/VPH11HA, B16-F0E1-CT/VPH6HA o B16-F0 en presencia de anti-CD107a/b-Alexa Fluor 488, anti-CD8-Brillant Violet 421 y anti-CD3-APC. El aumento de CD107a/b expuesto en la superficie celular indica actividad citotóxica de linfocitos T CD8 +. La significancia estadística con *** $P < 0.05$, mediante ANOVA multiparamétrico de una vía y la prueba de Dunett se representa en el gráfico.

DISCUSIÓN

Actualmente las vacunas comerciales contra VPH no protegen contra infecciones ya establecidas, por lo que la inducción de una respuesta de linfocitos T CD8+ citotóxicos contra antígenos virales constituye el principal objetivo para el desarrollo de vacunas terapéuticas contra enfermedades virales crónicas, incluidas las relacionadas con algunas formas de cáncer, como el cáncer de cuello uterino. En el presente estudio evaluamos la respuesta antitumoral inducida por E1$_{202-654}$ de VPH-18 y α-GalCer en un modelo animal, para examinar su posible papel como inmunógeno en las infecciones por VPH. Este potencial efecto terapéutico tendría relevancia en infecciones tempranas o lesiones de bajo grado debido a que en estas etapas la proteína E1 es expresada durante la replicación del ADN viral. Sin embargo, un estudio reciente mostró que existe una elevada expresión del ARN mensajero de E1 en estadios tardíos como NIC-3 y carcinomas *in situ* [24] por lo que de confirmar estos hallazgos a nivel de proteína en futuros estudios, el potencial efecto terapéutico de la proteína E1 también tendría relevancia en etapas tardías.

Para evaluar esta respuesta inmunológica, células de melanoma murino B16F0 fueron transfectadas con el plásmido pE1$_{244-550}$, para ser usadas como blanco inmunológico tanto *in vivo* al ser inoculadas a los ratones, como *in vitro* al ser empleadas en los ensayos de actividad citotóxica. Para ambos casos, la secuencia clonada de E1 contiene una optimización de codones para un modelo ratón, que en contraste con la secuencia referencia de VPH18-E1 de longitud completa, se expresó de manera eficiente (Figura

13). Esto concuerda con lo reportado para la proteína E1 de COPV [67], en donde también se optimizó la secuencia de codones de dicho gen, con lo que se logró una eficiente expresión.

Para este estudio, se utilizó como adyuvante a α-GalCer ya que ha demostrado que coadministrado con un antígeno proteico es capaz de promover una fuerte respuesta de linfocitos T CD8+ antígeno-específica [59, 79]. De esta manera, se empleó el adyuvante α-GalCer junto con la proteína E1, con la finalidad de inducir una respuesta E1-especifica capaz de eliminar células tumorales que expresen E1.

Los ratones inoculados con el inmunógeno $E1_{202-654}$ más el adyuvante α-GalCer o con α-GalCer solo, alteraron el crecimiento de células $B16-F0/E1_{244-550}HA^{hi}$ tanto en el protocolo profiláctico como terapéutico.

Cabe señalar que la administración sola de α-GalCer ya ha sido relacionada con una respuesta antitumoral [80, 81], este efecto también fue demostrado en este estudio. Sin embargo, la mayor inhibición del crecimiento tumoral se presentó en ratones inmunizados con $E1_{202-654}$+α-GalCer; observamos que para el caso del modelo profiláctico cuatro de seis ratones no desarrollaron tumor hasta los 21 días, mientras que en modelo terapéutico disminuye el crecimiento de tumores ya establecidos en todos los ratones. Esto indica que la vacunación con E1+α-GalCer puede inducir una fuerte respuesta antitumoral contra células que expresan E1.

Posterior a la medición del crecimiento tumoral, se determinaron las principales poblaciones celulares del sistema inmunológico relacionadas con un efecto citotóxico contra células tumorales, como son los linfocitos NK y T CD8+. La infiltración de estos linfocitos en tejido tumoral es relevante para la regresión tumoral y el mejor pronóstico en pacientes con cáncer [82, 83].

En el caso de los linfocitos NK, son capaces de eliminar células tumorales sin necesidad de reconocer un antígeno por lo que su actividad citotóxica sería inespecífica de antígeno [84, 85], mientras que los linfocitos T CD8+ necesitan reconocer a través de su TCR, un antígeno proteico presentado en el MHC-I. Esta sinapsis es esencial para la eliminación de células blanco [86].

De esta manera, se examinó si el efecto antitumoral observado en cada uno de los grupos de ratones correlaciona con la capacidad de los linfocitos T CD8+ y NK de tener actividad citotóxica en presencia de células B16-F0 que expresan antígenos de E1.

Solo los ratones inmunizados con $E1_{202-654}$+α-GalCer mostraron una actividad citotóxica E1-específica de linfocitos T CD8+ en presencia de células B16-F0/$E1_{244-550}$, lo cual es consistente con los hallazgos reportados previamente en ratones inmunizados con el virus Ankara que codifica E1 de VPH-16 [68].

Los hallazgos de este trabajo demuestran que el único tratamiento capaz de favorecer una respuesta inmune adaptativa E1-especifica es la vacunación de $E1_{202-654}$+α-GalCer y que el efecto antitumoral observado por la inoculación de α-GalCer solo, no es dependiente de linfocitos T CD8+.

Adicionalmente, se determinó la respuesta de células NK y se observó que los ratones tratados con α-GalCer de ambos protocolos mostraron una actividad citotóxica, lo cual correlaciona con el efecto antitumoral inespecífico observado en estos grupos. La actividad citotóxica de NK también se detectó en ratones tratados con $E1_{202-654}$+α-GalCer, lo que indica que el efecto antitumoral en los modelos profiláctico y terapéutico involucran una respuesta innata y adaptativa, que actuando en conjunto podría contribuir a una respuesta antitumoral más fuerte.

Una vez demostrado que la inmunización con VPH18-$E1_{202-654}$+α-GalCer es capaz de inducir una respuesta de linfocitos T CD8+ capaz de reconocer antígenos E1, se determinó mediante ensayos de citotoxicidad si estos linfocitos eran capaces de tener una actividad citotóxica en presencia de células B16-F0 que expresan E1 de otros tipos virales (VPH-6, 11, 16, 31, 33 y 53). Este objetivo toma relevancia dado que los actuales estudios sobre vacunas terapéuticas en fase I y II [87] emplean a las proteínas de expresión temprana con menos homología: E6 y/o E7, además de que no proponen generar un amplio espectro de protección.

El único antecedente previo hasta la fecha en donde se demostró una reacción cruzada contra una proteína de VPH con alta homología, es el reportado por Ragonnaud E, et al, 2017, en donde usan una proteína E1-E2 de papiloma de Macaco (MfPV) contra E1 de otros tipos virales [69]. De esta manera, en el presente estudio se comparó la homología del dominio E1-carboxilo terminal de diferentes tipos virales contra la homología de otras

proteínas virales tanto de bajo como alto riesgo, y se determinó que el dominio E1CT es el más conservado de todas las proteínas virales de expresión temprana (Tabla 5).

Esta tabla muestra que el porcentaje de homología de las proteínas E6 y E7 es muy variado y bajo, mientras que el rango en porcentaje de homología de la proteína E1 es más estrecho y con porcentajes más altos.

Tabla 5.

5A) Análisis de las secuencias de péptidos E6 de VPH-6, 11, 53, 18, 33, 16 y 31 en Clustal omega. El análisis indica que todos los tipos en esta tabla muestran una identidad de **31.33 a 55.56%**, en comparación con <u>VPH18-E6</u> (columna en rojo).

VPH	6	11	53	18	33	16	31
6	100.00	81.33	38.67	31.33	33.56	35.33	32.89
11	81.33	100.00	35.33	34.00	33.56	34.00	31.54
53	38.7	35.33	100.00	42.76	51.01	47.40	54.36
18	31.33	34.00	42.76	100.00	46.31	55.56	51.68
33	33.56	33.56	51.01	46.31	100.00	62.42	58.39
16	35.33	34.00	47.40	55.56	62.42	100.00	64.43
31	32.89	31.54	54.36	51.68	58.39	64.43	100.00

5B) Análisis de las secuencias de péptidos E7 de VPH-6, 11, 53, 18, 33, 16 y 31 en Clustal omega. El análisis indica que todos los tipos en esta tabla muestran una identidad de **39.81 a 44.33%**, en comparación con <u>VPH18-E7</u> (columna en rojo).

VPH	6	11	53	18	33	16	31
6	100.00	85.71	37.76	42.86	51.04	53.61	49.48
11	85.71	100.00	36.73	43.88	51.04	55.67	50.52
53	37.76	36.73	100.00	39.81	47.42	42.86	43.88
18	42.86	43.88	39.81	100.00	47.42	42.86	38.78
33	51.04	51.04	47.42	44.33	100.00	60.82	59.79
16	53.61	55.67	42.86	42.86	60.82	100.00	73.47
31	49.88	50.52	43.88	38.78	59.79	73.47	100.00

5C) Análisis de secuencias de péptidos E2 de VPH-6, 11, 53, 18, 33, 16 y 31 en Clustal omega. El análisis indica que todos los tipos en esta tabla muestran una identidad de **38.64 a 44.69%**, en comparación con VPH18-E2 (Columna en rojo).

VPH	6	11	53	18	33	16	31
6	100.00	78.14	41.92	38.64	42.86	45.66	43.80
11	78.14	100.00	41.60	39.89	43.97	45.79	45.86
53	41.92	41.60	100.00	42.54	39.77	43.49	43.87
18	38.64	39.89	42.54	100.00	43.27	43.06	44.69
33	42.86	43.97	39.77	43.27	100.00	51.87	47.88
16	45.66	45.79	43.49	43.06	51.87	100.00	62.74
31	43.80	45.86	43.87	44.69	47.88	62.74	100.00

5D) Análisis de secuencias de péptidos E1 de VPH-6, 11, 53, 18, 33, 16 y 31 en Clustal omega. El análisis indica que todos los tipos en esta tabla muestran una identidad de **59.43 a 67.61%**, en comparación con VPH18-E1 (Columna en rojo).

VPH	6	11	53	18	33	16	31
6	100.00	93.12	61.44	59.75	58.04	57.37	62.70
11	93.12	100.00	62.07	59.43	58.99	59.87	63.01
53	61.44	62.07	100.00	64.26	62.26	67.81	68.71
18	59.75	59.43	64.26	100.00	67.61	64.58	67.40
33	58.04	58.99	62.26	67.61	100.00	70.75	74.53
16	57.37	59.87	67.81	64.58	70.75	100.00	81.25
31	62.70	63.01	68.75	67.40	74.53	81.25	100.00

Adicionalmente, a través de un análisis *in silico* encontramos péptidos altamente conservados en el dominio carboxilo terminal de las proteínas E1 de VPH-6, 11, 16, 18, 31, 33 y 53 (Tabla 3), que tienen la probabilidad de unión a las proteínas MHC-I. El análisis mostró que los dominios carboxilo terminal de VPH53-E1 y VPH18-E1 comparten el mayor número de péptidos predichos (Tabla 4). Estos datos *in-silico* concuerdan con los resultados obtenidos de los ensayos de actividad citotóxica, donde los linfocitos T CD8+ de ratones inmunizados con VPH18-E1$_{202-654}$+α-GalCer, co-cultivados con B16-F0/E1CT-VPH53HA tienen una alta expresión de CD107a/b en membrana, lo que indica que son capaces de reconocer y ser activamente citotóxicos en presencia de E1CT de VPH-53. También se detectó una reactividad cruzada significativa en los co-cultivos con células que expresan E1CT de los tipos de VPH de alto riesgo 33, 16 y 31 (Figura 26A), los cuales también tienen péptidos altamente conservados con E1CT de VPH-18. Aunque también se detectó actividad citotóxica contra células que expresan VPH-E1CT

de tipo 11 (2,11%), su nivel no fue estadísticamente significativo comparado con el control negativo.

Estos datos de reacción cruzada son relevantes ya que con un solo dominio proteico de VPH18-E1 se puede generar una inmunidad contra otros tipos virales, incluyendo VPH-53 que es un tipo viral no incluido en las vacunas actuales. Cabe resaltar que las vacunas actuales que generan una inmunidad humoral contra diferentes genotipos de VPH emplean desde 2 hasta 9 proteínas de acuerdo con la vacuna, protegiendo aproximadamente contra el 75% de los casos más frecuentes de CaCu [64]. De esta manera, los resultados del presente estudio muestran que una sola proteína genera reacción cruzada contra al menos 5 tipos virales diferentes, por lo que caracterizar inmunológicamente nuevos blancos terapéuticos plantea la posibilidad de generar terapias contra el 100% de los VPH de alto y bajo riesgo que producen cáncer y verrugas genitales.

Cabe resaltar que los resultados del presente trabajo soportan diversos hallazgos previamente reportados acerca del adyuvante α-GalCer donde reportan un efecto anti-tumoral en modelos animales [76, 77]. El α-GalCer junto con los vectores virales son adyuvantes que promueven una fuerte respuesta inmunológica mediada por linfocitos T CD8+, por lo que todos los hallazgos hasta el momento los ponen como adyuvantes ideales para ser usados en terapias contra cáncer o contra infecciones por patógenos intracelulares como VPH.

En síntesis, los datos de este trabajo indican que la vacunación con $E1_{202-654}$+α-GalCer genera una respuesta inmunológica antitumoral de linfocitos T CD8+ antígeno-específica y NK, la cual es capaz de proteger completamente en el modelo profiláctico a 4 de 6 ratones del desarrollo de tumores positivos a E1, mientras que en los 2 ratones restantes desarrollaron los tumores más pequeños de todo el modelo profiláctico. En tanto que, en el modelo terapéutico es capaz de reducir el crecimiento de tumores ya establecidos por lo que terapéuticamente también tiene una respuesta favorable. Estos datos son coincidentes con los publicados por Moore, et al, 2002 [67]; en donde muestran que, en un modelo terapéutico en perros, existe una reducción en el tamaño de verrugas orales causadas por papiloma. No obstante, los resultados del presente trabajo muestran adicionalmente que la inmunización de VPH-18/$E1_{202-654}$+α-GalCer genera una

respuesta de linfocitos T CD8+ capaces de reconocer y tener una actividad citotóxica ante una gran variedad antígenos presentes en E1CT de VPH-53, 31, 33, 16 y 11.

Cabe resaltar que los únicos tratamientos terapéuticos que existen contra lesiones producidas por VPH son la escisión quirúrgica, la cual no genera una protección contra futuras infecciones y que los tratamientos inmunoterapéuticos en fase I o II emplean a las oncoproteínas E6 y/o E7, las cuales son poco conservadas entre VPHs (Tabla 5).

También encontramos que α-Galcer es un adyuvante prometedor en inmunoterapias contra las infecciones relacionadas con el VPH o en la mejora de las vacunas contra el VPH, ya que promueve una respuesta antitumoral por NK, así como una respuesta E1-especifica de linfocitos T CD8+.

Cualquiera de estas terapias inmunológicas tendría como objetivo promover una respuesta inmunológica mediada por linfocitos T CD8+ capaz de eliminar células que estén expresando proteínas virales a través de la molécula MHC-I. La expresión de estas proteínas virales podría suscitarse tanto en etapas tempranas de la infección como en canceres *in situ*. Cabe resaltar que adyuvantes como el α-GalCer promoverían adicionalmente un efecto anti-tumoral mediado por linfocitos NK, lo que indica que los efectos profilácticos y terapéuticos de la inmunización de E1$_{202\text{-}654}$ + α-GalCer implican tanto una respuesta inmunológica adaptativa como innata, que actuando conjuntamente podría contribuir a una respuesta antitumoral más fuerte.

De esta manera, este estudio provee datos relevantes referentes al diseño de nuevos tratamientos para la eliminación de lesiones tanto de bajo grado como de alto grado [24] asociadas a diferentes tipos de VPH, mientras que las moléculas de MHC de clase I todavía presentan antígenos E1.

CONCLUSIONES

- La vacunación de E1$_{202\text{-}654}$ + α-GalCer genera una respuesta de linfocitos T CD8+/E1 antígeno especifica.
- La vacunación de E1$_{202\text{-}654}$ + α-GalCer promueve una respuesta de linfocitos T CD8+ E1-específico, que es capaz de eliminar células tumorales que expresan antígenos de E1, tanto de manera profiláctica como terapéutica.

- La inoculación de α-GalCer es capaz de promover una fuerte respuesta antitumoral mediada por NK.
- Linfocitos T CD8+ E1 antígeno-especifico (HPV18), tiene una actividad citotóxica contra antígenos de E1 de HPV-53, 33, 16, 31 y 11.

PERSPECTIVAS

- Caracterización de la respuesta de memoria por linfocitos T CD8+
- Caracterización de citocinas pro-inflamatorias y así como de citocinas involucradas en el establecimiento de fenotipos de memoria.
- Caracterización de linfocitos intra tumorales (Tregs, NK, CD8+, CD4+ y NKT).
- Caracterización de los péptidos más inmunógenos de E1 mediante ensayos funcionales.

Bibliografía

[1] Ferlay J, Soerjomataram I, Dikshit R, Eser S, Mathers C, Rebelo M, et al. Cancer incidence and mortality worldwide: sources, methods and major patterns in GLOBOCAN 2012. Int J Cancer. 2015;136:E359-86.
[2] zur Hausen H. Papillomaviruses and cancer: from basic studies to clinical application. Nat Rev Cancer. 2002;2:342-50.
[3] Turyk ME, Golub TR, Wood NB, Hawkins JL, Wilbanks GD. Growth and characterization of epithelial cells from normal human uterine ectocervix and endocervix. In Vitro Cell Dev Biol. 1989;25:544-56.
[4] Eifel L. Atlas of Clinical Oncology. 2001 ed. Hamilton London2001.
[5] Pudney J, Quayle AJ, Anderson DJ. Immunological microenvironments in the human vagina and cervix: mediators of cellular immunity are concentrated in the cervical transformation zone. Biol Reprod. 2005;73:1253-63.
[6] Harden ME, Munger K. Human papillomavirus molecular biology. Mutat Res Rev Mutat Res. 2017;772:3-12.
[7] Doorbar J, Quint W, Banks L, Bravo IG, Stoler M, Broker TR, et al. The biology and life-cycle of human papillomaviruses. Vaccine. 2012;30 Suppl 5:F55-70.
[8] Graham SV. Keratinocyte Differentiation-Dependent Human Papillomavirus Gene Regulation. Viruses. 2017;9.
[9] Doorbar J. Papillomavirus life cycle organization and biomarker selection. Dis Markers. 2007;23:297-313.
[10] Amador-Molina A, Gonzalez-Montoya JL, Garcia-Carranca A, Mohar A, Lizano M. Intratypic changes of the E1 gene and the long control region affect ori function of human papillomavirus type 18 variants. J Gen Virol. 2013;94:393-402.
[11] Arbyn M, Tommasino M, Depuydt C, Dillner J. Are 20 human papillomavirus types causing cervical cancer? J Pathol. 2014;234:431-5.

[12] Clifford GM, Smith JS, Plummer M, Munoz N, Franceschi S. Human papillomavirus types in invasive cervical cancer worldwide: a meta-analysis. Br J Cancer. 2003;88:63-73.

[13] Clifford GM, Smith JS, Aguado T, Franceschi S. Comparison of HPV type distribution in high-grade cervical lesions and cervical cancer: a meta-analysis. Br J Cancer. 2003;89:101-5.

[14] Raff AB, Woodham AW, Raff LM, Skeate JG, Yan L, Da Silva DM, et al. The evolving field of human papillomavirus receptor research: a review of binding and entry. J Virol. 2013;87:6062-72.

[15] Koonin EV. A common set of conserved motifs in a vast variety of putative nucleic acid-dependent ATPases including MCM proteins involved in the initiation of eukaryotic DNA replication. Nucleic Acids Res. 1993;21:2541-7.

[16] Fradet-Turcotte A, Moody C, Laimins LA, Archambault J. Nuclear export of human papillomavirus type 31 E1 is regulated by Cdk2 phosphorylation and required for viral genome maintenance. J Virol. 2010;84:11747-60.

[17] Bergvall M, Melendy T, Archambault J. The E1 proteins. Virology. 2013;445:35-56.

[18] Moody CA, Fradet-Turcotte A, Archambault J, Laimins LA. Human papillomaviruses activate caspases upon epithelial differentiation to induce viral genome amplification. Proc Natl Acad Sci U S A. 2007;104:19541-6.

[19] D'Abramo CM, Archambault J. Small molecule inhibitors of human papillomavirus protein - protein interactions. Open Virol J. 2011;5:80-95.

[20] Chiang CM, Ustav M, Stenlund A, Ho TF, Broker TR, Chow LT. Viral E1 and E2 proteins support replication of homologous and heterologous papillomaviral origins. Proc Natl Acad Sci U S A. 1992;89:5799-803.

[21] Wang J, Sampath A, Raychaudhuri P, Bagchi S. Both Rb and E7 are regulated by the ubiquitin proteasome pathway in HPV-containing cervical tumor cells. Oncogene. 2001;20:4740-9.

[22] Doorbar J. The E4 protein; structure, function and patterns of expression. Virology. 2013;445:80-98.

[23] Romanczuk H, Howley PM. Disruption of either the E1 or the E2 regulatory gene of human papillomavirus type 16 increases viral immortalization capacity. Proc Natl Acad Sci U S A. 1992;89:3159-63.

[24] Baedyananda F, Chaiwongkot A, Bhattarakosol P. Elevated HPV16 E1 Expression Is Associated with Cervical Cancer Progression. Intervirology. 2017;60:171-80.

[25] Woodman CB, Collins SI, Young LS. The natural history of cervical HPV infection: unresolved issues. Nat Rev Cancer. 2007;7:11-22.

[26] Hu Z, Zhu D, Wang W, Li W, Jia W, Zeng X, et al. Genome-wide profiling of HPV integration in cervical cancer identifies clustered genomic hot spots and a potential microhomology-mediated integration mechanism. Nat Genet. 2015;47:158-63.

[27] Sano D, Oridate N. The molecular mechanism of human papillomavirus-induced carcinogenesis in head and neck squamous cell carcinoma. Int J Clin Oncol. 2016;21:819-26.

[28] Stanley MA, Pett MR, Coleman N. HPV: from infection to cancer. Biochem Soc Trans. 2007;35:1456-60.

[29] Sterling JC, Skepper JN, Stanley MA. Immunoelectron microscopical localization of human papillomavirus type 16 L1 and E4 proteins in cervical keratinocytes cultured in vivo. J Invest Dermatol. 1993;100:154-8.

[30] Stanley MA. Replication of human papillomaviruses in cell culture. Antiviral Res. 1994;24:1-15.

[31] Maglennon GA, McIntosh P, Doorbar J. Persistence of viral DNA in the epithelial basal layer suggests a model for papillomavirus latency following immune regression. Virology. 2011;414:153-63.

[32] Gravitt PE. Evidence and impact of human papillomavirus latency. Open Virol J. 2012;6:198-203.

[33] Nestle FO, Di Meglio P, Qin JZ, Nickoloff BJ. Skin immune sentinels in health and disease. Nat Rev Immunol. 2009;9:679-91.

[34] Black AP, Ardern-Jones MR, Kasprowicz V, Bowness P, Jones L, Bailey AS, et al. Human keratinocyte induction of rapid effector function in antigen-specific memory CD4+ and CD8+ T cells. Eur J Immunol. 2007;37:1485-93.

[35] Nasu K, Narahara H. Pattern recognition via the toll-like receptor system in the human female genital tract. Mediators Inflamm. 2010;2010:976024.

[36] Takeda K, Kaisho T, Akira S. Toll-like receptors. Annu Rev Immunol. 2003;21:335-76.

[37] Sanghavi SK, Reinhart TA. Increased expression of TLR3 in lymph nodes during simian immunodeficiency virus infection: implications for inflammation and immunodeficiency. J Immunol. 2005;175:5314-23.

[38] Yang K, Puel A, Zhang S, Eidenschenk C, Ku CL, Casrouge A, et al. Human TLR-7-, -8-, and -9-mediated induction of IFN-alpha/beta and -lambda Is IRAK-4 dependent and redundant for protective immunity to viruses. Immunity. 2005;23:465-78.

[39] Lebre MC, van der Aar AM, van Baarsen L, van Capel TM, Schuitemaker JH, Kapsenberg ML, et al. Human keratinocytes express functional Toll-like receptor 3, 4, 5, and 9. J Invest Dermatol. 2007;127:331-41.

[40] Miller LS, Modlin RL. Human keratinocyte Toll-like receptors promote distinct immune responses. J Invest Dermatol. 2007;127:262-3.

[41] Um SJ, Rhyu JW, Kim EJ, Jeon KC, Hwang ES, Park JS. Abrogation of IRF-1 response by high-risk HPV E7 protein in vivo. Cancer Lett. 2002;179:205-12.

[42] Li S, Labrecque S, Gauzzi MC, Cuddihy AR, Wong AH, Pellegrini S, et al. The human papilloma virus (HPV)-18 E6 oncoprotein physically associates with Tyk2 and impairs Jak-STAT activation by interferon-alpha. Oncogene. 1999;18:5727-37.

[43] Amador-Molina A, Hernandez-Valencia JF, Lamoyi E, Contreras-Paredes A, Lizano M. Role of innate immunity against human papillomavirus (HPV) infections and effect of adjuvants in promoting specific immune response. Viruses. 2013;5:2624-42.

[44] Ashrafi GH, Brown DR, Fife KH, Campo MS. Down-regulation of MHC class I is a property common to papillomavirus E5 proteins. Virus Res. 2006;120:208-11.

[45] Hou F, Ma D, Cui B. Treg cells in different forms of uterine cancer. Clin Chim Acta. 2013;415:337-40.

[46] Huang L, Baban B, Johnson BA, 3rd, Mellor AL. Dendritic cells, indoleamine 2,3 dioxygenase and acquired immune privilege. Int Rev Immunol. 2010;29:133-55.

[47] Munn DH, Sharma MD, Hou D, Baban B, Lee JR, Antonia SJ, et al. Expression of indoleamine 2,3-dioxygenase by plasmacytoid dendritic cells in tumor-draining lymph nodes. J Clin Invest. 2004;114:280-90.

[48] Textor S, Durst M, Jansen L, Accardi R, Tommasino M, Trunk MJ, et al. Activating NK cell receptor ligands are differentially expressed during progression to cervical cancer. Int J Cancer. 2008;123:2343-53.

[49] Vantourout P, Hayday A. Six-of-the-best: unique contributions of gammadelta T cells to immunology. Nat Rev Immunol. 2013;13:88-100.

[50] Silva-Santos B, Serre K, Norell H. gammadelta T cells in cancer. Nat Rev Immunol. 2015;15:683-91.

[51] Van Hede D, Polese B, Humblet C, Wilharm A, Renoux V, Dortu E, et al. Human papillomavirus oncoproteins induce a reorganization of epithelial-associated gammadelta T cells promoting tumor formation. Proc Natl Acad Sci U S A. 2017;114:E9056-E65.

[52] Pufnock JS, Cigal M, Rolczynski LS, Andersen-Nissen E, Wolfl M, McElrath MJ, et al. Priming CD8+ T cells with dendritic cells matured using TLR4 and TLR7/8 ligands together enhances generation of CD8+ T cells retaining CD28. Blood. 2011;117:6542-51.

[53] Hayakawa Y, Godfrey DI, Smyth MJ. Alpha-galactosylceramide: potential immunomodulatory activity and future application. Curr Med Chem. 2004;11:241-52.

[54] Godfrey DI, Stankovic S, Baxter AG. Raising the NKT cell family. Nat Immunol. 2010;11:197-206.

[55] Godfrey DI, Hammond KJ, Poulton LD, Smyth MJ, Baxter AG. NKT cells: facts, functions and fallacies. Immunol Today. 2000;21:573-83.

[56] Juno JA, Keynan Y, Fowke KR. Invariant NKT cells: regulation and function during viral infection. PLoS Pathog. 2012;8:e1002838.

[57] Van Kaer L, Parekh VV, Wu L. Invariant natural killer T cells: bridging innate and adaptive immunity. Cell Tissue Res. 2011;343:43-55.

[58] Liu K, Idoyaga J, Charalambous A, Fujii S, Bonito A, Mordoh J, et al. Innate NKT lymphocytes confer superior adaptive immunity via tumor-capturing dendritic cells. J Exp Med. 2005;202:1507-16.

[59] Adotevi O, Vingert B, Freyburger L, Shrikant P, Lone YC, Quintin-Colonna F, et al. B subunit of Shiga toxin-based vaccines synergize with alpha-galactosylceramide to break tolerance against self antigen and elicit antiviral immunity. J Immunol. 2007;179:3371-9.

[60] Kogo H, Shimizu M, Negishi Y, Uchida E, Takahashi H. Suppression of murine tumour growth through CD8(+) cytotoxic T lymphocytes via activated DEC-205(+) dendritic cells by sequential administration of alpha-galactosylceramide in vivo. Immunology. 2017;151:324-39.

[61] Alan R. Shaw MBF. Clinical Immunology (Third Edition). ScienceDirect ed: ScienceDirect; 2008.

[62] Peng S, Song L, Knoff J, Wang JW, Chang YN, Hannaman D, et al. Control of HPV-associated tumors by innovative therapeutic HPV DNA vaccine in the absence of CD4+ T cells. Cell Biosci. 2014;4:11.

[63] Sharma C, Khan MA, Mohan T, Shrinet J, Latha N, Singh N. A synthetic chimeric peptide harboring human papillomavirus 16 cytotoxic T lymphocyte epitopes shows therapeutic potential in a murine model of cervical cancer. Immunol Res. 2014;58:132-8.

[64] Human papillomavirus vaccines: WHO position paper, October 2014-Recommendations. Vaccine. 2015;33:4383-4.

[65] clinicaltrials.gov. U.S. National Library of Medicine. NIH2018.

[66] Herrero R. Human papillomavirus (HPV) vaccines: limited cross-protection against additional HPV types. J Infect Dis. 2009;199:919-22.

[67] Moore RA, Santos EB, Nicholls PK, White KL, Anderson DM, Lloyd A, et al. Intraepithelial DNA immunisation with a plasmid encoding a codon optimised COPV E1 gene sequence, but not the wild-type gene sequence completely protects against mucosal challenge with infectious COPV in beagles. Virology. 2002;304:451-9.

[68] Remy-Ziller C, Germain C, Spindler A, Hoffmann C, Silvestre N, Rooke R, et al. Immunological characterization of a modified vaccinia virus Ankara vector expressing the human papillomavirus 16 E1 protein. Clin Vaccine Immunol. 2014;21:147-55.

[69] Ragonnaud E, Andersson AC, Mariya S, Pedersen AG, Burk RD, Folgori A, et al. Therapeutic Vaccine Against Primate Papillomavirus Infections of the Cervix. J Immunother. 2017;40:51-61.

[70] Wang Z, Liu JQ, Liu Z, Shen R, Zhang G, Xu J, et al. Tumor-derived IL-35 promotes tumor growth by enhancing myeloid cell accumulation and angiogenesis. J Immunol. 2013;190:2415-23.

[71] Miller JP, Egbulefu C, Prior JL, Zhou M, Achilefu S. Gradient-Based Algorithm for Determining Tumor Volumes in Small Animals Using Planar Fluorescence Imaging Platform. Tomography. 2016;2:17-25.

[72] Betts MR, Brenchley JM, Price DA, De Rosa SC, Douek DC, Roederer M, et al. Sensitive and viable identification of antigen-specific CD8+ T cells by a flow cytometric assay for degranulation. J Immunol Methods. 2003;281:65-78.

[73] Newell EW, Sigal N, Bendall SC, Nolan GP, Davis MM. Cytometry by time-of-flight shows combinatorial cytokine expression and virus-specific cell niches within a continuum of CD8+ T cell phenotypes. Immunity. 2012;36:142-52.

[74] Aktas E, Kucuksezer UC, Bilgic S, Erten G, Deniz G. Relationship between CD107a expression and cytotoxic activity. Cell Immunol. 2009;254:149-54.

[75] Chavez-Blanco A, De la Cruz-Hernandez E, Dominguez GI, Rodriguez-Cortez O, Alatorre B, Perez-Cardenas E, et al. Upregulation of NKG2D ligands and enhanced natural killer cell cytotoxicity by hydralazine and valproate. Int J Oncol. 2011;39:1491-9.

[76] Ito H, Ando T, Seishima M. Inhibition of iNOS activity enhances the anti-tumor effects of alpha-galactosylceramide in established murine cancer model. Oncotarget. 2015;6:41863-74.

[77] Chennamadhavuni D, Saavedra-Avila NA, Carreno LJ, Guberman-Pfeffer MJ, Arora P, Yongqing T, et al. Dual Modifications of alpha-Galactosylceramide Synergize to Promote Activation of Human Invariant Natural Killer T Cells and Stimulate Anti-tumor Immunity. Cell chemical biology. 2018;25:571-84 e8.

[78] Bassiri H, Das R, Guan P, Barrett DM, Brennan PJ, Banerjee PP, et al. iNKT cell cytotoxic responses control T-lymphoma growth in vitro and in vivo. Cancer Immunol Res. 2014;2:59-69.

[79] Dolen Y, Kreutz M, Gileadi U, Tel J, Vasaturo A, van Dinther EA, et al. Co-delivery of PLGA encapsulated invariant NKT cell agonist with antigenic protein induce strong T cell-mediated antitumor immune responses. Oncoimmunology. 2016;5:e1068493.

[80] Stewart TJ, Smyth MJ, Fernando GJ, Frazer IH, Leggatt GR. Inhibition of early tumor growth requires J alpha 18-positive (natural killer T) cells. Cancer Res. 2003;63:3058-60.

[81] Cerundolo V, Barral P, Batista FD. Synthetic iNKT cell-agonists as vaccine adjuvants--finding the balance. Curr Opin Immunol. 2010;22:417-24.

[82] Butterfield LH. Cancer vaccines. BMJ. 2015;350:h988.

[83] Jung AC, Guihard S, Krugell S, Ledrappier S, Brochot A, Dalstein V, et al. CD8-alpha T-cell infiltration in human papillomavirus-related oropharyngeal carcinoma correlates with improved patient prognosis. Int J Cancer. 2013;132:E26-36.

[84] Rapp M, Wiedemann GM, Sun JC. Memory responses of innate lymphocytes and parallels with T cells. Semin Immunopathol. 2018;40:343-55.

[85] Della Chiesa M, Marcenaro E, Sivori S, Carlomagno S, Pesce S, Moretta A. Human NK cell response to pathogens. Semin Immunol. 2014;26:152-60.

[86] Zaiss DM, Boog CJ, van Eden W, Sijts AJ. Considerations in the design of vaccines that induce CD8 T cell mediated immunity. Vaccine. 2010;28:7716-22.

[87] Medicine. USNLo. https://clinicaltrials.gov/. In: Medicine. USNLo, editor. https://clinicaltrials.gov/2019.

ANEXOS

Número total de artículos publicados, en prensa y enviados, generados durante el desarrollo del proyecto de investigación y que se incluyen en el presente trabajo de tesis.

1. Amador-Molina Alfredo, Cesar Trejo-Moreno, Damaris Romero-Rodríguez, Isabel Sada-Ovalle, Enrique Pérez-Cárdenas, Edmundo Lamoyi, José Moreno and Marcela Lizano Vaccination with Human Papillomavirus-18 E1 protein plus α-Galactosyl-ceramide induces CD8+ cytotoxic response and impairs the growth of E1-expressing tumors. Vaccine. 2018.

2. Amador-Molina Alfredo, Amador-Molina Juan C, Arciniega Juan L. and Lizano Marcela. Cross-reactivity of HPV18 E1-antigen specific CD8+ T cells against cells expressing E1 from diverse HPV types. Viral Immunology. 2019 **"ENVIADO".**

3. Amador-Molina A, Hernandez-Valencia JF, Lamoyi E, Contreras-Paredes A, Lizano M. Role of innate immunity against human papillomavirus (HPV) infections and effect of adjuvants in promoting specific immune response. Viruses. 2013;5:2624-42.

4. Amador-Molina A, Gonzalez-Montoya JL, Garcia-Carranca A, Mohar A, Lizano M. Intratypic changes of the E1 gene and the long control region affect ori function of human papillomavirus type 18 variants. The Journal of general virology. 2013; 94:393-402.

Vaccination with human papillomavirus-18 E1 protein plus α-galactosyl-ceramide induces CD8+ cytotoxic response and impairs the growth of E1-expressing tumors

Alfredo Amador-Molina [a], Cesar Trejo-Moreno [a], Damaris Romero-Rodríguez [b], Isabel Sada-Ovalle [b], Enrique Pérez-Cárdenas [a], Edmundo Lamoyi [c], José Moreno [d], Marcela Lizano [a,e,∗]

[a] Unidad de Investigación Biomédica en Cáncer, Instituto Nacional de Cancerología, Av. San Fernando No. 22, Col. Sección XVI, Tlalpan, Ciudad de México 14080, Mexico
[b] Laboratorio de Inmunología Integrativa, Instituto Nacional de Enfermedades Respiratorias Ismael Cosío Villegas, Calzada de Tlalpan 4502, Tlalpan, Ciudad de México 14080, Mexico
[c] Departamento de Inmunología, Instituto de Investigaciones Biomédicas, Universidad Nacional Autónoma de México, Ciudad Universitaria, Ciudad de México 04510, Mexico
[d] Dirección de Investigación, Hospital Juárez de México, Ciudad de México 07760, Mexico
[e] Departamento de Medicina Genómica y Toxicología Ambiental, Instituto de Investigaciones Biomédicas, Universidad Nacional Autónoma de México, Ciudad Universitaria, Ciudad de México 04510, Mexico

ARTICLE INFO

ABSTRACT

CD8+ T cell-mediated immune response plays a major role in the clearance of virus-infected cells, including human papillomavirus (HPV). The effective treatment of women with normal cytology but persistent high risk-HPV infection or with low-grade intraepithelial lesions could take advantage of novel strategies based on vaccination with viral immunological targets with a wide spectrum of cross-protection. The helicase E1, expressed early during viral replication in HPV infection, is among the most conserved papillomavirus proteins, which makes it a good vaccine candidate. In the present study, we examined E1-specific CD8+ T cell and NK immune responses in a mouse model with α-galactosylceramide (α-GalCer) as an adjuvant. We found that mice immunized with E1 combined with α-GalCer elicited an E1-specific CD8+ T and NK cell cytotoxic responses, which correlated with growth inhibition of grafted melanoma B16-F0 cells expressing E1, both in prophylactic and therapeutic protocols.

1. Introduction

Cervical cancer is the fourth most frequent cancer in women worldwide [1] with high-risk human papillomavirus (HPV) as its etiologic agent [2]. According to their oncogenic potential, HPVs are classified as high- (HR-HPV) or low-risk (LR-HPV), being HPV16 and HPV18 the most common viral types found in cervical cancer patients [4,5]. Persistent infection with high-risk HPV can lead to cervical intraepithelial neoplasia (CIN) that, without treatment, could progress to *in situ* carcinoma [3].

During an HPV infection, viral genes are differentially and sequentially expressed along the various layers of the cervical epithelium [6]. HPV proteins E1 and E2 regulate viral replication [7,8], of which the E1 helicase is necessary for DNA double-strand separation during viral replication [9] and is the most conserved among early expressed HPV proteins [10,11].

Malignant transformation is not a common occurrence of an HPV infection, as only a minor number of cervical lesions infected with HR-HPV types evolve into cervical cancer [12]. However, for unclear reasons the HPV genome, in some cases, integrates randomly into the host DNA leading to cervical transformation, which is mainly due to overexpression of the major HPV viral oncoproteins, E6 and E7 [13,14].

Although the adaptive immune system plays an important role in the elimination of HPV infected cells [2,15], an estimated 15% of women infected with HR-HPV fail to develop an effective response against the virus due to viral immune evasion mechanisms [16], leading to HPV persistent infections [15]. HPV prophylactic vaccines activate the adaptive immune system and induce neutralizing antibodies that prevent infections by viral types covered by the vaccines but cannot eliminate established HPV infections. On the other hand, therapeutic vaccine candidates must be directed at inducing cell-mediated adaptive immune responses through the induction of HPV-specific CD8+ cytotoxic T lymphocytes (CTL) [17,18].

∗ Corresponding author at: Unidad de Investigación Biomédica en Cáncer, Instituto Nacional de Cancerología, Av. San Fernando No. 22, Col. Sección XVI, Tlalpan, Ciudad de México 14080, Mexico.
E-mail address: lizano@unam.mx (M. Lizano).

An ideal therapeutic vaccine candidate should be able to induce cross-reactivity among different HPV types with activation of tumor-specific CD8+ cytotoxic T cells, as well as CD4 + helper T cells [19,20]. A number of lines of evidence have shown that HPV-specific T cells and tumor infiltration by CD8+ T cells are associated with a better outcome in patients [21,22] and tumor regression in experimental models [23]. Although the most common HPV antigens employed for vaccination have been the major oncoproteins E6 and E7, which have shown some benefit against HPV and cervical cancer [24], these oncoproteins differ substantially among HPV types, affecting their potential as wide spectrum HPV therapeutic immunogens. On the other hand, as the HPV-E1 sequence is highly conserved among all known HPV types [10], it could constitute a good target for a universal HPV vaccine.

E1 protein expressed in a plasmid encoding codon-optimized canine oral papillomavirus (COPV) led to therapeutic immunization of COPV-infected Beagle dogs [25,26], which was better than that achieved with plasmids encoding E2 or E7 COPV. Moreover, E1 and E2 from cottontail rabbit papillomavirus (CRPV) induced strong immunity against infection with CRPV particles in rabbits [27,28]. In both models, the adaptive immune system cleared virally-induced papillomas. Recently, it was found that immunization of macaques with E1/E2 sequences in an adenoviral vector induced antigen-specific T cell immunity against established primate papillomavirus (MfPV) infections [29]. Moreover, immunization of mice with HPV-16 E1 in a vaccinia vector induced specific CTL immune responses [30].

Protein antigens contain a variable number of T-cell-epitopes capable of binding to major histocompatibility complex class I and class II molecules (MHC-I and MHC-II) and are recognized by CD8+ CTLs or CD4 + T cells, respectively. However, purified soluble proteins generally fail to induce robust CTL responses [31] unless they are administered together with adjuvants of different chemical natures, which activate innate immunity and inflammation, leading to the induction of costimulatory signals which are critical for antigen-presenting cell (APC) [32] induction of T cell activation. In addition to being an adjuvant, α-galactosylceramide (α-GalCer) that increases the numbers of antigen-specific CD8+ T cells when co-administered with antigens [33,34], stimulates an NKT cell-dependent cell immune cascade involving dendritic cells, NK and T cells [35]. Moreover, α-GalCer appears to promote a better CTL immune response than other adjuvants, such as incomplete Freund's adjuvant, IFN-α, poly (I:C) or TLR-9 agonists [33].

Its high homology among different HPV types makes the E1 protein a good candidate for a therapeutic vaccine against most HPV types in early HR-HPV infections and low-grade cervical intraepithelial lesions, where the viral genome is replicating and E1 expression is at its highest. As yet, it is not known whether antigen-specific CD8+ T cells are capable to eliminate HPV E1-expressing cells in-vivo. Here, we used a combination of HPV-E1 with the strong adjuvant α-GalCer to induce specific CD8+ T cell immune responses against HPV18-E1 expressing grafted cells. This combination induced E1-specific CD8+ T cells in mice, which correlated with a decrease in the growth of E1-expressing cells both in prophylactic and therapeutic approaches.

2. Methods

2.1. Mice and cell line

Female C57BL/6 mice (C57BL/6NCrl, originally from Charles River Laboratories International, Inc.) were purchased from Instituto Nacional de Ciencias Médicas y Nutrición Salvador Zubirán, México. All animals were kept in a pathogen-free environment and fed ad lib. The Ethics Committees of the Universidad Nacional

Autónoma de México and of the Instituto Nacional de Cancerología, México, approved the procedures for care and use of animals. All applicable institutional regulations concerning the ethical use of animals were followed accordingly. The B16-F0 mouse melanoma-derived cell line (ATCC® CRL-6322™) was grown in Dulbecco's modified Eagle's medium F12 supplemented with 10% FBS.

2.2. E1-codon optimization and plasmid construction

The HPV18-E1 reference gene sequence was codon-optimized to improve its expression in mouse cells. Codon optimization was made by GenScript (New Jersey). The codon-optimized sequence was used to amplify the E1-FL full-length (E1-FL) sequence and three E1 fragments (E1-N-terminal, E1-DNA-binding domain, and E1$_{244-550}$) (Supplementary Fig. 1A). The E1$_{244-550}$ region contains part of the DNA binding domain and C-terminal domain. PCR products were amplified with the primers shown in Supplementary Table 1 and were cloned into pcDNA 3.3 Topo plasmid (Invitrogen) with a Kozak sequence and human influenza hemagglutinin (HA) tag.

2.3. MHCI peptide prediction

To determine whether the E1 protein and the E1$_{202-654}$ region contained enough peptides capable of binding mouse H2-D^b, H2-K^b and human HLA-A2 we took advantage of the RANKPEP software (http://imed.med.ucm.es/Tools/rankpep.html) [36]. Based on this software, with 2% threshold and with a percentile score (% OPT) $\geq$ 15%, we found 120 peptides capable of binding to H2-D^b and H2-K^b in E1 of which 62 were within E1$_{244-550}$ (Supplementary Table 2).

2.4. Cell cultures, transfection, and cell sorting

GFP and pE1-FL or plasmids with truncated E1 sequences (E1-N-Terminal, E1-DNA-binding domain, and E1$_{244-550}$) were co-transfected 24 h after the beginning of culture by means of Lipofectamine 2000 reagent (Invitrogen) into B16-F0 cells grown in supplemented culture medium in 60 mm^2 wells (6 X10^5 cells/well). Transfected cells were analyzed by flow cytometry for the expression of GFP and E1. As cells with high expression of GFP (GFP^{hi}) also had high expression of E1 (Supplementary Fig. 2A). these cells were isolated by fluorescence-activated cell sorting in a BD FACSJazz cell sorter to obtain an enriched population of 96% GFP^{hi} cells (Supplementary Fig. 2B). As pE1$_{244-550}$ yielded higher and more consistent expression than the other E1-expressing plasmids, this E1-truncated plasmid was used for the experiments described below.

2.5. Western blot analysis

Extracts from sorted B16-F0 cells expressing E1$_{244-550}$ (B16-F0/E1$_{244-550}$) and from cells transfected with pcDNA3.1/His empty vector were run on 10% SDS-PAGE and transferred onto nitrocellulose membranes, after which they were incubated with rabbit polyclonal anti-HA antibody (Santa Cruz Biotechnology,sc-805), followed by horseradish peroxidase-labeled goat anti-rabbit antibody (Santa Cruz Biotechnology,sc-2030). β-actin was used as loading control and it was detected with mouse monoclonal antibody sc-47778 (Santa Cruz Biotechnology) followed by mouse IgG kappa binding protein conjugated to horseradish peroxidase (Santa Cruz Biotechnology, sc-516102). E1 and β-actin were visualized with enhanced chemiluminescence [37] (Amersham). Western blots were performed three times to assure reproducibility.

2.6. Expression of $E1_{244-550}$ in tumors

To evaluate $E1_{244-550}$ expression *in vivo* (in tumor cells), 7.5×10^5 B16-F0/$E1_{244-550}$ cells with a viability of $\geq 97\%$ (trypan blue) were injected subcutaneously (s.c.) in the left flank of untreated C57BL/6 mice. Tumors were excised at different times from euthanized mice in accordance with the Animal Research Advisory Committee (ARAC)-NIH regulations. $E1_{244-550}$ was analyzed in Western blots of tumor lysates as described above.

2.7. Recombinant $E1_{202-654}$ protein

A bacterial protein expression system was used to produce and purify the E1 protein 202 to 654 ($E1_{202-654}$) that corresponds to the DNA-binding (DBD) and carboxyl-terminal domains (Supplementary Fig. 1A) plus a 6x histidine tag. This fragment was obtained and purified by GenScript and dissolved in PBS and 0.5 M L-arginine, pH 7.4, and loaded onto SDS-PAGE to corroborate its molecular weight and integrity (Supplementary Fig. 1B).

2.8. Prophylactic and therapeutic immunization protocols

For the prophylactic protocol, seven to eight-week-old female C57BL/6 mice were distributed into four groups of six mice each. Group P1 ($E1_{202-654}$): immunized subcutaneously (s.c.) with 4 μg recombinant $E1_{202-654}$; Group P2 ($E1_{202-654}$ + α-GalCer) immunized s.c. with 4 μg recombinant $E1_{202-654}$ plus 3 μg α-GalCer; Group P3 (α-GalCer): inoculated s.c. with 3 μg α-GalCer; and Group P4 (control): inoculated s.c with 70 μl PBS. Fourteen days later, a second identical dose was administered s.c. to mice of each group. The dose for $E1_{202-654}$ immunization was chosen because it elicited the highest number of CTL as determined by a dose-response curve, with the optimal timing for boosting also determined by measuring cytotoxic CTLs at different times after immunization (not shown). The dose of α-GalCer administered s.c. has been reported by others [33]. To examine the effect of the different treatments on the growth of B16-F0/$E1_{244-550}$ cells, immunized C57BL/6 mice were injected s.c. five days later in the left flank with 1.8×10^6 B16-F0/$E1_{244-550}$ cells ($\geq 97\%$ viability by trypan blue). In non-immunized mice, tumor masses were detectable 3 to 5 days after inoculation. Tumor growth was measured every three days with a digital caliper and the estimated volume was determined with the equation; Volume = (width$^2 \times$ length)/2 as described [38–41]. Mice were euthanized when the tumor mass size reached 20 mm in any one dimension, or up to a maximum of 21 days after inoculation.

For the therapeutic protocol, 24 seven to eight-week-old female C57BL/6 mice were inoculated with 1.8×10^6 B16-F0/$E1_{244-550}$ cells (viability of $\geq 97\%$ by trypan blue). Five days after cell inoculation, when all mice had palpable tumors, they were distributed into four groups of six mice each, and inoculated with the same antigen and adjuvant doses as those of the prophylactic protocol: groups were T1 ($E1_{202-654}$), T2 ($E1_{202-654}$ + αGalCer), T3 (αGalCer) and T4 (PBS). Fourteen days later, a second identical dose was administered s.c. to each group. Tumor growth was measured every three days and the estimated volume was determined as described above. Again, mice were euthanized when the tumor mass size reached 20 mm in any one dimension, or up to a maximum of 23 days after inoculation.

2.9. Preparation of splenocytes, NK and CD8+ T cell isolation

Spleens were excised, placed in PBS, sliced into small fragments, settled onto 70 μm mesh nylon cell strainers (Corning Life Sciences) and pressed through with a syringe plunger onto 50 mL conical tubes. Cells were washed with PBS and centrifuged at $500 \times g$ for 5 min. Cell pellets were incubated with lysing solution (Becton Dickinson PharmLyse™) for 2 min at 37 °C. The cell preparation was washed twice and centrifuged ($500 \times g$ /5 min). CD8+ T cells were isolated with CD8α$^+$ T Cell Isolation Kit II (Miltenyi Biotec), and NK cells were isolated with NK Cell Isolation Kit (Miltenyi Biotec), according to the manufacturers' protocols from viable splenocytes counted in a TC20 automated cell counter (BIORAD). Purity of CD8+ T cells was assessed by staining with CD8+/PE, CD3+/Alexa Fluor488 and with CD3+/Alexa Fluor488, NK 1.1/Alexa Fluor647 for NK cells (purity of 94% and 87%, respectively)

2.10. Ex-vivo cytotoxic activity assay for CD8+ T-cell or NK cell cytotoxicity

Purified CD8+ T and NK cells with a viability $\geq 90\%$ were used for the cytotoxic activity assays. Thus, 4×10^5 CD8+ T cells or 1×10^5 NK cells from each individual mouse of the four groups were co-cultured with B16-F0/$E1_{244-550}$ target cells (4×10^4 and 1×10^5, respectively). In both systems, fluorophore-labelled antibodies AF488-anti-CD107a (1D4B) and AF488-anti-CD107b (M3/84) directed at the granular membrane proteins CD107a and CD107b (0.25 μg/10^6 cells) or isotype controls were added to the cultures at the beginning of the assay. As it is a time-course curve, the exposure of CD107a/b molecules on cell membrane is indicative of living cells with cytotoxic activity. NK and CD8+ T cells from unimmunized mice stimulated with phorbol-12-myristate-13-acetate (PMA, 300 ng/ml, Sigma Chemical Company, St. Lous MO) and ionomycin (1,500 ng/ml, Sigma) were used as positive effector controls. In all cases, cell cultures were incubated for up to 5 h, and monensin 5 mg/ml (BD Biosciences) was added for the final 3 h of culture [42]. Cells were fixed with 1% paraformaldehyde and
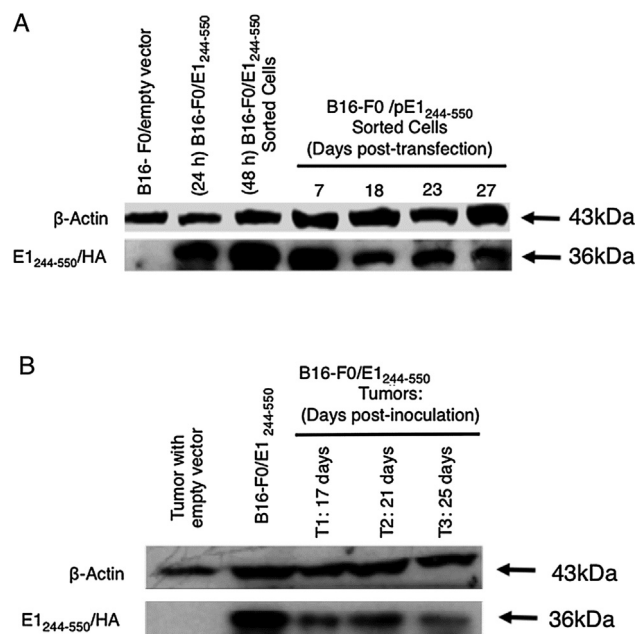
Fig. 1. Expression of codon-optimized $E1_{244-550}$. (A) Sorted B16-F0 cells expressing $E1_{244-550}$ were analyzed at different times post-transfection (7, 18, 23 and 27 days) by western blot using an anti-HA antibody. An extract from B16-F0 cells transfected with the empty vector was used as negative control. Extracts from un-sorted B16-F0 cells transfected with $pE1_{244-550}$ (24 h post-transfection) and sorted B16-F0 cells transfected with $pE1_{244-550}$ (48 h post-transfection) were used as positive controls. (B) Detection of $E1_{244-550}$ in tumors originated from sorted B16-F0/$E1_{244-550}$ cells. Untreated mice were inoculated with sorted B16-F0/$E1_{244-550}$ cells and the expression of $E1_{244-550}$ was analyzed in tumor extracts collected at different times post-inoculation (17, 21 and 25 days). B16-F0-$pE1_{244-550}$ cell extracts collected at 24 h post-transfection were used as positive control. Extracts from a tumor originated from B16-F0/empty vector was used as negative control.

CD107a/b expression on NK1.1 + and CD8+ T cells was analyzed by flow cytometry (see below).

2.11. Flow cytometry

Flow cytometry was achieved with a FACSAria II flow cytometer (Becton Dickinson, Mountain View, CA) using FACS Diva software 8.0.1 and further analyzed with FlowJo software (version 10.2). Typically, 50,000 events were acquired for CD8+ T cell cytotoxic activity assays and 10,000 events for NK cytotoxic activity assays. Monoclonal antibodies used for the flow cytometry and lineage-specific panels were: PerCP-labelled anti-CD8a (53-6.7), Alexa Fluor 488®-labelled anti-CD3 (17A2), Alexa Fluor 488® (AF488)-labelled anti-CD107a (1D4B), Alexa Fluor 488® (AF488)-labelled anti-CD107b (M3/84), PerCP-labelled anti-CD62L (MEL-14), brilliant violet 421™-labelled anti-CD127 (A7R34) and Alexa Fluor® 647 (AF647)-labelled anti-NK1.1 (all from Biolegend). To test E1-transfection efficiency in B16F0 melanoma cells, Alexa Fluor 647® (AF647)-labelled anti-HA.11 (16B12) antibody (Biolegend) was used.

2.12. Statistical analysis

Statistical analysis was performed by one-way ANOVA and Tukey's multiple comparison tests (GraphPad Prism Software, Inc.). Error bars represent standard error of the mean (SEM) and P values of < 0.05 were considered as statistically significant.

3. Results

3.1. Expression of codon-optimized $E1_{244-550}$ in B16-F0 cell line and mouse tumors

To generate cell lines expressing HPV-E1, four different plasmids encoding codon-optimized E1-full-length and three E1 fragments (E1-N-Terminal, E1-DNA-binding domain, and $E1_{244-550}$) were transfected into B16-F0 cells. All of the plasmids yielded transient expression of E1 sequences and although a stable expression could not be achieved with any of them, the $E1_{244-550}$ sequence remained expressed *in vitro* up to 27 days post-transfection (Fig. 1A). As high GFP-expressing cells were also $E1_{244-550}$ high expressers, with a mean 96% GFP + cells were used as targets in our experiments (Supplementary Fig. 2B).

$E1_{244-550}$ protein expression was clearly identified in western blots of *in vivo* grown tumor lysates up to 25 days after inoculation of mice with 7.5x10^5 B16-F0/$E1_{244-550}$ cells (Fig. 1B).

Therefore, the presence of a number of potential peptide binders to mouse H2-D^b, H2-K^b (Supplementary Table 2) and the high expression of $E1_{244-550}$ in these cells make them potential immunological targets for antigen-specific CTLs.

3.2. Immunization with $E1_{202-654}$ + α-GalCer protects against B16-F0/$E1_{244-550}$ tumor challenge (prophylactic approach)

To determine whether antigen-specific immune response impairs tumor formation and growth, we examined the protective efficacy of immunization with $E1_{202-654}$ + α-GalCer in a mouse tumor model (Fig. 2A). Tumor growth was monitored daily in the four different groups of mice implanted with syngeneic B16-F0/$E1_{244-550}$ cells at day 17th (Fig. 3A, B, C, and D). As seen, mean tumor size was significantly smaller in the group immunized with $E1_{202-654}$ + α-GalCer (Fig. 3E), when compared with mice receiving PBS (control), α-GalCer alone or $E1_{202-654}$ alone (n = 6 each). Importantly, four out of six mice in the $E1_{202-654}$ + α-GalCer group did not show any tumor growth after 21 days. Of interest, mean tumor size in mice inoculated with α-GalCer alone was also significantly smaller than those inoculated with PBS (Fig. 3E).
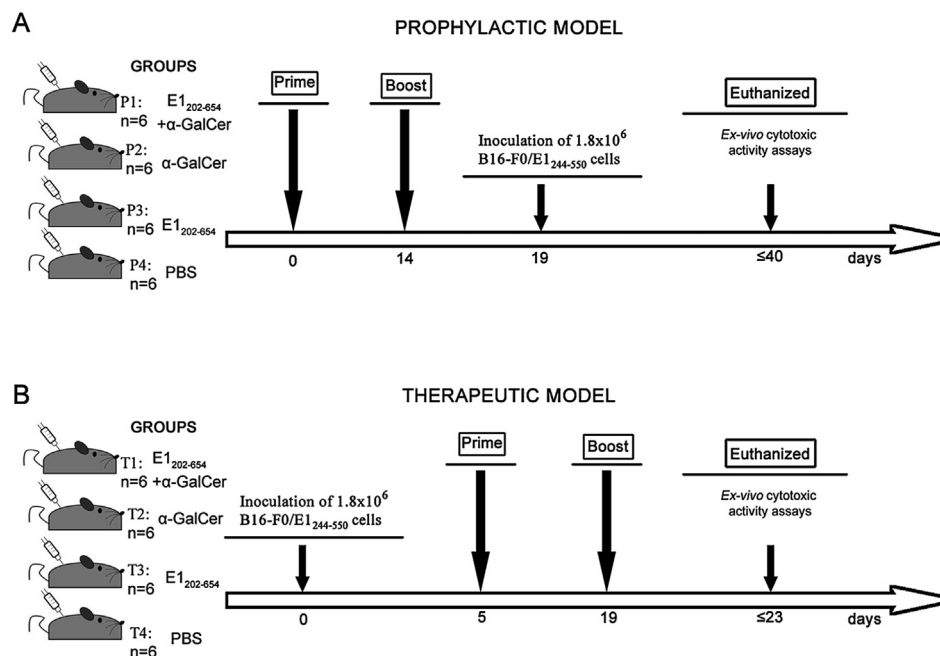
Fig. 2. Immunization protocol. (A) For the prophylactic immunization, six mice per group were used. They were inoculated and boosted at two-week after prime inoculation. Five days later, all mice were challenged with B16-F0/$E1_{244-550}$ cells. Mice were euthanized up to a maximum of 21 days after inoculation and spleens were removed to perform direct *ex-vivo* cytotoxic activity assays. (B) For the therapeutic immunization, twenty-four female C57BL/6 mice were inoculated with B16-F0/$E1_{244-550}$ cells. Five days after cell inoculation when all mice developed detectable tumors, they were distributed randomly into four groups of six mice each and inoculated as specified. Mice were euthanized up to a maximum of 23 days after inoculation and spleens were removed to perform direct *ex-vivo* cytotoxic activity assays.

3.3. $E1_{202-654}$ + α-GalCer inhibits the growth of established B16-F0/$E1_{244-550}$ tumors (therapeutic approach)

To examine whether $E1_{202-654}$ + α-GalCer inoculation confers protection to animals with established tumors derived from cells expressing E1, four groups of mice were initially inoculated with syngeneic B16-F0/$E1_{244-550}$ cells, and after five days, when, all mice had developed detectable tumors, were immunized as described in Methods (Fig. 2B). Tumor growth was monitored daily until day 23 after implantation of B16-F0/$E1_{244-550}$ cells. As shown in Fig. 4B, vaccination with $E1_{202-654}$ + α-GalCer impairs tumor growth, when compared with the other treatments (Fig. 4A, C, and D). As before,
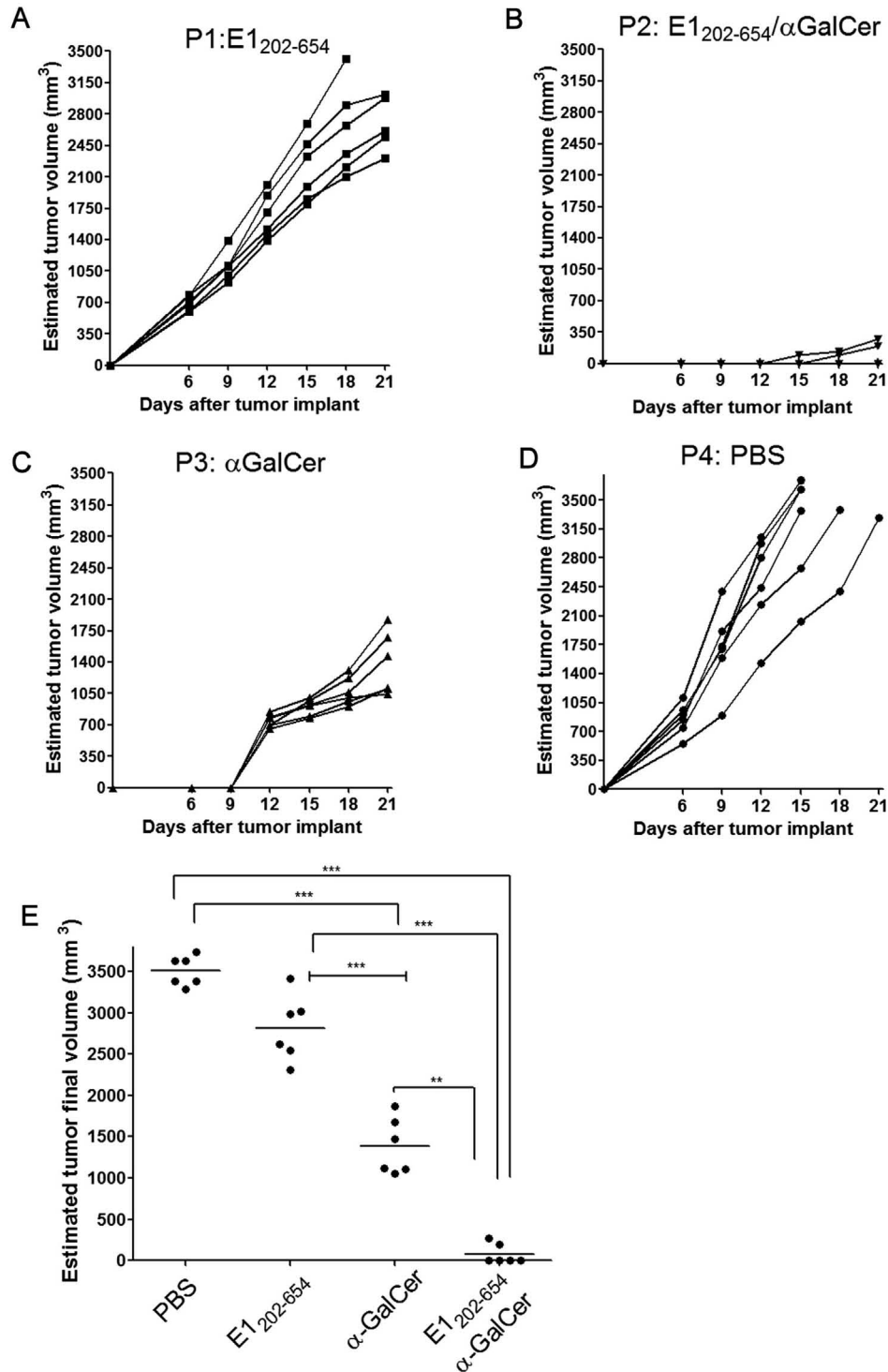
Fig. 3. Effect of prophylactic immunizations on tumor growth *in-vivo*. Each mouse group was inoculated with B16-F0/ $E1_{244-550}$ cells and tumor growth was monitored over time for (A) $E1_{202-654}$ (n = 6), (B) $E1_{202-654}$ + α-Galcer (n = 6), (C) α-GalCer (n = 6) and (D) PBS (n = 6) treatments. Tumor size was measured as described in "Methods" and its estimated volume was plotted over time. (E) Effect of immunizations on tumor growth. Once the mice were euthanized, the estimated final tumor size was determined as described in "Methods" and reported in mm³. Tumor size was plotted for each mouse and the mean is depicted for each group. The statistical significance with **p < 0.01 and ***p < 0.0001 (multiparametric one-way ANOVA and Tukey's Multiple Comparison Test).

the mean tumor size in mice inoculated with α-GalCer alone was significantly smaller (1937.6 mm^3) than that of PBS inoculated mice (3624 mm^3) (Fig. 4E). These results, indicate that immunization with $E1_{202-654}$ + α-GalCer is capable of reducing tumor mass when tumor growth has already started, and a role for α-GalCer alone can be seen, as mice of this group also had a reduced tumor size.

3.4. Immunization with $E1_{202-654}$ plus α-GalCer promotes antigen-specific CD8+ T cell cytotoxic response in both prophylactic and therapeutic protocols

As cytotoxic granule exocytosis leads to the expression of CD107a and CD107b on the surface of CD8+ T cells [42] their newly appearance on CD8+ T cells and NK cells are widely accepted as
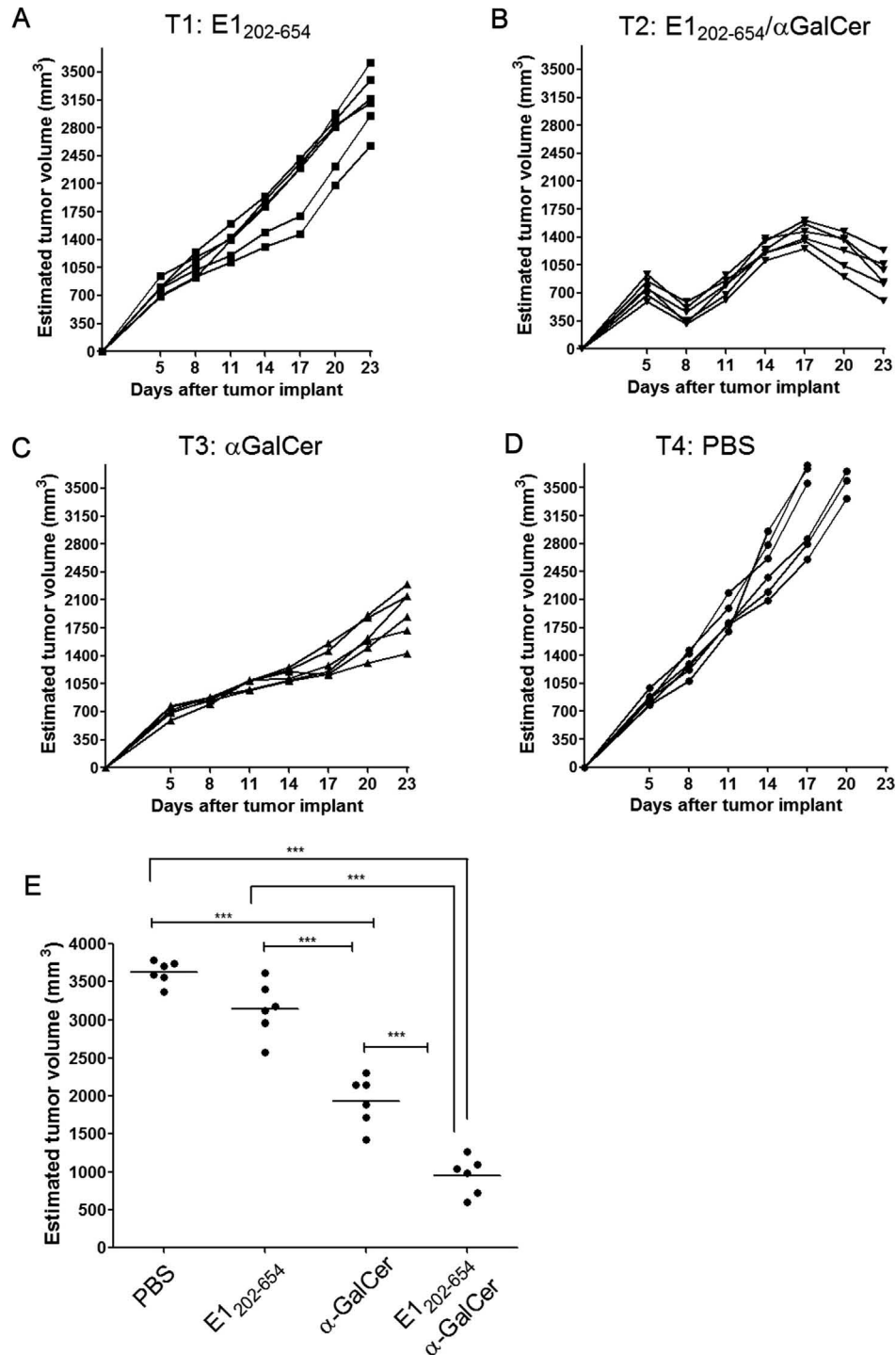
Fig. 4. Effect of therapeutic immunizations on tumor growth *in-vivo*. Each group was inoculated with B16-F0/ $E1_{244-550}$ cells and tumor growth was monitored over time for (A) $E1_{202-654}$ (n = 6), (B) $E1_{202-654}$ + α-Galcer (n = 6), (C) α-GalCer (n = 6) and (D) PBS (n = 6) treatments. Tumor size was measured as described in "Methods" and its estimated volume was plotted over time. (E) Effect of immunizations on established tumors. Once the mice were euthanized, the estimated final tumor size was determined as described in "Methods" and reported in mm^3. Tumor size was plotted for each mouse and the mean is depicted for each group. [***]p < 0.0001 (multiparametric one-way ANOVA and Tukey's Multiple Comparison Test).

markers of cytotoxicity [42–44]. Therefore, we examined first the time course of appearance of CD107a/b cytotoxic activity markers in splenic CD8+ T cells (Supplementary Fig. 3).

To examine E1 antigen-specific cytotoxic activity for the prophylactic and therapeutic protocols, CD8+ T cells from each individual mouse were co-cultured with B16-F0 and B16-F0/E1$_{244-550}$ cells as targets. We observed that in CD8+ T cells from E1 + α-GalCer immunized mice co-cultured with B16-F0/E1$_{244-550}$ cells, there was a striking increase in surface expression of CD107a/b, indicating the presence of an E1 antigen-specific CD8+ T cell cytotoxic activity (Fig. 5A and B), which correlated with the inhibition of B16-F0/E1$_{244-550}$ growth in both protocols. In the prophylactic (Fig. 5A) and therapeutic protocols (Fig. 5B), the PBS, E1 and α-GalCer groups did not show an E1 antigen-specific response, as measured through CD107a/b detection on CD8+ T cell surface.

We found that in the prophylactic as well as in therapeutic protocols, B16-F0/E1$_{244-550}$ growth inhibition seen in the α-GalCer only-treated mice was not due to CD8+ T cell activity, because CD8+ T cells fail to express CD107a/b in response to B16-F0 and B16-F0/E1$_{244-550}$ cells.

3.5. α-GalCer also promotes NK cell responses in the prophylactic and therapeutic protocols

As NK cell response has been associated with antitumor effects [34,45,46], and α-GalCer is a well-known NK cell activator, we examined the role of NK cells in tumor growth inhibition. First, we determined the time course of appearance of CD107a/b cytotoxic markers in splenic NK cells (Supplementary Fig. 4). To examine NK cytotoxic activity for the prophylactic and therapeutic protocols, NK cells from each individual mouse were co-cultured with B16-F0/E1$_{244-550}$ as targets. In both protocols, mice inoculated with α-GalCer alone showed the strongest NK cytotoxic activity (Fig. 6A for prophylactic and 6B for therapeutic) compared with all groups. Nevertheless, the inoculation of E1 + α-GalCer in both protocols also induced significant NK cytotoxic activity compared with PBS and E1$_{202-654}$ mice groups (Fig. 6A and B). E1$_{202-654}$ immunized mice from the prophylactic and therapeutic protocols showed a basal NK cytotoxic activity, similar to that observed in the PBS group (Fig. 6A and B). These results indicate that in addition to tumor-specific CD8+ cytotoxic responses, NK cells can
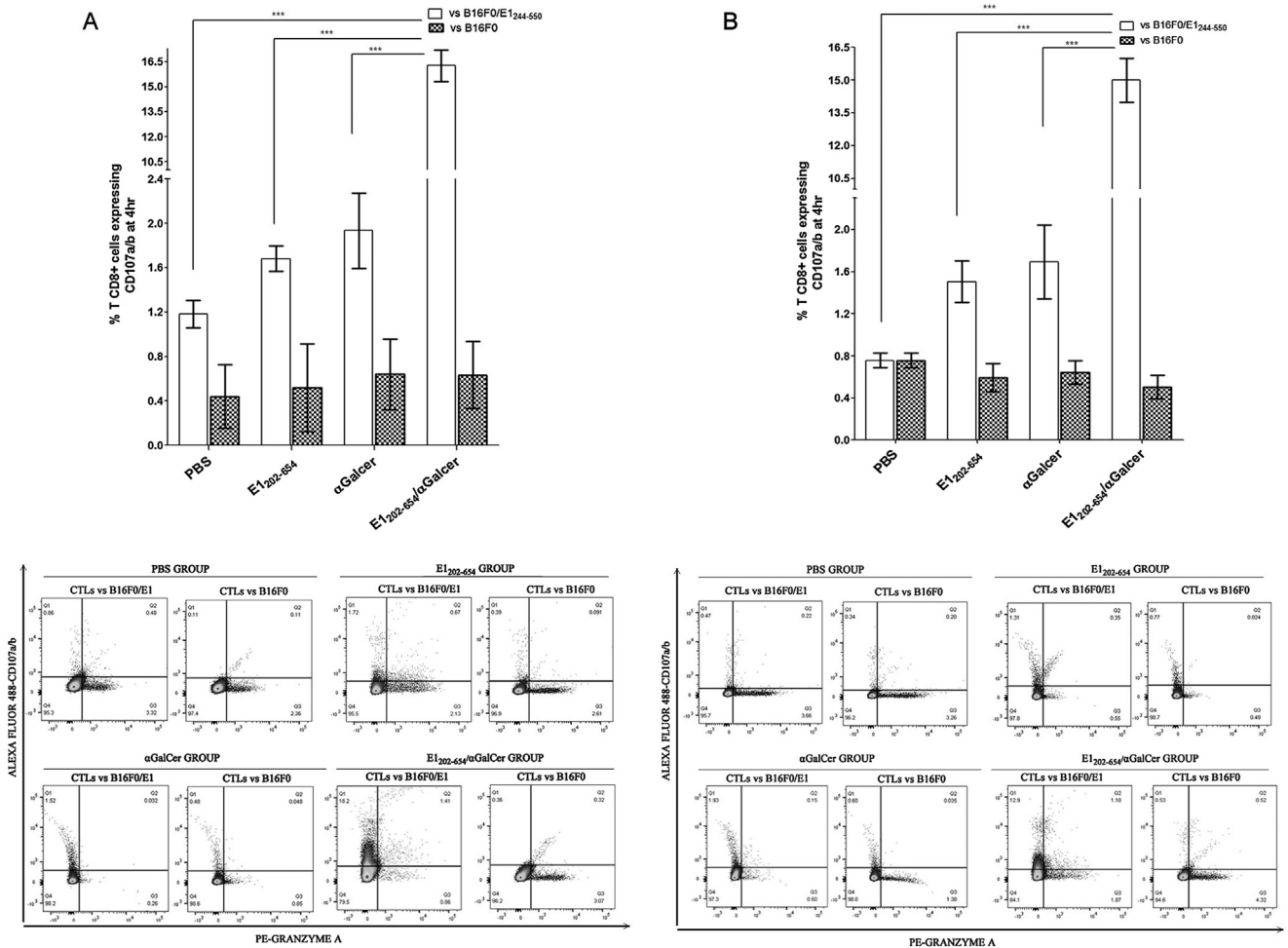
Fig. 5. E1-specific CD8+ T cell cytotoxic response by immunization with E1$_{202-654}$ + α-Galcer. CD107a/b expression on cell surface was measured in splenic CD8+ T cells from mice inoculated with E1$_{202-654}$ + α-Galcer (n = 6), PBS (n = 6), E1$_{202-654}$ (n = 6) and α-Galcer (n = 6) co-cultured with B16-F0 cells (empty bars) or B16-F0/E1$_{244-550}$ transfected cells (checkered bars) for up to 4 h in the presence of anti-CD107a/b-Alexa Fluor 488 to compare if the T CD8+ cells have an antigen-specific cytotoxic activity both in (A) prophylactic and (B) therapeutic protocols. The lower panels in A and B show representative flow cytometry images of cytotoxic assays where the CD107a/b molecules are detected at the cell surface. ***p < 0.0001 (multiparametric one-way ANOVA and Tukey's Multiple Comparison Test).
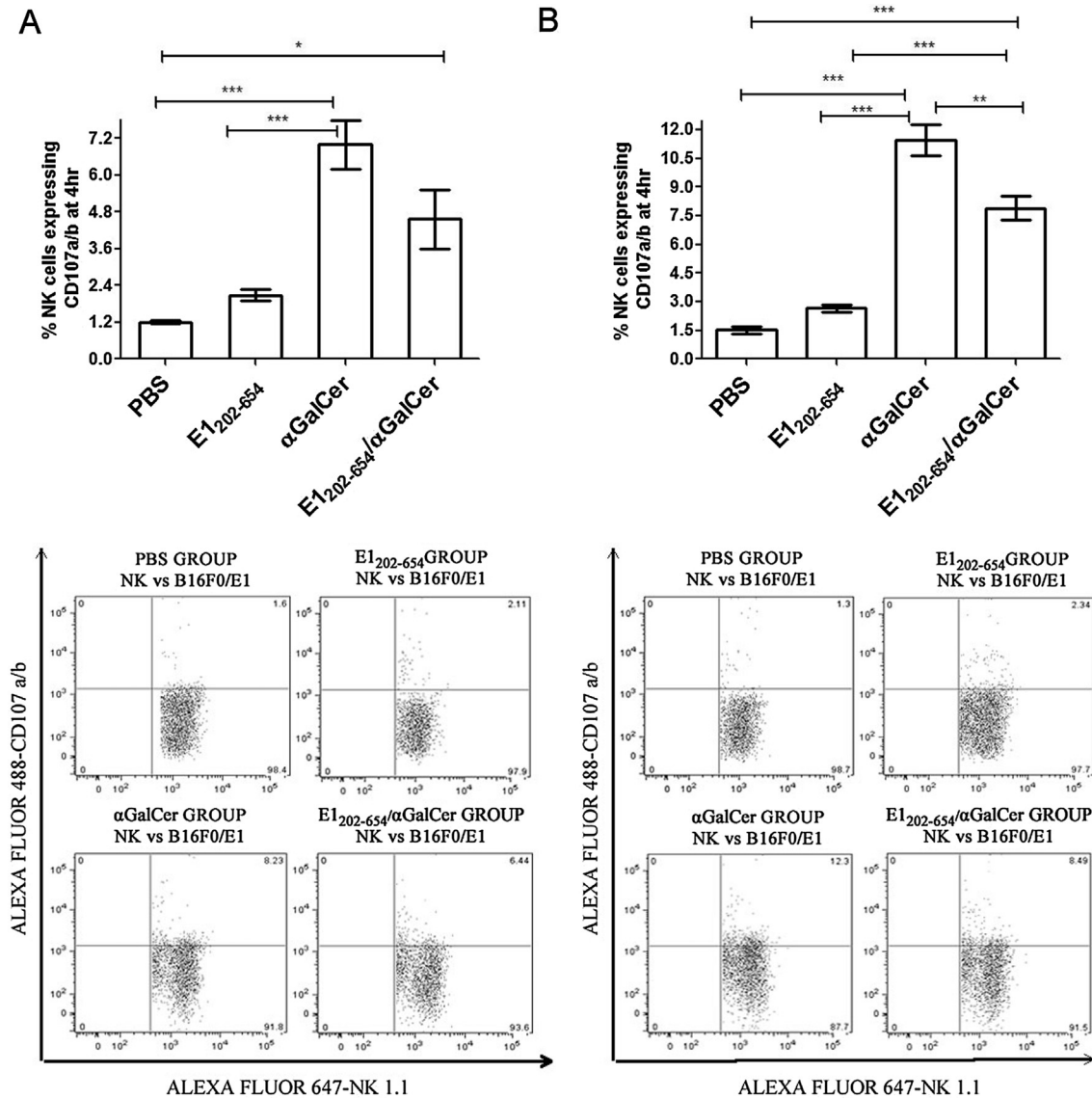
Fig. 6. Expression of CD107a/b on the cell surface of NK as a cytotoxic marker. Splenic NK cells from mice inoculated with $E1_{202-654}$ + α-Galcer (n = 6), PBS (n = 6), $E1_{202-654}$ (n = 6) and α-Galcer (n = 6) were co-cultured with $B16$-F0/$E1_{244-550}$ transfected cells for up to 4 h in the presence of anti-CD107a/b-Alexa Fluor 488 to evaluate NK cell cytotoxic activity against tumor cells, both in (A) prophylactic and (B) therapeutic protocols. The lower panels in A and B show representative flow cytometry images of cytotoxic assays where CD107a/b molecules are detected on the cell surface. $^{*}p < 0.05$, $^{**}p < 0.01$, and $^{***}p < 0.0001$ (multiparametric one-way ANOVA and Tukey's Multiple Comparison Test).

provide an additional antitumor activity that contributes to the therapeutic and prophylactic potential of E1 + α-GalCer immunization.

4. Discussion

Induction of cytotoxic T cell responses to viral antigens constitutes the main goal of therapeutic vaccination in chronic viral diseases, including those related to cancer, such as cervical cancer. In the current studies, we examined the role of an HPV-E1 protein fragment as an immunogen with therapeutic and/or prophylactic potential and capable of inducing HPV-E1-specific CD8+ cytotoxic T cells in a mouse model. For this, B16F0 murine melanoma cells were transfected with a codon-optimized $E1_{244-550}$ plasmid, which, in contrast to the full-length HPV18-E1 reference sequence, was efficiently expressed, as reported for COPV E1 [26].

We found that mice inoculated with $E1_{202-654}$ in combination with the potent adjuvant α-GalCer [33,34], impaired the growth of B16-F0/$E1_{244-550}$ bearing target cells in a therapeutic as well as

in a prophylactic protocol. The resulting tumors in mice of the therapeutic protocol were smaller than in control mice, whereas in the prophylactic model four out of six mice did not develop any tumor at all. This indicates that vaccination with E1 + α-GalCer can induce a strong antitumor and potentially therapeutic response.

As E1- bearing tumor growth inhibition was observed in the α-GalCer and $E1_{202-654}$ + α-GalCer immunized groups, although inhibition was stronger in the $E1_{202-654}$ + α-GalCer group, it was important to examine separately the ability of NK and CD8+ T cells from either mouse group *ex-vivo*. As expected, only mice immunized with $E1_{202-654}$ + α-GalCer showed specific cytotoxic activity against B16-F0/$E1_{244-550}$ cells, which is consistent with previous findings in mice immunized with Ankara vaccinia virus encoding E1 from HPV-16 [30]. We next measured an NK cell response in the α-GalCer treated mice from both protocols, which showed an NK cytotoxic activity, correlating with the unspecific antitumor effect observed in these groups. Moreover, NK cytotoxic activity was also detected in mice treated with $E1_{202-654}$ + α-GalCer,

indicating that the protective and therapeutic effects of $E1_{202-654}$ + α-GalCer against HPV involve an adaptive branch represented by CD8+ CTLs plus an increase in NK cell activity, which acting together could contribute to a stronger anti-tumor response.

The fact that the mean tumor size of the $E1_{202-654}$ + α-GalCer group was much smaller than that of the α-GalCer inoculated group in both protocols indicates that immunization with $E1_{202-654}$ plus α-GalCer, which induces a strong CD8+ T cell E1 antigen-specific immune response, is involved in the elimination of B16-F0/$E1_{244-550}$ cells. It should be noted that the percentage of CD8+ T cells actively cytotoxic is greater than the percentage of NK cells actively cytotoxic.

The current results could be the basis to propose that E1-specific CD8+ adaptive immune response could play a role in the clearance of HPV infected cells in patients with early HPV-infection, including those with normal cytology or with low-grade cervical intraepithelial lesions, where E1 is necessary for viral replication. Moreover, as the most conserved of early HPV proteins, E1 could potentially induce immunity against various HPV types. This remains to be tested in models inoculated with tumors bearing E1 from other HPV types. It is important to note that the finding that tumor cells transiently expressing $E1_{244-550}$ antigen were eliminated, strengthens the potential role of E1 as an immunizing antigen for broad-spectrum therapeutic vaccines against HPV. Additionally, α-GalCer served as a potent adjuvant to elicit $E1_{244-550}$ antigen-specific CD8+ T cell response also inducing a strong innate immune response through NK cells.

With these results, it is now important to predict whether a similar response could be obtained in humans immunized with the same E1 sequences. Thus, we used the same analysis criteria to predict peptides for HLA-A2, which is the largest and most diverse allele family in humans [47]. This revealed that the E1 full-length protein contains 303 highest-scoring predicted peptides and $E1_{244-550}$ sequence contains 243 (Supplementary Table 2).

Finally, although we did not address CD4 + T cell help in these studies, the $E1_{202-654}$ fragment is long enough and contains potential epitopes that, together with the adjuvant effect of α-GalCer, should have induced CD4 help to enhance CD8 T cell responses. This will be the subject of further studies. This is an important issue because, depending on the phenotype of the CD4 + T cells induced, they would lead to distinct types of responses, including help or suppression, which could affect the outcome of tumor-infiltrating CTLs.

5. Authors' contributions

AAM participated in the study design, cytotoxic and flow cytometry assays, analysis, interpretation of data and writing of the manuscript. CTM was involved in the cytotoxic and flow cytometry assays. DRR and ISO participated in the analysis and interpretation of flow cytometry assays. EPC coordinated the management of the mouse model and analysis of the data. EL and JM participated in the study design, data analysis and writing of the manuscript. ML designed the study and was involved in the analysis and interpretation of the data and writing of the manuscript. All authors reviewed and approved the final manuscript for submission.

Ethical statement

The Ethics Committees of the Universidad Nacional Autónoma de México (UNAM, Mexico City) and of the Instituto Nacional de Cancerología, México (017/001/IBI), approved the procedures for care and use of animals. All applicable institutional regulations concerning the ethical use of animals were followed accordingly.

Conflicts of interest

The authors declare to have no conflicts of interest.

Acknowledgments

Appendix A. Supplementary material

Supplementary data to this article can be found online at https://doi.org/10.1016/j.vaccine.2018.12.036.

References

[1] WHO. World Health Organization. Human papillomavirus (HPV) and cervical cancer. http://wwwwhoint/mediacentre/factsheets/fs380/en/ Accessed date, September 19, 2017.
[2] zur Hausen H. Papillomavirus infections–a major cause of human cancers. Biochim Biophys Acta 1996;1288:F55–78.
[3] Parkin DM, Bray F, Ferlay J, Pisani P. Global cancer statistics, 2002. CA Cancer J Clin 2005;55:74–108.
[4] Clifford GM, Smith JS, Aguado T, Franceschi S. Comparison of HPV type distribution in high-grade cervical lesions and cervical cancer: a meta-analysis. Br J Cancer 2003;89:101–5.
[5] Clifford GM, Smith JS, Plummer M, Munoz N, Franceschi S. Human papillomavirus types in invasive cervical cancer worldwide: a meta-analysis. Br J Cancer 2003;88:63–73.
[6] Doorbar J. Papillomavirus life cycle organization and biomarker selection. Dis Markers 2007;23:297–313.
[7] Abbate EA, Berger JM, Botchan MR. The X-ray structure of the papillomavirus helicase in complex with its molecular matchmaker E2. Genes Dev 2004;18:1981–96.
[8] Demeret C, Goyat S, Yaniv M, Thierry F. The human papillomavirus type 18 (HPV18) replication protein E1 is a transcriptional activator when interacting with HPV18 E2. Virology 1998;242:378–86.
[9] Wilson VG, West M, Woytek K, Rangasamy D. Papillomavirus E1 proteins: form, function, and features. Virus Genes 2002;24:275–90.
[10] Koonin EV. A common set of conserved motifs in a vast variety of putative nucleic acid-dependent ATPases including MCM proteins involved in the initiation of eukaryotic DNA replication. Nucleic Acids Res 1993;21:2541–7.
[11] Cote-Martin A, Moody C, Fradet-Turcotte A, D'Abramo CM, Lehoux M, Joubert S, et al. Human papillomavirus E1 helicase interacts with the WD repeat protein p80 to promote maintenance of the viral genome in keratinocytes. J Virol 2008;82:1271–83.
[12] Bosch FX, Lorincz A, Munoz N, Meijer CJ, Shah KV. The causal relation between human papillomavirus and cervical cancer. J Clin Pathol 2002;55:244–65.
[13] Magaldi TG, Almstead LL, Bellone S, Prevatt EG, Santin AD, DiMaio D. Primary human cervical carcinoma cells require human papillomavirus E6 and E7 expression for ongoing proliferation. Virology 2012;422:114–24.
[14] Romanczuk H, Howley PM. Disruption of either the E1 or the E2 regulatory gene of human papillomavirus type 16 increases viral immortalization capacity. Proc Natl Acad Sci USA 1992;89:3159–63.
[15] Tindle RW. Immune evasion in human papillomavirus-associated cervical cancer. Nat Rev Cancer 2002;2:59–65.
[16] Stanley MA, Pett MR, Coleman N. HPV: from infection to cancer. Biochem Soc Trans 2007;35:1456–60.
[17] Morrow MP, Kraynyak KA, Sylvester AJ, Shen X, Amante D, Sakata L, et al. Augmentation of cellular and humoral immune responses to HPV16 and HPV18 E6 and E7 antigens by VGX-3100. Mol Ther Oncolytics 2016;3:16025.
[18] Kim TJ, Jin HT, Hur SY, Yang HG, Seo YB, Hong SR, et al. Clearance of persistent HPV infection and cervical lesion by therapeutic DNA vaccine in CIN3 patients. Nat Commun 2014;5:5317.
[19] Liang X, Crepeau RL, Zhang W, Speck SH, Usherwood EJ. CD4 and CD8 T cells directly recognize murine gammaherpesvirus 68-immortalized cells and prevent tumor outgrowth. J Virol 2013;87:6051–4.

[20] Melief CJ, van Hall T, Arens R, Ossendorp F, van der Burg SH. Therapeutic cancer vaccines. J Clin Investig 2015;125:3401–12.
[21] Butterfield LH. Cancer vaccines. Bmj. 2015;350:h988.
[22] Jung AC, Guihard S, Krugell S, Ledrappier S, Brochot A, Dalstein V, et al. CD8-alpha T-cell infiltration in human papillomavirus-related oropharyngeal carcinoma correlates with improved patient prognosis. Int J Cancer 2013;132:E26–36.
[23] van Duikeren S, Fransen MF, Redeker A, Wieles B, Platenburg G, Krebber WJ, et al. Vaccine-induced effector-memory CD8+ T cell responses predict therapeutic efficacy against tumors. J Immunol 2012;189:3397–403.
[24] Yin W, Duluc D, Joo H, Xue Y, Gu C, Wang Z, et al. Therapeutic HPV cancer vaccine targeted to CD40 elicits effective CD8+ T-cell immunity. Cancer Immunol Res 2016;4:823–34.
[25] Johnston KB, Monteiro JM, Schultz LD, Chen L, Wang F, Ausensi VA, et al. Protection of beagle dogs from mucosal challenge with canine oral papillomavirus by immunization with recombinant adenoviruses expressing codon-optimized early genes. Virology 2005;336:208–18.
[26] Moore RA, Santos EB, Nicholls PK, White KL, Anderson DM, Lloyd A, et al. Intraepithelial DNA immunisation with a plasmid encoding a codon optimised COPV E1 gene sequence, but not the wild-type gene sequence completely protects against mucosal challenge with infectious COPV in beagles. Virology 2002;304:451–9.
[27] Han R, Reed CA, Cladel NM, Christensen ND. Intramuscular injection of plasmid DNA encoding cottontail rabbit papillomavirus E1, E2, E6 and E7 induces T cell-mediated but not humoral immune responses in rabbits. Vaccine 1999;17:1558–66.
[28] Han R, Reed CA, Cladel NM, Christensen ND. Immunization of rabbits with cottontail rabbit papillomavirus E1 and E2 genes: protective immunity induced by gene gun-mediated intracutaneous delivery but not by intramuscular injection. Vaccine 2000;18:2937–44.
[29] Ragonnaud E, Andersson AC, Mariya S, Pedersen AG, Burk RD, Folgori A, et al. Therapeutic vaccine against primate papillomavirus infections of the cervix. J Immunother 2017;40:51–61.
[30] Remy-Ziller C, Germain C, Spindler A, Hoffmann C, Silvestre N, Rooke R, et al. Immunological characterization of a modified vaccinia virus Ankara vector expressing the human papillomavirus 16 E1 protein. Clin Vaccine Immunol 2014;21:147–55.
[31] Haicheur N, Bismuth E, Bosset S, Adotevi O, Warnier G, Lacabanne V, et al. The B subunit of Shiga toxin fused to a tumor antigen elicits CTL and targets dendritic cells to allow MHC class I-restricted presentation of peptides derived from exogenous antigens. J Immunol 2000;165:3301–8.
[32] Pufnock JS, Cigal M, Rolczynski LS, Andersen-Nissen E, Wolfl M, McElrath MJ, et al. Priming CD8+ T cells with dendritic cells matured using TLR4 and TLR7/8 ligands together enhances generation of CD8+ T cells retaining CD28. Blood 2011;117:6542–51.
[33] Adotevi O, Vingert B, Freyburger L, Shrikant P, Lone YC, Quintin-Colonna F, et al. B subunit of Shiga toxin-based vaccines synergize with alpha-galactosylceramide to break tolerance against self antigen and elicit antiviral immunity. J Immunol 2007;179:3371–9.
[34] Dolen Y, Kreutz M, Gileadi U, Tel J, Vasaturo A, van Dinther EA, et al. Co-delivery of PLGA encapsulated invariant NKT cell agonist with antigenic protein induce strong T cell-mediated antitumor immune responses. Oncoimmunology 2016;5:e1068493.
[35] Smyth MJ, Crowe NY, Pellicci DG, Kyparissoudis K, Kelly JM, Takeda K, et al. Sequential production of interferon-gamma by NK1.1(+) T cells and natural killer cells is essential for the antimetastatic effect of alpha-galactosylceramide. Blood 2002;99:1259–66.
[36] Reche PA, Glutting JP, Reinherz EL. Prediction of MHC class I binding peptides using profile motifs. Hum Immunol 2002;63:701–9.
[37] Haicheur N, Benchetrit F, Amessou M, Leclerc C, Falguieres T, Fayolle C, et al. The B subunit of Shiga toxin coupled to full-size antigenic protein elicits humoral and cell-mediated immune responses associated with a Th1-dominant polarization. Int Immunol 2003;15:1161–71.
[38] Faustino-Rocha A, Oliveira PA, Pinho-Oliveira J, Teixeira-Guedes C, Soares-Maia R, da Costa RG, et al. Estimation of rat mammary tumor volume using caliper and ultrasonography measurements. Lab Animal 2013;42:217–24.
[39] Miller JP, Egbulefu C, Prior JL, Zhou M, Achilefu S. Gradient-based algorithm for determining tumor volumes in small animals using planar fluorescence imaging platform. Tomography 2016;2:17–25.
[40] Ringvall M, Thulin A, Zhang L, Cedervall J, Tsuchida-Straeten N, Jahnen-Dechent W, et al. Enhanced platelet activation mediates the accelerated angiogenic switch in mice lacking histidine-rich glycoprotein. PLoS ONE 2011;6:e14526.
[41] Wang Z, Liu JQ, Liu Z, Shen R, Zhang G, Xu J, et al. Tumor-derived IL-35 promotes tumor growth by enhancing myeloid cell accumulation and angiogenesis. J Immunol 2013;190:2415–23.
[42] Betts MR, Brenchley JM, Price DA, De Rosa SC, Douek DC, Roederer M, et al. Sensitive and viable identification of antigen-specific CD8+ T cells by a flow cytometric assay for degranulation. J Immunol Methods 2003;281:65–78.
[43] Newell EW, Sigal N, Bendall SC, Nolan GP, Davis MM. Cytometry by time-of-flight shows combinatorial cytokine expression and virus-specific cell niches within a continuum of CD8+ T cell phenotypes. Immunity 2012;36:142–52.
[44] Aktas E, Kucuksezer UC, Bilgic S, Erten G, Deniz G. Relationship between CD107a expression and cytotoxic activity. Cell Immunol 2009;254:149–54.
[45] Ito H, Ando T, Seishima M. Inhibition of iNOS activity enhances the anti-tumor effects of alpha-galactosylceramide in established murine cancer model. Oncotarget 2015;6:41863–74.
[46] Chennamadhavuni D, Saavedra-Avila NA, Carreno LJ, Guberman-Pfeffer MJ, Arora P, Yongqing T, et al. Dual modifications of alpha-galactosylceramide synergize to promote activation of human invariant natural killer T cells and stimulate anti-tumor Immunity. Cell Chem Biol 2018.
[47] Ellis JM, Henson V, Slack R, Ng J, Hartzman RJ, Katovich Hurley C. Frequencies of HLA-A2 alleles in five U.S. population groups. Predominance Of A*02011 and identification of HLA-A*0231. Hum Immunol 2000;61:334–40.

HPV18 E1 protein plus α-Galactosylceramide elicit in mice CD8+ T cell cross reactivity against cells expressing E1 from diverse HPV types

Journal:	*Viral Immunology*
Manuscript ID	Draft
Manuscript Type:	Brief Report
Date Submitted by the Author:	n/a
Complete List of Authors:	Amador-Molina, Alfredo; Instituto Nacional de Cancerologia Amador-Molina, Juan; Tecnológico de Monterrey, Campus Estado de México. Carretera Lago de Guadalupe Km. 3.5. Atizapán de Zaragoza, Estado de México. 52926. Arciniega, Juan; Biologics Consulting (Affiliate), 1555 King St., Suite 300. Alexandria, VA 22314, United States. Lizano, Marcela; Instituto Nacional de Cancerologia,
Keyword:	Vaccines
Manuscript Keywords (Search Terms):	Human papillomavirus, E1 protein, α-Galactosyl-Ceramide, CD8+ T cells, cross-reactivity.

SCHOLARONE™
Manuscripts

HPV18 E1 protein plus α-Galactosylceramide elicit in mice CD8+ T cell cross reactivity against cells expressing E1 from diverse HPV types

Alfredo Amador-Molina[1], Juan C. Amador-Molina[2], Juan L. Arciniega[3] and Marcela Lizano[1, 4,*].

[1]Unidad de Investigación Biomédica en Cáncer, Instituto Nacional de Cancerología, Av. San Fernando No. 22, Col. Sección XVI, Tlalpan 14080, México.

[2] Tecnológico de Monterrey, Campus Estado de México. Carretera Lago de Guadalupe Km. 3.5. Atizapán de Zaragoza, Estado de México. 52926.

[3]Biologics Consulting (Affiliate), 1555 King St., Suite 300. Alexandria, VA 22314, United States.

[4]Departamento de Medicina Genómica y Toxicología Ambiental, Instituto de Investigaciones Biomédicas, Universidad Nacional Autónoma de México, Ciudad Universitaria, Ciudad de México 04510, México.

*Correspondence: email: lizanosoberon@gmail.com. Phone number: +5255 56280400 ext.31035.

ABSTRACT

CD8+ T cell immune response plays a critical role in the clearance of Human Papillomavirus (HPV)-infected cells. During the natural history of HPV infection, the E1 protein, an early-expressed helicase highly conserved among papillomaviruses, is involved in the replication of HPV genomes. We have previously shown, in a murine model, that immunization with HPV18 E1 protein combined with α-Galactosyl-Ceramide elicits a specific CD8+ T cell response. We further proved those findings by analyzing whether CD8+ T cells from mice immunized with α-Galactosyl-Ceramide plus HPV18-E1 protein could effect cytotoxicity in cells expressing the carboxyl-terminal domain from E1 proteins of other HPV types. Interestingly, CD8+ T cells raised against HPV18 E1-antigen presented cross-reactivity against E1 protein from HPV53, 33, 16 and 31. Poor cross-reactivity was observed for HPV11 and none for HPV6. This outcome may be relevant for the design of broad spectrum immune-protective agents against HPV infections.

Keywords

Human papillomavirus; E1 protein; α-Galactosyl-Ceramide; CD8+ T cells; cross-reactivity.

Introduction

Persistent infection with human papillomavirus (HPV) is the main risk factor for the development of cervical cancer (15). HPV types are classified as high-risk (HR-HPV) or low-risk (LR-HPV), according with their oncogenic potential. HPV16 is the type most frequently found in cervical cancer, followed by HPV18; while, HPV6 and 11 are the LR-HPV types most frequently found in genital warts and premalignant lesions (6, 7). During viral infection, E1 protein participates in HPV DNA replication through its helicase function (1, 8). In some cases, for unclear reasons, the HPV genome integrates randomly into the host DNA, commonly disrupting E1/E2 open reading frame (11, 17). Nevertheless, it has been reported that the expression of E1 is found increased in patients with cervical intraepithelial neoplasia-3 (CIN3) and squamous cell carcinoma (SSC), in relation to low grade cervical lesions (4).

E1 belongs to the helicase superfamily III(14). This protein has an N-terminal domain that contains nuclear localization signals, a DNA binding domain (DBD) and a carboxyl-terminal (CT) domain that harbors the ATP-dependent DNA helicase(1). The CT is the most conserved domain of E1 and displays a set of three motifs conserved among large groups of DNA-dependent ATPases, such as helicase superfamily III and the DnaA family (14).

CD8+ T cell immune response plays a significant role in the clearance of HPV-infected cells (19). However, HPV can evade the immune system and promote a persistent infection (18, 19). In fact, an important proportion of HPV-infected women do not develop a successful immune response against HR-HPV (18).

Although licensed HPV vaccines are effective to prevent infections with the viral types of the L1 proteins included in their formulation, they are not useful to treat HPV infections already in progress (10). Thus, experimental HPV vaccines for therapeutic use have been designed, mostly for the treatment of established HPV-16 and HPV-18 infections, which elicit an antigen-specific CD8+ T cell immune response to the E6 and/or E7 oncoproteins,(20) Some of these therapeutic vaccines use novel adjuvants to achieve preferentially a CTL response. The adjuvant KRN7000, a chemically-synthesized α-Galactosylceramide (α-GalCer), has shown superiority in promoting a CTL immune

response, as compared with other adjuvants such as the incomplete Freund adjuvant, IFN-α, poly(I:C) or TLR-9 agonists, used in combination with internalization molecules such as the B subunit of Shiga toxin (2). Besides, α-GalCer alone has demonstrated to increase cross-presentation by Dendritic cells, thus enhancing CD8+ T cell response against tumors generated in mice (13). α-GalCer can stimulate NKT cells, and when co-administered with proteins, it has shown to increase the population of antigen-specific CD8+ T cells (2, 3, 9).

Previously, we reported that immunization of mice with the recombinant $E1_{202-654}$ protein along with α-GalCer induces an antigen-specific CD8+ T cell immune response, able to eliminate B16-F0 melanoma cells expressing HPV18-E1 protein (3). In the present study we analyzed if CD8+ T cell from mice immunized with HPV18 E1 protein can cross react against E1 from diverse HPV types.

Materials and methods

Plasmids

The E1 carboxyl-terminal domains from HPV types 6, 11,16, 31, 33 and 53 were amplified from pBR322-HPV6 and pBR322-HPV11 (kindly donated by EM de Villiers, Division of Episomal-Persistent DNA in Cancer and Chronic Diseases, Deutsches Krebsforschungszentrum, Heidelberg, Germany); pBR322-HPV16 (kindly donated by M Dürst, Department of Gynecology, Friedrich Schiller University Hospital, Jena, Germany); pT712-HPV31 and pLink-HPV33 (kindly donated by Professor H zur Hausen, Division of Episomal-Persistent DNA in Cancer and Chronic Diseases, Deutsches Krebsforschungszentrum, Heidelberg, Germany) and pEMBL-HPV53 (kindly donated by L Gissmann, Deutsches Krebsforschungszentrum, Heidelberg, Germany). The carboxyl-terminal domain from E1 HPV18 was amplified from a codon-optimized E1 HPV18 plasmid (3). PCR products were cloned into pcDNA 3.3 Topo plasmid (Invitrogen; Thermo Fisher, Cat# K830001) with a Kozak sequence and human influenza hemagglutinin (HA) tag, to obtain pE1-CT/HPV6HA, pE1-CT/HPV11HA, pE1-CT/HPV16HA, pE1-

CT/HPV18HA, pE1-CT/HPV31HA, pE1-CT/HPV33HA and pE1-CT/HPV53HA. The plasmid constructions were confirmed by sequencing.

Cell culture and transfection

B16-F0 cell line (ATCC; Cat# CRL-6322) was grown in Dulbecco's modified Eagle's medium F12 supplemented with 10% FBS and transiently transfected with pE1-CT/HPV6HA, pE1-CT/HPV11HA, pE1-CT/HPV16HA, pE1-CT/HPV18HA, pE1-CT/HPV31HA, pE1-CT/HPV33HA, pE1-CT/HPV53HA or pcDNA3.1, as previously described (3).

Western blot analysis

Protein extracts from B16-F0 cells transiently transfected with pE1-CT/HPV plasmids or pcDNA3.1 control vector were loaded onto SDS-PAGE and transferred onto nitrocellulose membranes. Afterwards, membranes were sequentially incubated with rabbit polyclonal anti-HA antibody (Cell Signaling Technology; Cat# 3724), and horseradish peroxidase-labelled goat anti-rabbit antibody (Santa Cruz Biotechnology; Cat# sc-2030). E1 proteins were revealed by enhanced chemiluminescence (Amersham; GE Healthcare Life Sciences, Cat #RPN2236). β-actin was used as loading control (Santa Cruz Biotechnology Cat# sc-47778) followed by mouse IgG kappa conjugated to horseradish peroxidase (Santa Cruz Biotechnology, Cat# sc-516102). Western blotting was performed in triplicate in every case to ensure reproducibility.

$E1_{202-654}$ Recombinant Protein

The $E1_{202-654}$ protein that contains the DNA-binding and the carboxyl-terminal domains was produced by GenScript as previously described (3).

MHC class I peptide binding prediction and multiple sequence alignment.

The RANKPEP server (http://imed.med.ucm.es/Tools/rankpep.html) was used to predict peptide-binding affinities to mouse H2-D^b and H2-K^b, with 2% threshold. We considered all possible immunogenic peptides with a percentile score (% OPT) ≥ 1%. Peptides from 8 to 11 aminoacid residues were analyzed in E1-aligned sequences using Clustal Omega multiple sequence alignment (https://www.ebi.ac.uk/Tools/msa/clustalo/), to find conserved immunogenic peptides among the E1-carboxyl terminal domains of HPV6, 11, 16, 18, 31, 33 and 53. Clustal Omega multiple sequence alignment analysis was also used to determine the homology of E6, E7, E2 and E1-CT genes among different HPV types.

Mice and Immunizations

Female C57BL/6 mice were purchased from Instituto Nacional de Ciencias Médicas y Nutrición Salvador Zubirán (INCMNSZ), Mexico City, Mexico. The Ethics Committees of the Universidad Nacional Autónoma de México (UNAM, Mexico City) and of the Instituto Nacional de Cancerología, México City, approved the procedures for care and use of animals. All applicable institutional regulations concerning the ethical use of animals were followed accordingly. Seven to eight-week-old female mice, distributed in groups of four mice each, were immunized as previously described (3); 1) $E1_{202-654}$ group: immunized with recombinant $E1_{202-654}$; 2) $E1_{202-654}$+α-GalCer group: immunized with recombinant $E1_{202-654}$ plus α-GalCer; 3) α-GalCer group: inoculated with α-GalCer; and 4) PBS group: inoculated with PBS. This animal experiment was replicated two additional times with identical design.

Preparation of murine splenocytes and CD8+ T cell isolation

Seven days after the last immunization, the mice were euthanized, and murine spleens were excised to proceed with the preparation of splenocytes, followed by CD8+ T cell isolation using $CD8\alpha^+$ T Cell Isolation Kit II (Miltenyi Biotec; Cat# 130104075) as previously described (3). Cells of each mice group were pooled.

Direct ex-vivo cytotoxic activity assay for CD8+ T cells

B16-F0 cells transiently transfected with pE1-CT/HPV6HA, pE1-CT/HPV11HA, pE1-CT/HPV16HA, pE1-CT/HPV31HA, pE1-CT/HPV33HA, pE1-CT/HPV53HA or pE1-CT/HPV18HA were co-cultured with CD8+ T cells (with a viability $\geq$90%) from mice immunized with recombinant HPV18-E1$_{202\text{-}654}$ protein plus α-GalCer, or HPV18-E1$_{202\text{-}654}$ protein, or α-GalCer or PBS, to perform the cytotoxic activity assay as previously described (3).

Flow cytometry

Samples from all assays were acquired in a FACSAria II flow cytometer (Becton Dickinson;) using FACS Diva software 8.0.1 and analyzed with FlowJo software (version 10.2). Typically, 40,000 events were acquired for cytotoxic activity.

For the flow cytometry panel and lineage-specific panels, the following monoclonal antibodies were used: Brillant Violet 421™ anti-CD8a (Clone 53-6.7, Cat# 100753), Allophycocyanin (APC)-anti-CD3 (Clone 17A2, Cat# 100210), Alexa Fluor 488® (AF488)-anti-CD107a (Clone 1D4B, Cat# 121608), and Alexa Fluor 488® (AF488)- anti-CD107b (Clone M3/84, Cat# 108510), (all from Biolegend; San Diego, CA).

Statistical analysis

Statistical analysis was performed by one-way ANOVA and Dunett post-tests (JMP® 13.0.0   Copyrigh 2016, SAS Institute Inc.). Error bars represent standard error of the mean (SEM) and *P* values of <0.05 were considered statistically significant.

Results

Expression of E1 proteins from HPV 6, 11, 16, 18, 31, 33 and 53 in B16-F0 cells

E1 carboxyl-terminal domain was detected in B16-F0 cells after 24 h post- transfection with plasmids expressing E1 fragments from different HPV types. The expression of E1

carboxyl-terminal domain from HPV 6, 11, 16, 18, 31, 33 and 53 was detected by western blot as 32 kDa hybrid polypeptides (Figure 1A.). Protein extracts from B16-F0 cells transfected with empty vector were used as negative control. The B16-F0 cells expressing different types of E1 were used as targets to determine the CD8+ T cell cytotoxic activity from mice immunized with HPV 18-E1.

In silico analysis of immunogenic peptides of the carboxyl-terminal domain of E1-HPV18.

The E1-carboxyl terminal domain is highly conserved among different HPV types (1). Moreover, this region contains a set of three motifs highly conserved among a large group of DNA-dependent ATPases (14). Thus, we analyzed this domain in the RANKPEP server to predict peptides with the ability to bind to MHC class I in a murine context. After obtaining a large variety of predicted peptides, we aligned the carboxyl-terminal domains in the Clustal Omega server to find conserved peptides among E1 proteins from HPV types 6, 11, 18, 16, 31, 33 and 53. The analysis showed that at least 15 predicted peptides are conserved among the seven E1 HPV types (columns in Table 1). Besides, E1-CT/HPV53 and E1-CT/HPV18 share twenty identical or highly homologous predicted peptides (Data not shown).

Cross reactivity against other HPV types

To determine if CD8+ T cells from mice immunized with HPV18-E1 could have cytotoxic activity against other E1-HPV types, splenic CD8+ T cells from mice immunized with HPV18 E1$_{202-654}$ plus α-GalCer were co-cultured with B16-F0 cells expressing the carboxyl-terminal domains from HPV6, 11, 16, 31, 33 and 53. As a negative control, non-transfected B16-F0 cells were used; and as a positive control, B16-F0 cells expressing E1-CT/HPV18HA were used, as previously reported (3). Activation-induced granule exocytosis leads to the exposure of CD107a and CD107b on the surface of CD8+ T cells (5). Co-cultures were monitored up to 4h, time at which they reached the highest CD107a/b cell surface expression.

A significant increase in cell surface exposure of CD107a/b was detected in the co-cultures of CD8+ T cells with B16-F0 cells individually expressing the E1 proteins of HPV types 53, 33, 16, 31 and 11, in relation to the co-culture with B16-F0 non-transfected cells (Figure 1B.). The highest percentage of cell surface CD107a/b exposure was obtained in the co-cultures of cells expressing E1-CT/HPV53, and the lowest was obtained for E1-CT/HPV11. No cell surface exposure of CD107a/b was detected in splenic CD8+ T cells when co-cultured with cells expressing E1-CT/HPV6 (Figure 1B.). These data indicate that CD8+ T cells from mice immunized with HPV18/E1plus α-GalCer can also display cytotoxic activity against cells expressing E1-CT/HPV53HA, E1-CT/HPV33HA, E1-CT/HPV16HA, E1-CT/HPV31HA and E1-CT/HPV11HA.

Splenic CD8+ T cells from mice injected with PBS (Figure 1C.), α-GalCer (Figure 1D.), or immunized exclusively with HPV18 $E1_{202-654}$ protein (Figure 1E.) showed no cytotoxic activity against any E1-carboxyl-terminal domain. Therefore, immunization with HPV18/E1 promotes a cytotoxic response against E1 from different HPV types, only when combined with α-GalCer.

Discussion

Cervical cancer is the fourth cause of cancer death in women worldwide[12], and HPV is the main etiological agent. The current efforts to develop therapeutic vaccines against HPV are mainly directed against E6 and/or E7 from HPV16 and/or HPV18. Since E6 and E7 HPV proteins are poorly conserved among HPV types (supplementary Table 1), their cross-reactivity with other HPV types could be limited. A therapeutic vaccine based on the most conserved HPV proteins, such as E1, could ideally elicit a wider-spectrum protection against several HPV types.

In the current study we evaluated ex-vivo the ability of HPV18 E1 antigen specific CD8+ T cells induced in mice, to cross react against B16-F0 cells expressing E1 proteins from other HPV types. Through in silico analysis we found highly conserved peptides, which would predictably bind to MHC class I proteins, in the carboxyl terminal domain of E1 proteins from HPV6, 11, 16, 18, 31, 33 and 53 (Table 1). It is remarkable that the carboxyl-terminal domain from HPV53 E1 share with E1-CT/HPV18 the highest number of

predicted peptides that bind to MHC class I proteins (Data not shown). This latter data matches the results obtained from ex-vivo cytotoxic activity assays, where splenic CD8+ T cells from mice immunized with HPV18 $E1_{202-654}$ plus α-GalCer, co-cultured with B16-F0/E1-CT/HPV53HA showed the highest cell surface CD107a/b exposure, a sign of cytotoxicity.

Significant cross-reactivity was also detected in co-cultures with cells expressing E1-CT from high risk HPV types 33, 16 and 31 (Figure 1B.). Nevertheless, although cross-reactive cytotoxic activity against cells expressing HPV type 11 was detected, it was non-significant (2.11%). Thus, these data suggest that immunization with E1 from HPV18 could contribute to the clearance of low-grade and high-grade(4) lesions associated to different HPV types, when MHC class I molecules are still presenting E1 antigens. It is worth mentioning that most of the low grade cervical intraepithelial lesions express E1 and E2 proteins (11, 16). Even that it has been reported that the expression of E2 decreases while the lesions advance, it has been shown that E1 is expressed in high grade lesions and cervical cancer (4, 11).

We previously demonstrated that immunizing mice with HPV18 E1 plus α-GalCer promoted an E1-specific CD8+ T cell cytotoxic response, involved in growth inhibition of melanoma B16-F0 cells expressing HPV18 E1 antigens(3). Therefore, in order to test its broad-spectrum protective potential, it would be necessary to test if growth inhibition could also be achieved with grafted B16-F0 cells expressing E1 antigens of diverse HPV types. In summary, this report provides evidence that immunization with HPV18- $E1_{202-654}$ protein plus α-GalCer can elicit a CTL immune response against E1 from diverse HPV types.

Further studies on therapeutic vaccines able to generate an efficient, broad spectrum protection against HPV, based on cross-reactive CTL immune response to early-expressed proteins, may be warranted.

Author Disclosure Statement

No competing financial interest exist

Acknowledgments

Alfredo Amador Molina is a Doctoral student at "Programa de Maestría y Doctorado en Ciencias Bioquímicas, Universidad Nacional Autónoma de México".

Funding

Ethics approval and consent to participate

The Ethics Committees of the Universidad Nacional Autónoma de México (UNAM, Mexico City) and of the Instituto Nacional de Cancerología, México (017/001/IBI), approved the procedures for care and use of animals. All applicable institutional regulations concerning the ethical use of animals were followed accordingly.

References

1. Abbate EA, Berger JMand Botchan MR. The X-ray structure of the papillomavirus helicase in complex with its molecular matchmaker E2. Genes Dev 2004;18:1981-1996.
2. Adotevi O, Vingert B, Freyburger L, et al. B subunit of Shiga toxin-based vaccines synergize with alpha-galactosylceramide to break tolerance against self antigen and elicit antiviral immunity. J Immunol 2007;179:3371-3379.
3. Amador-Molina A, Trejo-Moreno C, Romero-Rodriguez D, et al. Vaccination with human papillomavirus-18 E1 protein plus alpha-galactosyl-ceramide induces CD8(+) cytotoxic response and impairs the growth of E1-expressing tumors. Vaccine 2019.
4. Baedyananda F, Chaiwongkot Aand Bhattarakosol P. Elevated HPV16 E1 Expression Is Associated with Cervical Cancer Progression. Intervirology 2017;60:171-180.
5. Betts MR, Brenchley JM, Price DA, et al. Sensitive and viable identification of antigen-specific CD8+ T cells by a flow cytometric assay for degranulation. J Immunol Methods 2003;281:65-78.
6. Clifford GM, Smith JS, Aguado T, et al. Comparison of HPV type distribution in high-grade cervical lesions and cervical cancer: a meta-analysis. Br J Cancer 2003;89:101-105.
7. Clifford GM, Smith JS, Plummer M, et al. Human papillomavirus types in invasive cervical cancer worldwide: a meta-analysis. Br J Cancer 2003;88:63-73.
8. Demeret C, Goyat S, Yaniv M, et al. The human papillomavirus type 18 (HPV18) replication protein E1 is a transcriptional activator when interacting with HPV18 E2. Virology 1998;242:378-386.
9. Dolen Y, Kreutz M, Gileadi U, et al. Co-delivery of PLGA encapsulated invariant NKT cell agonist with antigenic protein induce strong T cell-mediated antitumor immune responses. Oncoimmunology 2016;5:e1068493.
10. Herrero R. Human papillomavirus (HPV) vaccines: limited cross-protection against additional HPV types. J Infect Dis 2009;199:919-922.
11. Hu Z, Zhu D, Wang W, et al. Genome-wide profiling of HPV integration in cervical cancer identifies clustered genomic hot spots and a potential microhomology-mediated integration mechanism. Nat Genet 2015;47:158-163.

12. International Agency for Research on Cancer WHO. Estimated number of deaths in 2018, worldwide, all cancers, female, all ages. (Last accessed on February 5, 2019).

13. Kogo H, Shimizu M, Negishi Y, et al. Suppression of murine tumour growth through CD8(+) cytotoxic T lymphocytes via activated DEC-205(+) dendritic cells by sequential administration of alpha-galactosylceramide in vivo. Immunology 2017;151:324-339.

14. Koonin EV. A common set of conserved motifs in a vast variety of putative nucleic acid-dependent ATPases including MCM proteins involved in the initiation of eukaryotic DNA replication. Nucleic Acids Res 1993;21:2541-2547.

15. Parkin DM, Bray F, Ferlay J, et al. Global cancer statistics, 2002. CA Cancer J Clin 2005;55:74-108.

16. Romanczuk Hand Howley PM. Disruption of either the E1 or the E2 regulatory gene of human papillomavirus type 16 increases viral immortalization capacity. Proc Natl Acad Sci U S A 1992;89:3159-3163.

17. Sano Dand Oridate N. The molecular mechanism of human papillomavirus-induced carcinogenesis in head and neck squamous cell carcinoma. Int J Clin Oncol 2016;21:819-826.

18. Stanley MA, Pett MRand Coleman N. HPV: from infection to cancer. Biochem Soc Trans 2007;35:1456-1460.

19. Tindle RW. Immune evasion in human papillomavirus-associated cervical cancer. Nat Rev Cancer 2002;2:59-65.

20. Yang A, Farmer E, Wu TC, et al. Perspectives for therapeutic HPV vaccine development. J Biomed Sci 2016;23:75.

Viral Immunology

FIGURE LEGENDS

Figure 1. Expression of E1 carboxyl-terminal domains and cross-reactivity of CD8+ T cells against B16-F0 cells expressing E1-ct from several HPVs. **A)** B16-F0 cells were transfected with pE1-CT/HPV6HA, pE1-CT/HPV11HA, pE1-CT/HPV16HA, pE1-CT/HPV31HA, pE1-CT/HPV33HA, pE1-CT/HPV53HA or pE1-CT/HPV18HA. The carboxyl-terminal domains were detected as 32 kDa hybrid polypeptides 24 h post-transfection by western blot, using an anti-HA antibody. Protein extracted from B16-F0 cells transfected with empty vector was used as negative control. β-actin expression ensures that a similar amount of lysate was loaded in each lane.

Acquisition of cell surface CD107a/b was measured as CD8+ T cell cytotoxic activity marker. Splenic T CD8+ cells from mice immunized or inoculated with: **B)** HPV18-E1$_{202\text{-}654}$ protein plus α-GalCer, **C)** PBS, **D)** α-GalCer and **E)** E1$_{202\text{-}654}$, were co-cultured for up to 4 h with B16-F0/E1-CT/HPV18HA, B16-F0/E1-CT/HPV53HA, B16-F0/E1-CT/HPV33HA, B16-F0/E1-CT/HPV16HA, B16-F0/E1-CT/HPV31HA, B16-F0/E1-CT/HPV11HA, B16-F0/E1-CT/HPV6HA or B16-F0 in the presence of anti-CD107a/b-Alexa Fluor 488, anti-CD8-Brillant Violet 421 and anti-CD3-APC. The increase of exposed cell surface CD107a/b indicates CD8+ T cell cytotoxic activity. The lower panels show representative flow cytometry images of cytotoxic activity assays where CD107a/b molecules are detected on cell surface. The statistical significance with $^{**}p < 0.01$ and $^{***}p < 0.0001$, by one-way ANOVA and Dunett post-tests Comparison is represented in the graph.
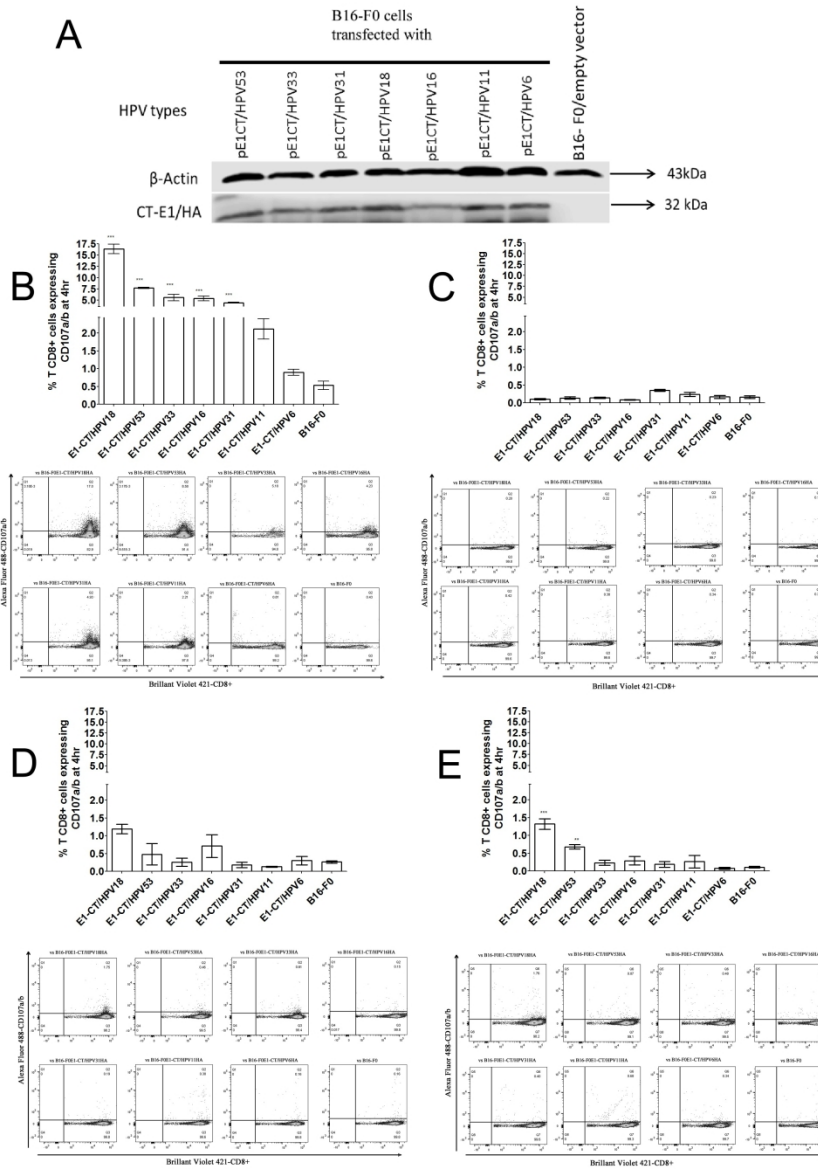
Figure 1. Expression of E1 carboxyl-terminal domains and cross-reactivity of CD8+ T cells against B16-F0 cells expressing E1-ct from several HPVs.

TABLE 1. Predicted conservation of peptides in the carboxyl-terminal domains of several E1-HPVs, which bind MHC class I murine proteins

	Peptide for MHC-I H2D^b 10 aa	Peptide for MHC-I H2D^b and H2K^b 9 aa	Peptide for MHC-I H2D^b 8 aa	Peptide for MHC-I H2D^b 8 aa	Peptide for MHC-I H2D^b and H2K^b 9 aa	Peptide for MHC-I H2D^b 10 aa	Peptide for MHC-I H2K^b 9 aa	Peptide for MHC-I H2D^b 8 aa
E1-CT/HPV18	KCPPILLTTN	NTGKSYFGM	PANTGKSY	KNGNPVYE	DSNSNAAAF	CGPANTGKSY	VQFLRYQQI	KNWKCFFE
E1-CT/HPV6	KCPPLLVTSN	DTGKSYFCM	PDDTGKSY	RNGNAVYE	DFDSNARAF	VGPPDTGKSY	VQFLRHQNI	ANWKCFFE
E1-CT/HPV11	KCPPLLVTSN	DTGKSCFCM	PDDTGKSC	RNGNAVYE	DFDSNARAF	VGPPDTGKSC	VQFLRHQNI	ANWKCFFE
E1-CT/HPV16	KCPPLLITSN	NTGKSLFGM	AANTGKSL	KNGNPVYE	DTNSNASAF	YGAANTGKSL	VMFLRYQGV	KNWKSFFS
E1-CT/HPV31	KCPPLLITSN	NTGKSYFGM	APNTGKSY	KNGNPVYE	DSDSNACAF	HGAPNTGKSY	VKFLRYQQI	KNWKSFFS
E1-CT/HPV33	KCPPLLLTSN	NTGKSYFGM	PANTGKSY	ENGNPVYA	DSNSNAAAF	CGPANTGKSY	VQLLRYQNI	ENWKSFFS
E1-CT/HPV53	KCPPVLITTN	NTGKSCFAM	PPNTGKSC	VNGNPVYQ	DVDSNAQAF	YGPPNTGKSC	VQFLRYQGV	ANWKCFFE

TABLE 1. Predicted conservation of peptides in the carboxyl-terminal domains of several E1-HPVs, which bind MHC class I murine proteins (Cont.)

	Peptide for MHC-I H2D^b 8 aa	Peptide for MHC-I H2K^b 9 aa	Peptide for MHC-I H2K^b 8 aa	Peptide for MHC-I H2K^b 8 aa	Peptide for MHC-I H2K^b 8 aa	Peptide for MHC-I H2D^b 9 aa	Peptide for MHC-I H2K^b 8 aa
E1–CT/HPV18	WKCFFERT	CKHYRRAQK	KHYRRAQK	RTWSRLDL	NSTSHFWL	GTPKKNCLV	SHFWLEPL
E1–CT/HPV6	WKCFFERL	CRHYKRAQQ	RHYKHAEM	RLSSSLDI	NSSSHFWL	GTPKKNCIA	SHFWLQPL
E1–CT/HPV11	WKCFFERL	CRHYKKAEK	RHYKHAEM	RLSSSLDI	NSCSHFWL	GTPKKNCIA	SHFWLQPL
E1–CT/HPV16	WKSFFSRT	CRHYKRAEK	RHYKRAEK	RTWSRLSL	NSKSHFWL	GIPKKNCIL	SHFWLQPL
E1–CT/HPV31	WKSFFSRT	CRHYKRAEK	RHYKRAEK	RTWCRLNL	NSKSHFWL	GVPKKNCIL	SHFWLQPL
E1–CT/HPV33	WKSFFSRT	CRHYKHAEM	RHYKRAEK	RTWCKLDL	NSKSHFWL	GIPKKSCML	SHFWLQPL
E1–CT/HPV53	WKCFFERT	CRHYKHAEM	RHYKRAQQ	RTWSRLDL	NSHSHFWL	GTPKHNCLV	SHFWLEPL

■ Indicates fully conserved residue with respect to the HPV18 sequence.

■ Indicates residues with strongly similar properties with respect to the HPV18 sequence.

■ Not conserved residue with respect to the HPV18 sequence

1
2
3
4
5
6
7
8
9
10
11
12
13
14
15
16
17
18
19
20
21
22
23
24
25
26
27
28
29
30
31
32
33
34
35
36
37
38
39
40
41
42
43
44
45
46
47
48
49
50
51
52
53
54
55
56
57
58
59
60

Supplementary Table 1

A) Clustal omega analysis of E6 peptide sequences from HPV6, 11, 53, 18, 33, 16 and 31.
    The analysis indicates that E6 from HPV types included in this table show identity from
    31.33 to 55.56%, compared with HPV18-E6.

HPV´s	6	11	53	18	33	16	31
6	100.00	81.33	38.67	31.33	33.56	35.33	32.89
11	81.33	100.00	35.33	34.00	33.56	34.00	31.54
53	38.7	35.33	100.00	42.76	51.01	47.40	54.36
18	31.33	34.00	42.76	100.00	46.31	55.56	51.68
33	33.56	33.56	51.01	46.31	100.00	62.42	58.39
16	35.33	34.00	47.40	55.56	62.42	100.00	64.43
31	32.89	31.54	54.36	51.68	58.39	64.43	100.00

B) Clustal omega analysis of E7 peptide sequences from HPV6, 11, 53, 18, 33, 16 and 31.
    The analysis indicates that E7 from HPV types included in this table show identity from
    39.81 to 44.33%, compared with HPV18-E7.

HPV´s	6	11	53	18	33	16	31
6	100.00	85.71	37.76	42.86	51.04	53.61	49.48
11	85.71	100.00	36.73	43.88	51.04	55.67	50.52
53	37.76	36.73	100.00	39.81	47.42	42.86	43.88
18	42.86	43.88	39.81	100.00	47.42	42.86	38.78
33	51.04	51.04	47.42	44.33	100.00	60.82	59.79
16	53.61	55.67	42.86	42.86	60.82	100.00	73.47
31	49.88	50.52	43.88	38.78	59.79	73.47	100.00

C) Clustal omega analysis of E2 peptide sequences from HPV6, 11, 53, 18, 33, 16 and 31.
    The analysis indicates that E2 from HPV types included in this table show identity from
    38.64 to 44.69%, compared with HPV18-E2.

HPV´s	6	11	53	18	33	16	31
6	100.00	78.14	41.92	38.64	42.86	45.66	43.80
11	78.14	100.00	41.60	39.89	43.97	45.79	45.86
53	41.92	41.60	100.00	42.54	39.77	43.49	43.87
18	38.64	39.89	42.54	100.00	43.27	43.06	44.69
33	42.86	43.97	39.77	43.27	100.00	51.87	47.88
16	45.66	45.79	43.49	43.06	51.87	100.00	62.74
31	43.80	45.86	43.87	44.69	47.88	62.74	100.00

D) Clustal omega analysis of E1-CT peptide sequences from HPV6, 11, 53, 18, 33, 16 and 31. The analysis indicates that E1-CT from HPV types in this table show identity from 59.43 to 67.61%, compared with HPV18-E1.

HPV´s	6	11	53	18	33	16	31
6	100.00	93.12	61.44	59.75	58.04	57.37	62.70
11	93.12	100.00	62.07	59.43	58.99	59.87	63.01
53	61.44	62.07	100.00	64.26	62.26	67.81	68.71
18	59.75	59.43	64.26	100.00	67.61	64.58	67.40
33	58.04	58.99	62.26	67.61	100.00	70.75	74.53
16	57.37	59.87	67.81	64.58	70.75	100.00	81.25
31	62.70	63.01	68.75	67.40	74.53	81.25	100.00

viruses

Review

Role of Innate Immunity against Human Papillomavirus (HPV) Infections and Effect of Adjuvants in Promoting Specific Immune Response

Alfredo Amador-Molina [1], José Fernando Hernández-Valencia [1], Edmundo Lamoyi [2], Adriana Contreras-Paredes [1] and Marcela Lizano [1,2,*]

[1] Unidad de Investigación Biomédica en Cáncer, Instituto Nacional de Cancerología, Av. San Fernando No. 22, Col. Sección XVI, Tlalpan 14080, Mexico; E-Mails: E-Mails: aamf17@hotmail.com (A.A.-M.); ferhv@hotmail.com (J.F.H.-V.); adrycont@yahoo.com.mx (A.C.-P.)

[2] Instituto de Investigaciones Biomédicas, Universidad Nacional Autónoma de México, Apartado postal 70228, Ciudad Universitaria, Distrito Federal CP 04510, Mexico; E-Mail: lamoyi@biomedicas.unam.mx

* Author to whom correspondence should be addressed; E-Mail: lizanosoberon@gmail.com; Tel.:+52-55-5573-4662.

Abstract: During the early stages of human papillomavirus (HPV) infections, the innate immune system creates a pro-inflammatory microenvironment by recruiting innate immune cells to eliminate the infected cells, initiating an effective acquired immune response. However, HPV exhibits a wide range of strategies for evading immune-surveillance, generating an anti-inflammatory microenvironment. The administration of new adjuvants, such as TLR (Toll-like receptors) agonists and alpha-galactosylceramide, has been demonstrated to reverse the anti-inflammatory microenvironment by down-regulating a number of adhesion molecules and chemo-attractants and activating keratinocytes, dendritic (DC), Langerhans (LC), natural killer (NK) or natural killer T (NKT) cells; thus, promoting a strong specific cytotoxic T cell response. Therefore, these adjuvants show promise for the treatment of HPV generated lesions and may be useful to elucidate the unknown roles of immune cells in the natural history of HPV infection. This review focuses on HPV immune evasion mechanisms and on the proposed response of the innate immune system,

suggesting a role for the surrounding pro-inflammatory microenvironment and the NK and NKT cells in the clearance of HPV infections.

1. Introduction

Cervical cancer is the second most common cancer in women worldwide, and human papillomavirus (HPV) infection is the main risk factor for developing this disease [1]. More than 100 HPV types have been identified [2] and 38 of them can infect the anogenital tract. According to their oncogenic potential, HPVs are classified as high- (HR-HPV) or low-risk (LR-HPV), with the former being associated with anogenital cancer and the latter, with genital warts or epithelial lesions. HPV16 is the type that is most frequently found in cases of cervical cancer, followed by HPV18 [3,4].

HPV is a DNA virus with a circular genome of approximately 8000 bp that contains an early region, encoding the early viral proteins E6, E7, E8, E1, E2, E4 and E5, and a late region, encoding L1 and L2 proteins, which are components of the viral capsid. The long control region (LCR) is a non-encoding region involved in replication and viral transcription.

The expression of the viral proteins is associated with the cell differentiation program, and these proteins are therefore differentially expressed in the layers of the cervical epithelium [5]. The proteins that are first expressed are E1 and E2, which regulate viral replication and transcription. The formation of an E1-E2 complex is required for the stable binding of the E1 helicase to the LCR ori site [6]. E2 is a transcriptional regulator of early expressed HPV genes; when E2 binds to the four E2-binding-domains in the LCR it controls the transcriptional levels of E6 and E7 viral oncogenes.

The transformation step is not a common occurrence of an HPV infection, and only a small number of cervical lesions infected with high-risk HPV types evolve into cervical cancer [7]. Sometimes, for yet unknown reasons, the HPV genome integrates randomly into the host DNA. During this process, the HPV DNA often breaks at any position within the E1-E2 region. When E2 is lost, E6 and E7 become actively expressed, promoting cervical transformation [8–10].

The immune response plays an important role in clearing most of these infections, but some infections cannot be eliminated and persist for several years, becoming an additional risk factor [11].

During the early stages of an HPV infection, the host innate immune response becomes the first line of defense against the infection. Dendritic (DC), Langerhans (LC), natural killer (NK), natural killer T (NKT) cells and keratinocytes, among others, are important cells involved in promoting a good adaptive immune response against HPV infection and are the focus of this review. Most of these cell types can promote a cytokine-mediated pro-inflammatory process, which links the innate with the adaptive immune response. Moreover, NK cells are able to directly eliminate HPV infected cells [12].

However, HPV can evade the immune response, mainly through the action of E6 and E7 proteins. The viral mechanisms of immune evasion range from modulation of cytokines and chemo-attractant

Figure 1. Schematic representation of the immunological microenvironment in a human papillomavirus (HPV) infection. (**a**) The predominant microenvironment induced by HPV promotes a down-regulation of antigen presentation, which triggers the following phenomena: (1) modulation of the cytokine-mediated inflammatory response of keratinocytes as the first line of defense against infection; (2) the inhibition of the activation and migration of Langerhans (LCs); and (3) evasion of the infiltration of dendritic cells (DCs) from the stroma. (**b**) The possible pro-inflammatory microenvironment in keratinocytes adjacent to the lesion. This microenvironment is characterized by   down-regulation of the anti-inflammatory cytokine IL-10 and the presence of activated   T-cells. The arrows with a question mark indicate an unknown process that could reverse the HPV-induced microenvironment.
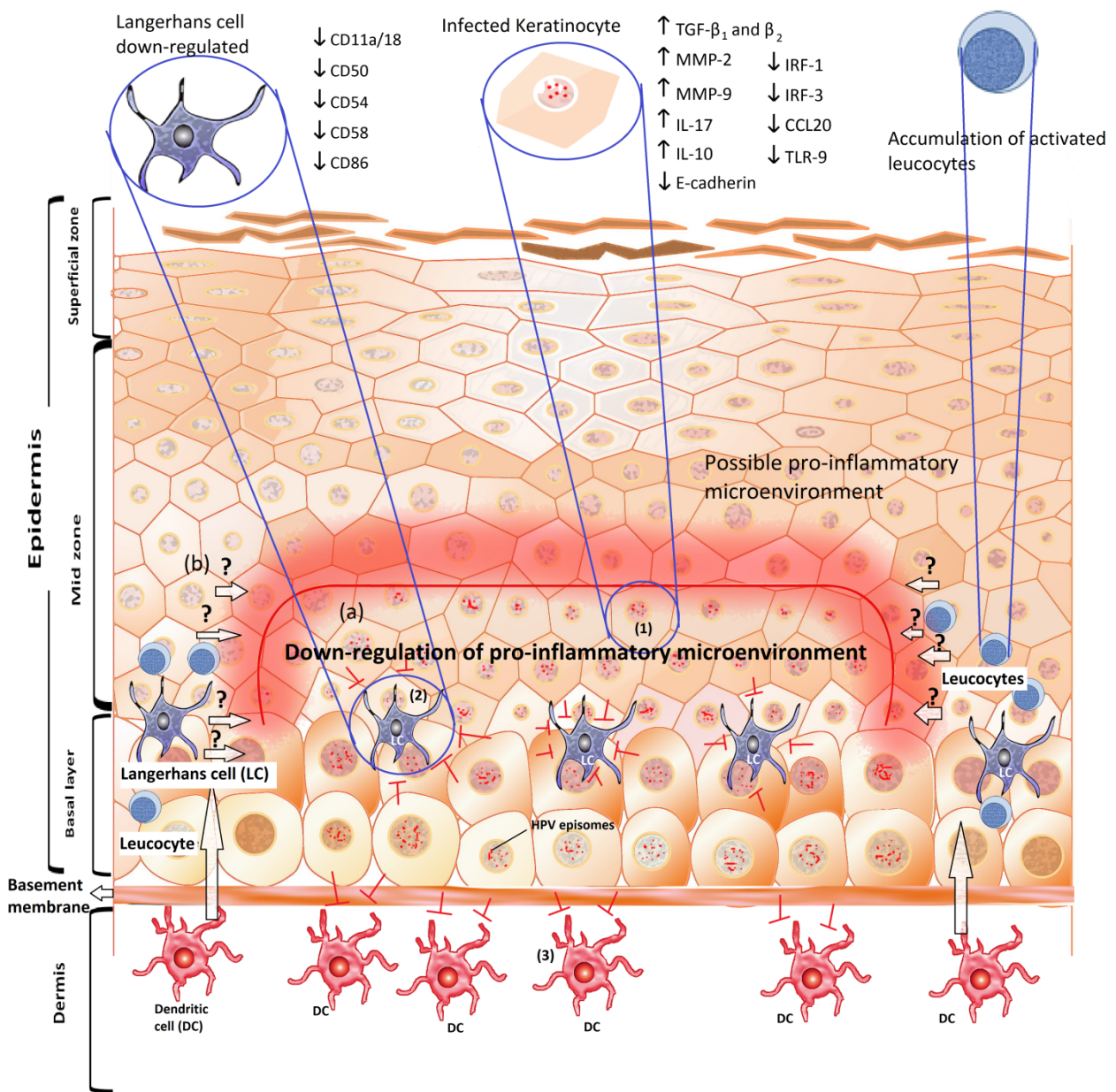
expression to alteration of antigen presentation, and down-regulation of IFN-pathways and adherence molecules [13]. Evasion of the immune response by HPV is critical for a successful infection.

Thus, stimulation of the innate immune response through strong adjuvants has turned out to be a promising therapeutic strategy for disrupting the evasion mechanisms of HPV and has been useful to understand the function of some innate immune cells during HPV infections.

2. Keratinocytes at the Initiation of HPV Infections

HPV infects keratinocytes of the basal layer of the cervical epithelium [14,15] and possibly stem cells [16,17]. As the main target of HPV, the keratinocyte plays an important role during the initiation of the HPV infection and subsequently becomes a link to promote an effective adaptive immune response. The keratinocytes are part of the innate immune defence system and have been considered as immune sentinels [18]. They can function as non-professional antigen presenting cells, and are able to induce the expression of T_{H1} and T_{H2} type cytokines and cytotoxic responses in CD4+ and CD8+ memory T cells, respectively [19]. Keratinocytes in female genital tracts express several Toll-like receptors (TLRs), located either on the cell surface (TLR-1, TLR-2, TLR-4, TLR-5 and TLR-6) or in the endosomes (TLR-3 and TLR-9) [20]. The TLRs are a family of immunological receptors that recognize pathogen-associated molecular patterns (PAMPs), their activation initiates signaling pathways that result in innate and adaptive immune responses. Endosomal TLRs play an important role in combating viral infections and in the recognition of viral nucleic acids; TLR-3 recognizes double-stranded RNA (dsRNA), TLR-7 and TLR-8 single-stranded RNA (ssRNA), and TLR-9 double stranded CpG-rich DNA. The activation of these receptors promotes the production of cytokines and creates a powerful pro-inflammatory environment [21–23], in particular, activation of TLR-9 in keratinocytes results in production of TNF-α, IL-8, CCL2, CCL20, CXCL9 and type 1 IFN [24,25]

HPV is able to modify cytokine levels as an immune evasion mechanism [26]. This strategy is mainly directed to down-regulate the pro-inflammatory response in cervical keratinocytes [18]. Figure 1 shows the up- and down-regulated cytokines that can be found in the microenvironment of an HPV infected tissue.

Interferons (IFNs) are components of the innate immune system that mediate intracellular protection against viruses through antiviral, anti-proliferative and immunostimulatory mechanisms [27]. The regression of HPV lesions could be related to an interferon response. However, HPV oncoproteins reduce the IFN and MCP1 secretion by the keratinocyte; HPV18-E7 can reduce IRF-1 expression in cervical tissue from transgenic mice expressing HPV18 E6/E7 [28], while HPV18-E6 can inhibit the phosphorylation of molecules involved in IFN signaling as Tyk2 kinase, STAT1 and STAT2, in cervical cancer cell lines [29]. Interestingly, HPV16 positive patients with pre-malignant lesions respond to IFN-α treatment more effectively when the levels of E7 transcripts are low.

Keratinocytes containing episomal copies of HR-HPV display a large number of deregulated genes involved in chemotactic and pro-inflammatory mechanisms; down-regulated genes are involved in an innate and adaptive immune response as well as KC differentiation [30]. These results emphasise the importance of the keratinocyte as an initiator of the immune response against HPV and as a link to the adaptive immune response.

3. Role of DCs in HPV Infections

The professional antigen presenting cells (APC) orchestrate a T-cell-inducing response, which has been correlated with good clinical prognosis [31]. DCs are APC that promote T-cell immune response through the capture and presentation of antigens [32]. Human DCs in skin comprise LC cells in epidermis and three subsets in dermis, characterized by the expression of CD1a+, CD14+, or CD141+ [33]. There are several functional and phenotypic differences between LCs and DCs in skin: LC express fewer TLRs including -1, -2, -3, -6, -10 and promote CD8+ T cell responses through IL-15 [34,35], whereas dermal CD14+ DCs express TLR-2, -4, -5, -6, -8, -10 [36] and produce IL-1α, TGF-β, IL-10, IL-12, GM-CSF, IL-6 and IL-8 [35,36]. To generate an effective immune cellular response, the epithelium should be communicated with LCs and DCs.

Immunosuppressive DC subsets have also been described in humans. Nevertheless, their role in HPV infections is not yet clear. The suppressive role of some DC subsets has been explained through the activation of regulatory T cells (T$_{reg}$) [37]. A suppressive phenotype on murine DCs can also be conferred by immune-regulatory molecules as indoleamine 2,3-dioxygenase (IDO) 1; conventional and plasmacytoid dendritic cells expressing IDO1 mediate a potent T cell suppression that predominates over the T cell stimulatory properties of other DCs, promoting suppression of antitumor immune responses [38,39]. A skin graft of HPV16-E7 transgenic mice with infiltrating langerin^{-ve} dermal dendritic cells expressing IDO1 is not rejected in non-transgenic mice; but the inhibition of IDO1 activity promotes E7-skin graft rejection [40].

The immune-regulatory programmed death-1 (PD-1) molecule and its ligand (PD-L1) are molecules that can also confer a DC immunosuppressive phenotype. PD-1 and PDL-1 are both commonly expressed on lymphocytes; the interaction of PD-1 on T-cells with its ligand expressed on APC promotes T-cell functional exhaustion and anergy [41,42]. The DC-PD-L1+ population is more abundant in cervical cells from HR-HPV (+) patients without intraepithelial neoplasia than in HR-HPV (−) patients; therefore, DC-PD-L1+ subset is possibly associated with the down-regulation of T$_{H1}$-type cytokines in HR-HPV (+) patients [43].

The complete characterization of DC subsets will be necessary to understand the role of APC in HPV immune evasion mechanisms as well as to identify the success or failure of future treatments through vaccines and/or new adjuvants.

The migration and adhesion of APC are essential mechanisms during the initiation of an immune response against HPV infection, but unfortunately for the host, HPV can modulate APC adhesion and migration [44,45]. Down-regulation of E-cadherin by E6 and E7 disrupts the adhesion of keratinocytes to LCs [44]. However, silencing of E7 oncogene in HPV16-infected keratinocytes has been shown to restore E-cadherin expression [46]. Silencing both E6 and E7 allows the re-expression of CCL20 in HPV-positive cell lines; CCL20 is an important chemokine involved in the infiltration of immature LC to the epithelium [45,47].

A decrease in LC numbers has been found in cervical intraepithelial neoplasia (CIN) and is associated with the severity of the lesion [48]. LCs in CIN show little or no expression of the adhesion/costimulatory molecules CD11a/18, CD50, CD54, CD58 and CD86, suggesting a poor antigen-presenting environment. On the other hand, the expression of HLA-DR, CD54 and CD58 in keratinocytes increases with disease severity, which together with the observed accumulation of

activated leucocytes below the lesion, point to the development of a CIN-related but weak immune response since TNFα is down-regulated and IL-10 expression is increased [49]. Whether such a response causes spontaneous regression of the lesion or clearance of the infection is uncertain.

Escape from the immune-surveillance induced by HPV also impacts the number of LC. In α-, γ- and μ-HPV infections, the LC population decreases, in contrast to β-HPV infections [50]. Therefore, important effects of HPV infection on the development of a cervical neoplasia include interference of the keratinocyte response, a decrease in the number of LC and down-regulation of LC activation markers. Figure 1b illustrates a CIN-related immune response, with a possible pro-inflammatory microenvironment at the epithelium adjacent to the lesion.

4. Down-Regulation of Toll-Like Receptors by HPV and the Use of TLR Agonists to Improve Immunity

The main TLR in relation to double-stranded DNA virus infection is TLR-9. The expression of this TLR is down-regulated in keratinocytes expressing the HPV16 and HPV-18 E6 and E7 proteins, in HPV16-positive cervical cancer samples and in HPV positive cell lines. TLR-9 expression can be rescued by silencing of E6 and E7 using siRNAs [51].

TLR-9 synthetic agonists have been used as a strategy against E7-expressing tumors in animal model systems. Figure 2a–c displays the proposed modulation of the innate immune response following adjuvant stimulation during HPV infection. In mice challenged with tumor cells constitutively expressing E6 and E7, the coinjection of recombinant E7 with ODN—oligodeoxinucleotide composed of unmethylated CpGs motifs (as depicted in Figure 2c)—induce a strong immunostimulatory effect resulting in a significant suppression of tumor formation, both prophylactically and therapeutically. The tumor protection appears to be driven by the activation of CD4+ and mostly by CD8+ T-cells, as demonstrated by *in vivo* T-cell subset depletion [52,53]. Table 1 describes different treatments that have been applied in order to improve immune response against HPV antigens.

Other TLR agonists that show non-canonical action against DNA virus infections also promote an efficient response against HPV proteins. Such agonists include 3M-002 (TLR-8 agonist) and resiquimod (TLR-8 and 7 agonist), which together with virus-like-particle VLP-L1-L2 or VLP-L1-L2-E7 (Table 1), are able to activate LCs, to induce the overexpression of chemokines and pro-inflammatory T_{H1} cytokines (MIP, IL-6, TNF-α, IL-12 and IL-8), to stimulate LC migration related to CCL21, and to induce a specific CD8+ T-cell response [54]. In contrast, the single antigenic stimulation with either of the HPV16 antigens is not sufficient to initiate an effective immune response and promote cytokine production [54]. A possible role of 3M-002 and resiquimod in human HPV-infected tissue is depicted in Figure 2c. The Lipopolysaccharide TLR-4 agonist (LPS) and the polyinosinic acid-polycytidylic acid TLR-3 agonist (PIC), together with HPV11/E7 epitopes, can up-regulate CD40, CD80, CD86, CD83, HLA-DR, cytokines, as IL-12 and IFN-γ, in monocyte-derived dendritic cells (mdDC), and can also promote specific cytotoxic T lymphocyte response [55] (Table 1). A possible role of PIC and LPS in human HPV infected tissue is depicted in Figure 2c.

Figure 2. Schematic representation of the role of the innate immune response following adjuvant stimulation during HPV infection. (**a**) Stimulation of natural killer T (NKT) cells using α-GalCer, together with HPV-antigens, promotes CD4+ and CD8+ T cells antigen-specific responses and the rapid release of high levels of inflammatory cytokines, such as IFN-γ. (**b**) NK cells can kill HPV-infected cells, following their indirect activation through adjuvants such as α-GalCer and Toll-like receptor (TLR) agonists, via IFN-γ. (**c**) The induction of a pro-inflammatory response through TLR agonists rescues keratinocytes from the HPV-induced microenvironment to promote antigen presentation.
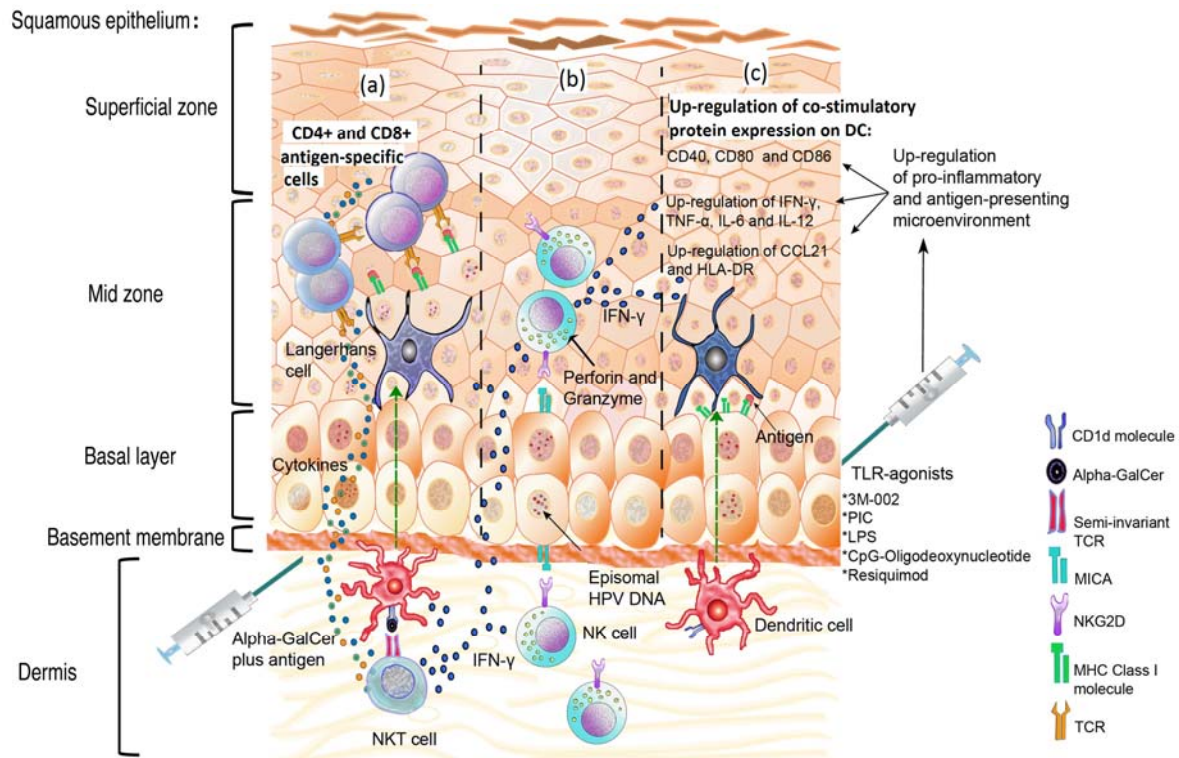
The ability to induce CD8+ T cells using TLR agonists is a useful finding, obtained from the study of adjuvants that aimed to promote a successful long-term immune response against intracellular pathogens. Therefore, the examination of TLR agonists against HPV proteins has become a promising field of inquiry, offering new possibilities for using adjuvants to promote a cellular response for the production of future HPV vaccines. TLR agonists could be useful in treatments intended to disrupt the anti-inflammatory microenvironment generated by E6-E7 HPV positive cells and the tolerance produced by HPV oncoproteins.

Table 1. Treatments used to improve immune response against HPV antigens.

Treatment	Effect	Model	Reference
CpG ODN (TLR-9 agonist) + E7 recombinant protein	Suppression of tumor formation.	Mouse	[52,53]
3M002 (TLR-8 agonist), resiquimod or (TLR-8 and 7 agonist) + VLP-L1-L2 or VLP-L1-L2-E7	Overexpression of chemokines and pro-inflammatory T_{H1} cytokines (MIP, IL-6, TNF-α, IL-12, IL-8). Stimulation of LC migration related to CCL21. Induction of specific CD8+ T cell response.	Human immune cells isolated from peripheral blood lymphocyte (PBL)	[54]
LPS (Lipopolysaccharide) TLR-4 agonist or polyinosinic acid-polycytidylic acid (PIC, TLR-3 agonist) + HPV11-E7 epitopes.	Up-regulation of CD40, CD80, CD86, CD83, HLA-DR, IL-12 and IFN-γ, in monocyte-derived dendritic cells (mdDC). Promotion of specific cytotoxic T lymphocyte response.	Human immune cells isolated from PBL	[55]
Live or inactivated *Listeria monocytogenes* or endotoxin.	Promote E7-specific T CD8+ cell immune response.	E7-Skin graft challenge.	[56]
Hydralazine and valproate	Decrease of soluble MICA and increase of susceptibility of target cells to NK attack.	NK cells isolated from PBL and tumor cells lines.	[57]
Short hairpin RNA (shRNA) plasmid targeting the IDO gene	Susceptibility to NK cell attack.	*In vitro* assays.	[58]
Gardasil HPV vaccine	Induction of protective antibodies. Increase NK cell population following immunization. Increase of the expression of NKG2D, NKp30, Nkp46 and ILT2 receptors.	Peripheral blood samples from vaccinated patients.	[26,59]
α-GalCer + DNA vaccine encoding the HPV16-E7 oncoprotein.	Increase of E7-specific CD8+ T cells and inhibition of tumor growth.	Mouse	[60]
β-GalCer	Inhibition of TC-1-tumor growth.	Mouse	[61]
B subunit of Shiga toxin coupled with ovalbumin or the E7 polypeptide + α-GalCer	Break tolerance generated against self Ag-elicited antiviral immunity	Mouse	[62]

5. The Pro-Inflammatory Response: Deregulation of the Link between the Innate and the Acquired Immune Responses

Some findings have suggested that HPV immune evasion mechanisms may act in the early stages of infection as a necessary mechanism for successful viral infection. The microenvironment of low-grade cervical lesions is predominantly anti-inflammatory, and is modified in a way that favors HPV infection. In cervical secretions obtained from low-grade squamous intraepithelial lesions (LSIL) from HPV-positive patients, higher levels of IL-10 are found compared to HPV-negative patients [63].

IL-10 is not always found in LSIL; nevertheless, there is evidence of over-expression of other anti-inflammatory cytokines, such as TGF-β1 and TGF-β2 [64].

Once the infection has been established, E6 expression leads to IL-17 up-regulation, which might constitute an important step for tumor development and progression, as demonstrated in E6-positive lung tumor cells [65]. IL-17 promotes angiogenesis and tumor growth [66], and as a component of the IL-17 signaling pathway, the IL-8, which is involved in angiogenesis and metastasis, is also up-regulated by E6 in adenocarcinoma lung cells. This IL-8 up-regulation is correlated with the expression of the MMP-2 and MMP-9 metalloproteinases, which are involved in angiogenic mechanisms [67] (Figure 1a). Modulation of the pro-inflammatory response may be an important step during HPV-carcinogenesis, a process that includes the establishment of the infection, persistence, progression, angiogenesis and metastasis.

The induction of a pro-inflammatory response can be used as a tool to break the tolerance induced by HPV [56]. The effectiveness of this approach has been demonstrated in models of E7-transgenic as well as non-transgenic mice, that when receiving an E7 transgenic skin graft were unable to respond to the E7 antigen. In these mice, stimulation with live or inactivated *Listeria monocytogenes* or endotoxin was sufficient to promote an E7-specific, CD8+ T cell immune response leading to the rejection of E7-grafts [56] (Table 1). Therefore, the successful initiation of pro-inflammatory signaling is important for developing new treatments to induce an effective immune response and disrupt the anti-inflammatory barrier triggered by HPV infections.

6. Natural Killer Cells: An Important Barrier against Cells Expressing HPV Antigens

NK cells represent an important barrier and a key component of the innate immune system. These cells have the capacity to recognize and kill virus-infected and transformed cells through two mechanisms: granule-dependent cytotoxicity; and the apoptosis pathway in the target cells [68] Nevertheless, tumor cells have developed mechanisms to evade being attacked by NK cells, and viruses such as HPV display intrinsic strategies for preventing infected cells from being easily eliminated by NK cells.

NK cell activity is tightly regulated through a balance between inhibitory and activating receptors [69]. However, deregulation of these receptors is common in cancer and HPV infections. NKp30 and NKp46 receptors are found at low levels in NK cells from patients with cervical cancer and precursor lesions, which is correlated with low cytotoxic activity of NK cells [70].

Another important receptor in NK cells that is related to cytotoxicity is NKG2D. This receptor is involved in cell lysis through the interaction with the major histocompatibility complex class I-related chain A (MICA) proteins. Both NKG2D and MICA are modulated in the presence of HPV-infection. Furthermore, the levels of free-MICA in serum are increased in association with cervical cancer progression, which suggests that a significant factor that contributes to HPV persistence or tumor progression could be the presence of soluble MICA in the serum [71]. In a NK cell line (NKL), it was found that the NKG2D receptor was down-regulated when the NKL was co-cultured with cervical cancer cell lines HeLa, SiHa, or C33A, but not with immortalized keratinocytes HaCaT [72]. This down-regulation of NKG2D in the NKL was associated with a reduced cytotoxic activity after contact

with the HPV-positive cancer cell lines (HeLa, SiHa), but not after contact with HPV-negative cell line C33, or non-tumorigenic HaCat cell line [72].

Certain drugs are able to reduce MICA plasmatic levels, allowing the attack of NK cell to target cells that express MICA. For example, the administration of hydralazine and valproate can increase the expression of MICA and MICB ligands in the CaSki cervical cancer cell line and reduce their shedding to the supernatant, allowing NK attack; while cells without hydralazine and valproate are not susceptible to NK attack [57] (Table 1).

Several studies have evaluated the association of HLA class I and class II genes with susceptibility to cervical cancer [73,74], and their findings support the association of HLA polymorphisms with the risk of cervical neoplasia.

HPV can affect NK cells through different target molecules. Carcinoembryogenic antigen-related cell adhesion molecule 1 (CEA-CAM1) mediates NK cytotoxicity. CEA-CAM1 expression is increased in patients with high-grade squamous intraepithelial lesions (HSIL) in contrast to what is observed in LSIL, in which CEA-CAM1 is undetectable or present at a low level [75].

HPV can also evade the cytotoxic mechanisms of NK cells through the alteration of immunosuppressive enzyme indoleamine-2,3-dioxygenase (IDO), and IDO expression is correlated with the escape of tumor cells from immune surveillance [76]. The absence of IDO is related to increased NK cell activity. CaSki cells transfected with a short hairpin RNA (shRNA) plasmid targeting the IDO gene (shIDO) are more susceptible to NK cell attack *in vitro* than control cells (CaSki/Mock). Additionally, an *in vivo* assay performed in BALB/c nude mice revealed a greater accumulation of NK cells in the stroma of CaSki/shIDO formed tumors than in control subcutaneous tumors. Moreover, low level of IDO increases the susceptibility of cervical cancer cells to NK cells, suggesting that IDO-targeted shRNAs may represent an effective molecular targeted therapy for cervical cancer [58] (Table 1).

Although some of the mechanisms employed by HPV to avoid NK cell activity are known, the role of NK cells in the natural history of infection is not entirely clear. Moreover, there are few studies addressing the effects of adjuvants or drugs that might increase the number of NK cells and their cytotoxic activity against HPV infected cells during the early stages of infection or against HPV-positive tumor cells, in the later stages. As shown in Figure 2, some adjuvants may indirectly activate NK cells via IFN-γ (Figure 2).

The currently available Gardasil HPV vaccine can increase the NK cell population following immunization, which is associated with increased expression of NKG2D, NKp30, Nkp46 and ILT2 receptors in NK cells, suggesting the contribution of other pathways, besides the increase in neutralizing antibodies, involved in vaccine effectiveness [59] (Table 1). A detailed understanding of NK cell responses could lead to the generation of new and more effective immunotherapies against HPV-related cancer and/or early infections.

7. The Promising Role of NKT Cells in Controlling HPV Infection

Invariant or type 1 natural killer T cells (iNKT) are a group of T lymphocytes defined as CD1d1-restricted T cells that express a semi-invariant αβ T cell antigen receptor (TCR) and surface antigens typically associated with natural killer cells such as CD161 in humans [77–79].

The TCR found on type 1 NKT cells recognize glycolipid antigens presented by the MHC class I-related glycoprotein CD1d, which are expressed abundantly on antigen-presenting cells and other cell types. There are two ways in which iNKT cells are activated: directly, via engagement of the invariant TCR with glycolipid antigens and CD1d molecules, and indirectly, via activated antigen-presenting cells. After stimulation, iNKT cells rapidly secrete large amounts of various cytokines including IFN-γ, TNF, IL-4, IL-10 and IL-3, among others [80,81].

Due to the reciprocal activation of NKT cells and DC, synthetic NKT ligands constitute promising new vaccine adjuvants [82]. One of the best-studied antigens is α-galactosylceramide (α-GalCer), a molecule originally isolated from sponge *Agelas mauritianus*; closely related glycolipids are found in a broad range of microorganisms including bacteria of the genera *Novosphingobium*, *Borrelia* and *Streptococcus* [83,84]. A potent variant of α-GalCer called KRN7000 can enhance the immune system response against tumors, viruses, bacteria and parasites [83,85].

While the α-GalCer is one molecule that has been demonstrated to strongly stimulate NKT cells, there are endogenous antigens that can also stimulate NKT cells [86]; however, their activation capacity is lower than that of α-GalCer. Although HPV does not have NKT-stimulating glycolipids, whether HPV infection can modify the profile of endogenous glycolipids which can be presented to iNKT cells is unclear.

NKT cells have long been implicated in tumor immunity. In a murine model of adoptive immunotherapy using an established tumor expressing E7 from HPV16 (TC-1), NKT cells were necessary to inhibit early but not late tumor growth [87].

The role of NKT cells in the spontaneous regression of HPV lesions is uncertain. Results from immunodeficient or immunocompetent individuals suggest that the immune system has a significant role in the success or failure of spontaneous clearance [88]. However, the level of circulating NKT cells is not associated with the severity of infection or progression to cervical cancer [89]. Since HPV is a local infection, understanding the contribution of NKT cells in infected cervical tissue is necessary to identify the determinants of HPV clearance.

Despite the unclear role of NKT cells in HPV infections, there is evidence of immune evasion mechanisms that have been developed by HPV to avoid NKT cell activity. Some of these mechanisms are related to decreased CD1d expression, as observed *in vivo* in cervical HPV-infected tissues and *in vitro* in the C33A/CD1d+ and Vag/CD1d+ cell lines, which are stably transfected with HPV6 E5 and HPV16 E5, respectively. In these cell lines, the E5 protein targets CD1d to the cytosolic proteolytic pathway by inhibiting calnexin-related CD1d trafficking [90]. Thus, reduced CD1d expression may represent a strategy for HPV-infected cells to evade protective immunological surveillance during early stages of infection.

Research on α-GalCer has made an important contribution to the understanding of the role of NKT cells during HPV-infection (as depicted in Figure 2). In a mouse model, with TC-1 tumor cells (expressing E6 and E7), the number of E7-specific CD8+ T-cells was found to be increased when α-GalCer was administered as an adjuvant in addition to DNA vaccine encoding the HPV16 E7 oncoprotein; in addition, this treatment generated potent anti TC-1 tumor effects [60] (Table 1). Administration of β-GalCer(C12) without HPV antigen was also able to inhibit the growth of TC-1 at the early stages of tumor progression [61] (Table 1).

As depicted in Figure 2a,b α-GalCer coadministered with several immunogens such as proteins, recombinant virus and tumor cells has been shown to augment the level of antigen-specific CD8 T cell response [91–93]. Administration of the B subunit of Shiga toxin coupled with ovalbumin or the E7 polypeptide plus α-GalCer results in a powerful CD8 response, breaking tolerance generated against self-antigen and protection against a challenge with OVA-expressing vaccinia virus; the effect was not observed with other adjuvants such as TLR-9 or TLR-3 agonists, or IFN-α [62] (Table 1). Treatment of antigen-activated CD8+ T cells with α-GalCer before adoptive transfer to tumor-bearing mice resulted in increased numbers of antigen-specific CD8+ T cells and cytotoxic activity; this effect involved iNKT and DC cells [94]. These results demonstrate the potential of NKT ligands to be used as therapeutic molecules for treating HPV-associated cancers.

Recently, immunosuppressive functions of NKT cells in transgenic mouse models expressing the HPV16 E7 protein in epidermal keratinocytes have been described [95,96]. CD1d-restricted NKT cells infiltrating E7-positive skin grafts inhibit their rejection, through the secretion of IFN-γ [95]. In addition, NKT cells from the lymph nodes draining the skin graft were capable of suppressing CD8 T cell proliferation, cytokine production and cytotoxic activity [96].

There are currently few available reports addressing the role of NKT cells in precancerous and cervical cancer lesions and their impact on the microenvironment surrounding HPV-infected cervical tissue. Understanding the role of NKT cells in cervical cancer will be useful for the design of alternative ways for immunotherapy.

8. Perspectives

Despite the great efforts exerted in HPV-vaccination programs, cervical cancer still represents the second most common cancer in women. Therefore, the mechanisms involved in HPV clearance and HPV immune evasion should be settled.

Innate immunity is the first barrier associated with HPV clearance through promoting humoral or cellular immune responses. The study of new molecules that stimulate the innate immune response, mainly through adjuvants, represents a new possibility to understand the mechanisms of innate immune evasion induced by HPV and the unclear role of the microenvironment surrounding an HPV infection. Such research could aid in the identification of new targets and the design of efficient therapies for treating HPV infections, where the complexity of tumor immunosuppressive mechanisms should be considered.

Recent studies using TLR agonists and α-GalCer adjuvants have shed light on the unclear roles of the surrounding environment and NKT cells, respectively, during HPV infections. However, exploring new adjuvants, or other molecules such as shRNAs targeting immunosuppressive molecules, will be necessary to improve our understanding of the role of NK cells in HPV infections.

Acknowledgments

Conflicts of Interest

The authors declare no conflict of interest.

References

1. Parkin, D.M.; Bray, F.; Ferlay, J.; Pisani, P. Global cancer statistics, 2002. *CA Cancer J. Clin.* **2005**, *55*, 74–108.
2. Walboomers, J.M.; Jacobs, M.V.; Manos, M.M.; Bosch, F.X.; Kummer, J.A.; Shah, K.V.; Snijders, P.J.; Peto, J.; Meijer, C.J.; Munoz, N. Human papillomavirus is a necessary cause of invasive cervical cancer worldwide. *J. Pathol.* **1999**, *189*, 12–19.
3. Clifford, G.M.; Smith, J.S.; Aguado, T.; Franceschi, S. Comparison of HPV type distribution in high-grade cervical lesions and cervical cancer: a meta-analysis. *Br. J. Cancer* **2003**, *89*, 101–105.
4. Clifford, G.M.; Smith, J.S.; Plummer, M.; Munoz, N.; Franceschi, S. Human papillomavirus types in invasive cervical cancer worldwide: A meta-analysis. *Br. J. Cancer* **2003**, *88*, 63–73.
5. Doorbar, J. Papillomavirus life cycle organization and biomarker selection. *Dis. Markers* **2007**, *23*, 297–313.
6. Kasukawa, H.; Howley, P.M.; Benson, J.D. A fifteen-amino-acid peptide inhibits human papillomavirus E1-E2 interaction and human papillomavirus DNA replication *in vitro*. *J. Virol.* **1998**, *72*, 8166–8173.
7. Bosch, F.X.; Lorincz, A.; Munoz, N.; Meijer, C.J.; Shah, K.V. The causal relation between human papillomavirus and cervical cancer. *J. Clin. Pathol.* **2002**, *55*, 244–265.
8. Jeon, S.; Allen-Hoffmann, B.L.; Lambert, P.F. Integration of human papillomavirus type 16 into the human genome correlates with a selective growth advantage of cells. *J. Virol.* **1995**, *69*, 2989–2997.
9. Spartz, H.; Lehr, E.; Zhang, B.; Roman, A.; Brown, D.R. Progression from productive infection to integration and oncogenic transformation in human papillomavirus type 59-immortalized foreskin keratinocytes. *Virology* **2005**, *336*, 11–25.
10. Jeon, S.; Lambert, P.F. Integration of human papillomavirus type 16 DNA into the human genome leads to increased stability of E6 and E7 mRNAs: Implications for cervical carcinogenesis. *Proc. Natl. Acad. Sci. USA* **1995**, *92*, 1654–1658.
11. Zur Hausen, H. Papillomavirus infections − a major cause of human cancers. *Biochim. Biophys. Acta* **1996**, *1288*, F55–F78.
12. Renoux, V.M.; Bisig, B.; Langers, I.; Dortu, E.; Clemenceau, B.; Thiry, M.; Deroanne, C.; Colige, A.; Boniver, J.; Delvenne, P.; Jacobs, N. Human papillomavirus entry into NK cells requires CD16 expression and triggers cytotoxic activity and cytokine secretion. *Eur. J. Immunol.* **2011**, 41, 3240-3252.
13. Kanodia, S.; Fahey, L.M.; Kast, W.M. Mechanisms used by human papillomaviruses to escape the host immune response. *Curr. Cancer Drug Targets* **2007**, *7*, 79–89.
14. Sterling, J.C.; Skepper, J.N.; Stanley, M.A. Immunoelectron microscopical localization of human papillomavirus type 16 L1 and E4 proteins in cervical keratinocytes cultured *in vivo*. *J. Investig. Dermatol.* **1993**, *100*, 154–158.

15. Stanley, M.A. Replication of human papillomaviruses in cell culture. *Antivir. Res.* **1994**, *24*, 1–15.

16. Maglennon, G.A.; McIntosh, P.; Doorbar, J. Persistence of viral DNA in the epithelial basal layer suggests a model for papillomavirus latency following immune regression. *Virology* **2011**, *414*, 153–163.

17. Gravitt, P.E. Evidence and impact of human papillomavirus latency. *Open Virol. J.* **2012**, *6*, 198–203.

18. Nestle, F.O.; di Meglio, P.; Qin, J.Z.; Nickoloff, B.J. Skin immune sentinels in health and disease. *Nat. Rev. Immunol.* **2009**, *9*, 679–691.

19. Black, A.P.; Ardern-Jones, M.R.; Kasprowicz, V.; Bowness, P.; Jones, L.; Bailey, A.S.; Ogg, G.S. Human keratinocyte induction of rapid effector function in antigen-specific memory CD4+ and CD8+ T cells. *Eur. J. Immunol.* **2007**, *37*, 1485–1493.

20. Nasu, K.; Narahara, H. Pattern recognition via the toll-like receptor system in the human female genital tract. *Mediat. Inflamm.* **2010**, *2010*, 976024.

21. Takeda, K.; Kaisho, T.; Akira, S. Toll-like receptors. *Annu. Rev. Immunol.* **2003**, *21*, 335–376.

22. Sanghavi, S.K.; Reinhart, T.A. Increased expression of TLR3 in lymph nodes during simian immunodeficiency virus infection: Implications for inflammation and immunodeficiency. *J. Immunol.* **2005**, *175*, 5314–5323.

23. Yang, K.; Puel, A.; Zhang, S.; Eidenschenk, C.; Ku, C.L.; Casrouge, A.; Picard, C.; von Bernuth, H.; Senechal, B.; Plancoulaine, S.; *et al*. Human TLR-7-, -8-, and -9-mediated induction of IFN-alpha/beta and -lambda Is IRAK-4 dependent and redundant for protective immunity to viruses. *Immunity* **2005**, *23*, 465–478.

24. Lebre, M.C.; van der Aar, A.M.; van Baarsen, L.; van Capel, T.M.; Schuitemaker, J.H.; Kapsenberg, M.L.; de Jong, E.C. Human keratinocytes express functional Toll-like receptor 3, 4, 5, and 9. *J. Investig. Dermatol.* **2007**, *127*, 331–341.

25. Miller, L.S.; Modlin, R.L. Human keratinocyte Toll-like receptors promote distinct immune responses. *J. Investig. Dermatol.* **2007**, *127*, 262–263.

26. Stanley, M.A. Epithelial cell responses to infection with human papillomavirus. *Clin. Microbiol. Rev.* **2012**, *25*, 215–222.

27. Le Bon, A.; Tough, D.F. Links between innate and adaptive immunity via type I interferon. *Curr. Opin. Immunol.* **2002**, *14*, 432–436.

28. Um, S.J.; Rhyu, J.W.; Kim, E.J.; Jeon, K.C.; Hwang, E.S.; Park, J.S. Abrogation of IRF-1 response by high-risk HPV E7 protein *in vivo*. *Cancer Lett.* **2002**, *179*, 205–212.

29. Li, S.; Labrecque, S.; Gauzzi, M.C.; Cuddihy, A.R.; Wong, A.H.; Pellegrini, S.; Matlashewski, G.J.; Koromilas, A.E. The human papilloma virus (HPV)-18 E6 oncoprotein physically associates with Tyk2 and impairs Jak-STAT activation by interferon-alpha. *Oncogene* **1999**, *18*, 5727–5737.

30. Karim, R.; Meyers, C.; Backendorf, C.; Ludigs, K.; Offringa, R.; van Ommen, G.J.; Melief, C.J.; van der Burg, S.H.; Boer, J.M. Human papillomavirus deregulates the response of a cellular network comprising of chemotactic and proinflammatory genes. *PLoS One* **2011**, *6*, e17848.

31. Eiben, G.L.; Velders, M.P.; Kast, W.M. The cell-mediated immune response to human papillomavirus-induced cervical cancer: Implications for immunotherapy. *Adv. Cancer Res.* **2002**, *86*, 113–148.

32. Banchereau, J.; Steinman, R.M. Dendritic cells and the control of immunity. *Nature* **1998**, *392*, 245–252.

33. Valladeau, J.; Saeland, S. Cutaneous dendritic cells. *Semin. Immunol.* **2005**, *17*, 273–283.

34. Van der Aar, A.M.; Sylva-Steenland, R.M.; Bos, J.D.; Kapsenberg, M.L.; de Jong, E.C.; Teunissen, M.B. Loss of TLR2, TLR4, and TLR5 on Langerhans cells abolishes bacterial recognition. *J. Immunol.* **2007**, *178*, 1986–1990.

35. Klechevsky, E.; Banchereau, J. Human dendritic cells subsets as targets and vectors for therapy. *Ann. N. Y. Acad. Sci.* **2013**, *1284*, 24–30.

36. Klechevsky, E.; Liu, M.; Morita, R.; Banchereau, R.; Thompson-Snipes, L.; Palucka, A.K.; Ueno, H.; Banchereau, J. Understanding human myeloid dendritic cell subsets for the rational design of novel vaccines. *Hum. Immunol.* **2009**, *70*, 281–288.

37. Huang, L.; Baban, B.; Johnson, B.A., 3rd; Mellor, A.L. Dendritic cells, indoleamine 2,3 dioxygenase and acquired immune privilege. *Int. Rev. Immunol.* **2010**, *29*, 133–155.

38. Munn, D.H.; Sharma, M.D.; Hou, D.; Baban, B.; Lee, J.R.; Antonia, S.J.; Messina, J.L.; Chandler, P.; Koni, P.A.; Mellor, A.L. Expression of indoleamine 2,3-dioxygenase by plasmacytoid dendritic cells in tumor-draining lymph nodes. *J. Clin. Investig.* **2004**, *114*, 280–290.

39. Sharma, M.D.; Baban, B.; Chandler, P.; Hou, D.Y.; Singh, N.; Yagita, H.; Azuma, M.; Blazar, B.R.; Mellor, A.L.; Munn, D.H. Plasmacytoid dendritic cells from mouse tumor-draining lymph nodes directly activate mature Tregs via indoleamine 2,3-dioxygenase. *J. Clin. Investig.* **2007**, *117*, 2570–2582.

40. Mittal, D.; Kassianos, A.J.; Tran, L.S.; Bergot, A.S.; Gosmann, C.; Hofmann, J.; Blumenthal, A.; Leggatt, G.R.; Frazer, I.H. Indoleamine 2,3-Dioxygenase Activity Contributes to Local Immune Suppression in the Skin Expressing Human Papillomavirus Oncoprotein E7. *J. Investig. Dermatol.* **2013**, doi:10.1038/jid.2013.222.

41. Butte, M.J.; Keir, M.E.; Phamduy, T.B.; Sharpe, A.H.; Freeman, G.J. Programmed death-1 ligand 1 interacts specifically with the B7-1 costimulatory molecule to inhibit T cell responses. *Immunity* **2007**, *27*, 111–122.

42. Francisco, L.M.; Salinas, V.H.; Brown, K.E.; Vanguri, V.K.; Freeman, G.J.; Kuchroo, V.K.; Sharpe, A.H. PD-L1 regulates the development, maintenance, and function of induced regulatory T cells. *J. Exp. Med.* **2009**, *206*, 3015–3029.

43. Yang, W.; Song, Y.; Lu, Y.L.; Sun, J.Z.; Wang, H.W. Increased expression of programmed death (PD)-1 and its ligand PD-L1 correlates with impaired cell-mediated immunity in high-risk human papillomavirus-related cervical intraepithelial neoplasia. *Immunology* **2013**, *139*, 513–522.

44. Hubert, P.; Caberg, J.H.; Gilles, C.; Bousarghin, L.; Franzen-Detrooz, E.; Boniver, J.; Delvenne, P. E-cadherin-dependent adhesion of dendritic and Langerhans cells to keratinocytes is defective in cervical human papillomavirus-associated (pre)neoplastic lesions. *J. Pathol.* **2005**, *206*, 346–355.

45. Caberg, J.H.; Hubert, P.; Herman, L.; Herfs, M.; Roncarati, P.; Boniver, J.; Delvenne, P. Increased migration of Langerhans cells in response to HPV16 E6 and E7 oncogene silencing: Role of CCL20. *Cancer Immunol. Immunother.* **2009**, *58*, 39–47.

46. Caberg, J.H.; Hubert, P.M.; Begon, D.Y.; Herfs, M.F.; Roncarati, P.J.; Boniver, J.J.; Delvenne, P.O. Silencing of E7 oncogene restores functional E-cadherin expression in human papillomavirus 16-transformed keratinocytes. *Carcinogenesis* **2008**, *29*, 1441–1447.

47. Sperling, T.; Oldak, M.; Walch-Ruckheim, B.; Wickenhauser, C.; Doorbar, J.; Pfister, H.; Malejczyk, M.; Majewski, S.; Keates, A.C.; Smola, S. Human papillomavirus type 8 interferes with a novel C/EBPbeta-mediated mechanism of keratinocyte CCL20 chemokine expression and Langerhans cell migration. *PLoS Pathog.* **2012**, *8*, e1002833.

48. Mota, F.F.; Rayment, N.B.; Kanan, J.H.; Singer, A.; Chain, B.M. Differential regulation of HLA-DQ expression by keratinocytes and Langerhans cells in normal and premalignant cervical epithelium. *Tissue Antigens* **1998**, *52*, 286–293.

49. Mota, F.F.; Rayment, N.B.; Chong, S.; Singer, A.; Chain, B.M. The antigen-presenting environment in normal and human papillomavirus (HPV)-related premalignant cervical epithelium. *Clin. Exp. Immunol.* **1999**, *116*, 33–40.

50. Leong, C.M.; Doorbar, J.; Nindl, I.; Yoon, H.S.; Hibma, M.H. Loss of epidermal Langerhans cells occurs in human papillomavirus alpha, gamma, and mu but not beta genus infections. *J. Investig. Dermatol.* **2010**, *130*, 472–480.

51. Hasan, U.A.; Bates, E.; Takeshita, F.; Biliato, A.; Accardi, R.; Bouvard, V.; Mansour, M.; Vincent, I.; Gissmann, L.; Iftner, T.; *et al.* TLR9 expression and function is abolished by the cervical cancer-associated human papillomavirus type 16. *J. Immunol.* **2007**, *178*, 3186–3197.

52. Kim, T.Y.; Myoung, H.J.; Kim, J.H.; Moon, I.S.; Kim, T.G.; Ahn, W.S.; Sin, J.I. Both E7 and CpG-oligodeoxynucleotide are required for protective immunity against challenge with human papillomavirus 16 (E6/E7) immortalized tumor cells: Involvement of CD4+ and CD8+ T cells in protection. *Cancer Res.* **2002**, *62*, 7234–7240.

53. Kim, T.G.; Kim, C.H.; Won, E.H.; Bae, S.M.; Ahn, W.S.; Park, J.B.; Sin, J.I. CpG-ODN-stimulated dendritic cells act as a potent adjuvant for E7 protein delivery to induce antigen-specific antitumour immunity in a HPV 16 E7-associated animal tumour model. *Immunology* **2004**, *112*, 117–125.

54. Fahey, L.M.; Raff, A.B.; Da Silva, D.M.; Kast, W.M. Reversal of human papillomavirus-specific T cell immune suppression through TLR agonist treatment of Langerhans cells exposed to human papillomavirus type 16. *J. Immunol.* **2009**, *182*, 2919–2928.

55. Chen, X.Z.; Mao, X.H.; Zhu, K.J.; Jin, N.; Ye, J.; Cen, J.P.; Zhou, Q.; Cheng, H. Toll like receptor agonists augment HPV 11 E7-specific T cell responses by modulating monocyte-derived dendritic cells. *Arch. Dermatol. Res.* **2010**, *302*, 57–65.

56. Frazer, I.H.; de Kluyver, R.; Leggatt, G.R.; Guo, H.Y.; Dunn, L.; White, O.; Harris, C.; Liem, A.; Lambert, P. Tolerance or immunity to a tumor antigen expressed in somatic cells can be determined by systemic proinflammatory signals at the time of first antigen exposure. *J. Immunol.* **2001**, *167*, 6180–6187.

57. Chavez-Blanco, A.; de la Cruz-Hernandez, E.; Dominguez, G.I.; Rodriguez-Cortez, O.; Alatorre, B.; Perez-Cardenas, E.; Chacon-Salinas, R.; Trejo-Becerril, C.; Taja-Chayeb, L.; Trujillo, J.E.; *et al.* Upregulation of NKG2D ligands and enhanced natural killer cell cytotoxicity by hydralazine and valproate. *Int. J. Oncol.* **2011**, *39*, 1491–1499.

58. Sato, N.; Saga, Y.; Mizukami, H.; Wang, D.; Takahashi, S.; Nonaka, H.; Fujiwara, H.; Takei, Y.; Machida, S.; Takikawa, O.; *et al.* Downregulation of indoleamine-2,3-dioxygenase in cervical cancer cells suppresses tumor growth by promoting natural killer cell accumulation. *Oncol. Rep.* **2012**, *28*, 1574–1578.

59. Colmenares, V.; Noyola, D.E.; Monsivais-Urenda, A.; Salgado-Bustamante, M.; Estrada-Capetillo, L.; Gonzalez-Amaro, R.; Baranda, L. Human papillomavirus immunization is associated with increased expression of different innate immune regulatory receptors. *Clin. Vaccine Immunol.* **2012**, *19*, 1005–1011.

60. Kim, D.; Hung, C.F.; Wu, T.C.; Park, Y.M. DNA vaccine with alpha-galactosylceramide at prime phase enhances anti-tumor immunity after boosting with antigen-expressing dendritic cells. *Vaccine* **2010**, *28*, 7297–7305.

61. Simova, J.; Indrova, M.; Bieblova, J.; Mikyskova, R.; Bubenik, J.; Reinis, M. Therapy for minimal residual tumor disease: Beta-galactosylceramide inhibits the growth of recurrent HPV16-associated neoplasms after surgery and chemotherapy. *Int. J. Cancer* **2010**, *126*, 2997–3004.

62. Adotevi, O.; Vingert, B.; Freyburger, L.; Shrikant, P.; Lone, Y.C.; Quintin-Colonna, F.; Haicheur, N.; Amessou, M.; Herbelin, A.; Langlade-Demoyen, P.; *et al*. B subunit of Shiga toxin-based vaccines synergize with alpha-galactosylceramide to break tolerance against self antigen and elicit antiviral immunity. *J. Immunol.* **2007**, *179*, 3371–3379.

63. Azar, K.K.; Tani, M.; Yasuda, H.; Sakai, A.; Inoue, M.; Sasagawa, T. Increased secretion patterns of interleukin-10 and tumor necrosis factor-alpha in cervical squamous intraepithelial lesions. *Hum. Pathol.* **2004**, *35*, 1376–1384.

64. Peghini, B.C.; Abdalla, D.R.; Barcelos, A.C.; Teodoro, L.; Murta, E.F.; Michelin, M.A. Local cytokine profiles of patients with cervical intraepithelial and invasive neoplasia. *Hum. Immunol.* **2012**, *73*, 920–926.

65. Chang, Y.H.; Yu, C.W.; Lai, L.C.; Tsao, C.H.; Ho, K.T.; Yang, S.C.; Lee, H.; Cheng, Y.W.; Wu, T.C.; Shiau, M.Y. Up-regulation of interleukin-17 expression by human papillomavirus type 16 E6 in nonsmall cell lung cancer. *Cancer* **2010**, *116*, 4800–4809.

66. Numasaki, M.; Fukushi, J.; Ono, M.; Narula, S.K.; Zavodny, P.J.; Kudo, T.; Robbins, P.D.; Tahara, H.; Lotze, M.T. Interleukin-17 promotes angiogenesis and tumor growth. *Blood* **2003**, *101*, 2620–2627.

67. Shiau, M.Y.; Fan, L.C.; Yang, S.C.; Tsao, C.H.; Lee, H.; Cheng, Y.W.; Lai, L.C.; Chang, Y.H. Human papillomavirus up-regulates MMP-2 and MMP-9 expression and activity by inducing interleukin-8 in lung adenocarcinomas. *PLoS One* **2013**, *8*, e54423.

68. Sutlu, T.; Alici, E. Natural killer cell-based immunotherapy in cancer: Current insights and future prospects. *J. Intern. Med.* **2009**, *266*, 154–181.

69. Bryceson, Y.T.; Long, E.O. Line of attack: NK cell specificity and integration of signals. *Curr. Opin. Immunol.* **2008**, *20*, 344–352.

70. Garcia-Iglesias, T.; del Toro-Arreola, A.; Albarran-Somoza, B.; del Toro-Arreola, S.; Sanchez-Hernandez, P.E.; Ramirez-Duenas, M.G.; Balderas-Pena, L.M.; Bravo-Cuellar, A.; Ortiz-Lazareno, P.C.; Daneri-Navarro, A. Low NKp30, NKp46 and NKG2D expression and reduced cytotoxic activity on NK cells in cervical cancer and precursor lesions. *BMC Cancer* **2009**, *9*, 186.

71. Arreygue-Garcia, N.A.; Daneri-Navarro, A.; del Toro-Arreola, A.; Cid-Arregui, A.; Gonzalez-Ramella, O.; Jave-Suarez, L.F.; Aguilar-Lemarroy, A.; Troyo-Sanroman, R.; Bravo-Cuellar, A.; Delgado-Rizo, V.; *et al.* Augmented serum level of major histocompatibility complex class I-related chain A (MICA) protein and reduced NKG2D expression on NK and T cells in patients with cervical cancer and precursor lesions. *BMC Cancer* **2008**, *8*, 16.

72. Jimenez-Perez, M.I.; Jave-Suarez, L.F.; Ortiz-Lazareno, P.C.; Bravo-Cuellar, A.; Gonzalez-Ramella, O.; Aguilar-Lemarroy, A.; Hernandez-Flores, G.; Pereira-Suarez, A.L.; Daneri-Navarro, A.; del Toro-Arreola, S. Cervical cancer cell lines expressing NKG2D-ligands are able to down-modulate the NKG2D receptor on NKL cells with functional implications. *BMC Immunol.* **2012**, *13*, 7.

73. Neuman, R.J.; Huettner, P.C.; Li, L.; Mardis, E.R.; Duffy, B.F.; Wilson, R.K.; Rader, J.S. Association between DQB1 and cervical cancer in patients with human papillomavirus and family controls. *Obstet. Gynecol.* **2000**, *95*, 134–140.

74. Wang, S.S.; Wheeler, C.M.; Hildesheim, A.; Schiffman, M.; Herrero, R.; Bratti, M.C.; Sherman, M.E.; Alfaro, M.; Hutchinson, M.L.; Morales, J.; *et al*. Human leukocyte antigen class I and II alleles and risk of cervical neoplasia: Results from a population-based study in Costa Rica. *J. Infect. Dis.* **2001**, *184*, 1310–1314.

75. Albarran-Somoza, B.; Franco-Topete, R.; Delgado-Rizo, V.; Cerda-Camacho, F.; Acosta-Jimenez, L.; Lopez-Botet, M.; Daneri-Navarro, A. CEACAM1 in cervical cancer and precursor lesions: Association with human papillomavirus infection. *J. Histochem. Cytochem.* **2006**, *54*, 1393–1399.

76. Uyttenhove, C.; Pilotte, L.; Theate, I.; Stroobant, V.; Colau, D.; Parmentier, N.; Boon, T.; van den Eynde, B.J. Evidence for a tumoral immune resistance mechanism based on tryptophan degradation by indoleamine 2,3-dioxygenase. *Nat. Med.* **2003**, *9*, 1269–1274.

77. Godfrey, D.I.; Stankovic, S.; Baxter, A.G. Raising the NKT cell family. *Nat. Immunol.* **2010**, *11*, 197–206.

78. Patel, O.; Cameron, G.; Pellicci, D.G.; Liu, Z.; Byun, H.S.; Beddoe, T.; McCluskey, J.; Franck, R.W.; Castano, A.R.; Harrak, Y.; *et al*. NKT TCR recognition of CD1d-alpha-C-galactosylceramide. *J. Immunol.* **2011**, *187*, 4705–4713.

79. Godfrey, D.I.; Hammond, K.J.; Poulton, L.D.; Smyth, M.J.; Baxter, A.G. NKT cells: Facts, functions and fallacies. *Immunol. Today* **2000**, *21*, 573–583.

80. Juno, J.A.; Keynan, Y.; Fowke, K.R. Invariant NKT cells: Regulation and function during viral infection. *PLoS Pathog.* **2012**, *8*, e1002838.

81. Van Kaer, L.; Parekh, V.V.; Wu, L. Invariant natural killer T cells: Bridging innate and adaptive immunity. *Cell Tissue Res.* **2011**, *343*, 43–55.

82. Cerundolo, V.; Barral, P.; Batista, F.D. Synthetic iNKT cell-agonists as vaccine adjuvants − finding the balance. *Curr. Opin. Immunol.* **2010**, *22*, 417–424.

83. Banchet-Cadeddu, A.; Henon, E.; Dauchez, M.; Renault, J.H.; Monneaux, F.; Haudrechy, A. The stimulating adventure of KRN 7000. *Org. Biomol. Chem.* **2011**, *9*, 3080–3104.

84. Kinjo, Y.; Wu, D.; Kim, G.; Xing, G.W.; Poles, M.A.; Ho, D.D.; Tsuji, M.; Kawahara, K.; Wong, C.H.; Kronenberg, M. Recognition of bacterial glycosphingolipids by natural killer T cells. *Nature* **2005**, *434*, 520–525.

85. Wu, L.; van Kaer, L. Natural killer T cells in health and disease. *Front. Biosci. (Schol. Ed.)* **2011**, *3*, 236–251.

86. Mattner, J.; Debord, K.L.; Ismail, N.; Goff, R.D.; Cantu, C., 3rd; Zhou, D.; Saint-Mezard, P.; Wang, V.; Gao, Y.; Yin, N.; *et al*. Exogenous and endogenous glycolipid antigens activate NKT cells during microbial infections. *Nature* **2005**, *434*, 525–529.

87. Stewart, T.J.; Smyth, M.J.; Fernando, G.J.; Frazer, I.H.; Leggatt, G.R. Inhibition of early tumor growth requires J alpha 18-positive (natural killer T) cells. *Cancer Res.* **2003**, *63*, 3058–3060.

88. Monnier-Benoit, S.; Mauny, F.; Riethmuller, D.; Guerrini, J.S.; Capilna, M.; Felix, S.; Seilles, E.; Mougin, C.; Pretet, J.L. Immunohistochemical analysis of CD4+ and CD8+ T-cell subsets in high risk human papillomavirus-associated pre-malignant and malignant lesions of the uterine cervix. *Gynecol. Oncol.* **2006**, *102*, 22–31.

89. Molling, J.W.; de Gruijl, T.D.; Glim, J.; Moreno, M.; Rozendaal, L.; Meijer, C.J.; van den Eertwegh, A.J.; Scheper, R.J.; von Blomberg, M.E.; Bontkes, H.J. CD4(+)CD25hi regulatory T-cell frequency correlates with persistence of human papillomavirus type 16 and T helper cell responses in patients with cervical intraepithelial neoplasia. *Int. J. Cancer* **2007**, *121*, 1749–1755.

90. Miura, S.; Kawana, K.; Schust, D.J.; Fujii, T.; Yokoyama, T.; Iwasawa, Y.; Nagamatsu, T.; Adachi, K.; Tomio, A.; Tomio, K.; *et al*. CD1d, a sentinel molecule bridging innate and adaptive immunity, is downregulated by the human papillomavirus (HPV) E5 protein: A possible mechanism for immune evasion by HPV. *J. Virol.* **2010**, *84*, 11614–11623.

91. Liu, K.; Idoyaga, J.; Charalambous, A.; Fujii, S.; Bonito, A.; Mordoh, J.; Wainstok, R.; Bai, X.F.; Liu, Y.; Steinman, R.M. Innate NKT lymphocytes confer superior adaptive immunity via tumor-capturing dendritic cells. *J. Exp. Med.* **2005**, *202*, 1507–1516.

92. Silk, J.D.; Hermans, I.F.; Gileadi, U.; Chong, T.W.; Shepherd, D.; Salio, M.; Mathew, B.; Schmidt, R.R.; Lunt, S.J.; Williams, K.J.; *et al*. Utilizing the adjuvant properties of CD1d-dependent NK T cells in T cell-mediated immunotherapy. *J. Clin. Investig.* **2004**, *114*, 1800–1811.

93. Ko, S.Y.; Ko, H.J.; Chang, W.S.; Park, S.H.; Kweon, M.N.; Kang, C.Y. alpha-Galactosylceramide can act as a nasal vaccine adjuvant inducing protective immune responses against viral infection and tumor. *J. Immunol.* **2005**, *175*, 3309–3317.

94. Choi, D.H.; Kim, K.S.; Yang, S.H.; Chung, D.H.; Song, B.; Sprent, J.; Cho, J.H.; Sung, Y.C. Dendritic cell internalization of alpha-galactosylceramide from CD8 T cells induces potent antitumor CD8 T-cell responses. *Cancer Res.* **2011**, *71*, 7442–7451.

95. Mattarollo, S.R.; Rahimpour, A.; Choyce, A.; Godfrey, D.I.; Leggatt, G.R.; Frazer, I.H. Invariant NKT cells in hyperplastic skin induce a local immune suppressive environment by IFN-gamma production. *J. Immunol.* **2010**, *184*, 1242–1250.

96. Mattarollo, S.R.; Yong, M.; Gosmann, C.; Choyce, A.; Chan, D.; Leggatt, G.R.; Frazer, I.H. NKT cells inhibit antigen-specific effector CD8 T cell induction to skin viral proteins. *J. Immunol.* **2011**, *187*, 1601–1608.

Intratypic changes of the E1 gene and the long control region affect *ori* function of human papillomavirus type 18 variants

Alfredo Amador-Molina, José Luis González-Montoya, Alejandro García-Carrancá, Alejandro Mohar and Marcela Lizano

Correspondence

Marcela Lizano

lizano@unam.mx

Unidad de Investigación Biomédica en Cáncer, Instituto Nacional de Cancerología, México/Instituto de Investigaciones Biomédicas, Universidad Nacional Autónoma de México. Av. San Fernando No. 22, Col. Sección XVI, Tlalpan 14080, Mexico

A persistent infection with high-risk human papillomavirus (HPV) constitutes the main aetiological factor for cervical cancer development. HPV16 and 18 are the most prevalent types found in cervical cancer worldwide. It has been proposed that HPV intratype variations may result in differences in biological behaviour. Three different HPV18 variants belonging to the Asian Amerindian (AsAi), European (E) and African (Af) branches have been associated with specific histological types of cervical cancer with different relative prognoses, suggesting that HPV18 genomic variations might participate in disease evolution. The E1 viral protein plays a critical role in controlling viral replication and load, requiring interaction with the E2 protein to bind to the long control region (LCR). In this work, we analysed if intratype variations in the LCR and E1 and E2 genes of HPV18 impact *ori* replication. While the changes found in E2 genes of the tested variants were irrelevant in replication, we found that variations in E1 and LCR in fact affect *ori* function. It was demonstrated that nucleotide differences in the LCR variants impact *ori* function. Nevertheless, HPV18 E1 Af gene was mainly involved in the highest *ori* replication, compared with the E and AsAi E1 variants. Immunofluorescence analysis showed increased levels of Af E1 in the nucleus, correlating with the enhanced *ori* function. Site-directed mutagenesis revealed that at least two positions in the N-terminal domain of E1 could impact its nuclear accumulation.

INTRODUCTION

Human papillomaviruses (HPVs) are classified as high- or low-risk according to their oncogenic potential. High-risk HPV types (HR-HPV) are those found in cervical cancer, with HPV types 16 and 18 accounting for almost 70 % of all cervical cancer cases (zur Hausen, 2002). It is well known that only a small number of cervical lesions infected with HR-HPVs evolve into high-grade lesions or cervical cancer (Bosch *et al.*, 2002). Many naturally occurring HPV intratype variants have been identified; furthermore, molecular and epidemiological data suggest that variants of the same type are biologically distinct and may confer different pathogenic risks (Berumen *et al.*, 2001; De la Cruz-Hernández *et al.*, 2005; Lizano *et al.*, 1997, 2006). In a previous work examining a Mexican population, three different HPV18 variants were identified, Asian Amerindian (AsAi), European (E) and African (Af), which have been associated with specific histological types of cervical cancer (Lizano *et al.*, 1997).

HPV replication has two stages in the natural history of infection: a persistent stage, which is characterized by a low copy number of viral episomes, occurring mainly in the basal layer without generating progeny virions (Hubert *et al.*, 1999; Hubert, 2005); and a productive stage, where viral genomes are amplified in high copy numbers, later genes are expressed and progeny virions are produced (Hubert, 2005). E1 and E2 viral proteins are essential for HPV replication. E1 is the most conserved protein among papillomaviruses (Koonin, 1993), harbouring a C-terminal domain involved in ATP-dependent DNA helicase activity (Abbate *et al.*, 2004; Wilson *et al.*, 2002). The N-terminal domain is the most variable region of E1 within all papillomaviruses (Abbate *et al.*, 2004); nevertheless, it contains two conserved nuclear localization signals (NLS) and a nuclear export signal (NES) (Fradet-Turcotte *et al.*, 2010). It has been reported that the E1 N-terminal region is essential for viral episome maintenance in undifferentiated primary human keratinocytes due to its interaction with the cellular protein p80, which co-localizes with E1 at the nucleus (Côté-Martin *et al.*, 2008). The long control region (LCR) contains the origin of replication, *ori*, harbouring a single E1- and three E2-binding sites (Demeret *et al.*, 1998). The keratinocyte enhancer (KE) domain contained in the LCR has been described as being directly involved in

Supplementary material is available with the online version of this paper.

modulating *ori* function (Hubert *et al.*, 1999). The E2 protein plays an important role in viral replication, forming E1–E2 complexes, which help E1 binding to the *ori* (Abbate *et al.*, 2004). The aim of this study was to determine whether nucleotide variations in the LCR and/or E1 or E2 genes of HPV18 intratype variants could affect viral replication. Our results demonstrate that nucleotide variations in these sequences affect replication, with the highest impact for E1-Af.

RESULTS

HPV18 E1 variations reside in the N-terminal region

E1 genes of HPV18 variants (AsAi, E and Af) were sequenced. Nucleotide sequences shared a 99 % of similarity with already reported HPV18 isolates (GenBank accession no. EF202155.1, for the Af variant; GenBank accession no. GQ180786.1, for the E variant). Table 1 lists the nucleotide and predicted amino acid changes found in different regions of the E1 variants. Few changes affecting amino acids were present in the Af or E variants compared to the reference AsAi. Nevertheless, variations were mainly located at the N-terminal region, which is essential for E1 nuclear localization.

Viral *ori* function is dependent on E1 and E2

Plasmid pORI replication was assessed in the presence and absence of E1 and E2 expressing plasmids, Fig. S1 (available in JGV Online). Semi-quantitative RT-PCR assay showed similar expression levels for E1 and E2 in each transfection, Fig. S2. No replication was found with pORI alone or pORI/E2 and minimal replication occurred with pORI/E1, compared when both E1 and E2 were present, where there was an approximately 24-fold amplification. The results confirm that pORI replication is dependent on the E1 and E2 genes. In these experiments it was ensured that the amount of input plasmid was uniform. It was demonstrated that input dam-methylated DNA was comparable in all experiments, after digesting unmethylated DNA with *Mbo*I enzyme, Fig. S3. Therefore, differences observed in replication should be due to the biological effect of variations in the tested genes.

Variations in the LCR affect *ori* function

The E1 and E2 DNA-binding domains (DBDs) are conserved within papillomaviruses, as well as the respective LCR-binding consensus sequences (Auster & Joshua-Tor, 2004; Hegde & Androphy, 1998; Titolo *et al.*, 2003;). Moreover, it has been previously suggested that viral proteins E1 and E2 may support the replication of homologous and heterologous papillomaviruses (Chiang *et al.*, 1992). In a previous study, variations in the LCR of HPV18 E and Af sequences were reported (López-Saavedra *et al.*, 2009), particularly in

the KE region, known to be involved in viral *ori* replication (Hubert, 2005). Hence, it was of our interest to analyse whether LCR variations could impact *ori* replication.

Plasmids expressing E1 and E2 (p40-E1AsAi and pCG-E2AsAi) were co-transfected with each of the LCR variants (pORI-AsAi, -E or -Af) as the only variable. Fig. 1(a) shows that pORI-AsAi had the highest *ori* function since pORI-Af and pORI-Eu were amplified to almost half of the number of copies of pORI-AsAi ($P<0.05$). A similar trend was observed for transfected C33 and HaCaT cell lines, where pORI-AsAi had the highest *ori* function, although some variations in pORI-Eu and pORI-Af replication occurred within cell lines, Fig. 1(b) and (c).

Variations in the E1 gene affect *ori* function

Next, we sought to determine whether the changes in E2 variant genes could modify *ori* function. Co-transfections of p40-E1AsAi and pORI-AsAi plasmids with those expressing E2 variants (AsAi, E or Af) as the only variable were performed. As shown in Fig. 2(a), no significant changes in pORI-AsAi amplification were found, related to the tested E2 variants in HEK-293. The same effect was observed for transfected C33 and HaCaT cells lines, Fig. 2(b) and (c). Therefore, the analysed E2 variations do not affect *ori* function.

To evaluate the effect of variations in E1, pCG-E2AsAi and pORI-AsAi were co-transfected in HEK-293 cell line, with plasmids expressing the different E1 variant genes (AsAi, E or Af) as the only variable. As observed in Fig. 3(a), the presence of E1-Af caused a significantly higher pORI-AsAi amplification than that observed with E1-AsAi or E1-E ($P<0.05$). This result shows that E1-Af, is able to augment the previously demonstrated strong *ori* function of pORI-AsAi, in comparison to E1-AsAi, Fig. 1. This trend was reproduced in other cell lines, as demonstrated when HaCat keratinocytes and cervical cancer-derived C33, were tested. As shown in Fig. 3(b) and (c), E1-Af promotes the highest replication level of pORI-AsAi in those cellular contexts.

We next tested the effect of variant homologous elements by the analysis of the *ori* function of each variant in the presence of the corresponding E2 and E1 variant genes in HEK-293. In this context, the highest effect was observed for pORI-Af-related amplification as shown in Fig. 4(a), even it previously appeared weaker than pORI-AsAi in the presence of E1- and E2-AsAi, Fig. 1. This effect was reproduced in the context of C33 and HaCaT cell lines, Fig. 4(b) and (c), respectively.

The observed effect on *ori* function was not due to slight differences in E1 concentration, as observed through transfections of HEK-293, C33 and HaCaT cell lines with p40-E1-Af in concentration gradient. Fig. S4(a), (b) and (c) show that E1-Af affect *ori* replication in a dose-dependent manner, where >0.8 µg p40-E1-Af plasmid overload E1 enzymic function in all cell lines. In the present study an amount of 1.75 µg p40-E1 was used for all transfections.

Table 1. Comparison of E1 nt and amino acid sequences of the HPV18 variants

Nucleotide and predicted amino acid changes, compared to the reference AsAi, are shown. The negative sign (–) indicate no change at the respective nucleotide or amino acid position. Changes affecting amino acid sequence are located in N- and C-terminal domains.

	E1-AsAi			E1-Af		E1-E	
	Position	Nucleotide	Amino acid	Nucleotide	Amino acid	Nucleotide	Amino acid
N-terminal: NLS and NES	1012	A	Ser 33	–	–	T	–
	1087	T	Cys 58	C	–	–	–
	1123	C	Phe 70	T	–	–	–
	1194	C	Thr 94	–	–	A	Lys
	1256	G	Glu 115	C	Gln	–	–
	1264	T	Thr 117	A	–	–	–
	1279	G	Gln 122	A	–	–	–
	1303	T	Phe 130	C	–	–	–
	1353	T	Ile 147	–	–	A	Asn
	1378	T	His 157	G	Gln	–	–
	1408	G	Thr 165	A	–	–	–
	1423	C	Asn 170	T	–	–	–
	1470	A	Asn 186	C	Thr	–	–
DNA-binding domain	1588	A	Ser 225	–	–	C	–
	1735	A	Thr 274	T	–	–	–
	1774	T	Arg 287	G	–	–	–
	1789	G	Lys 292	A	–	–	–
	1843	T	Thr 310	–	–	G	–
	1891	A	Leu 326	G	–	–	–
C-terminal: helicase/ATPase and E2-binding site	2101	A	Ala 396	G	–	–	–
	2270	C	Leu 453	T	–	–	–
	2335	C	Thr 474	T	–	–	–
	2401	T	Ser 496	C	–	–	–
	2440	G	Val 509	A	–	–	–
	2446	C	Ser 511	T	–	–	–
	2482	T	Thr 523	C	–	–	–
	2509	G	Thr 532	C	–	–	–
	2551	G	Ala 546	T	–	–	–
	2566	A	Pro 551	C	–	–	–
	2656	T	Asn 581	C	–	–	–
	2719	T	Asp 602	G	Glu	–	–
	2734	A	Pro 607	T	–	–	–

Nuclear localization of E1 variants

Nuclear localization of E1 is essential for its helicase function. Therefore, it is possible that E1 variations in the N-terminal domain, Table 1, could impact on protein localization explaining the observed differences related to *ori* replication.

To compare E1 nuclear localization among variants, immunofluorescence analysis was performed on C33 cells transfected with plasmids containing E1 variants tagged with HA. As shown in Fig. 5(a), a stronger HA signal was observed in the nucleus of cells transfected with E1-Af, compared to those with E1-AsAi, with only a subtle difference for E1-Eu. E1 real-time PCR assays were performed, confirming that there were no significant differences in RNA expression and neither in DNA-copy number of the introduced pE1-HA. This trend was reproducible when E1, E2 and LCR of each variant were transfected altogether, Fig. 5(b).

Three of the E1-Af nucleotide variations result in amino acid substitutions, related to the reference E1-AsAi. The participation of these variations in the observed nuclear accumulation was evaluated. Through direct mutagenesis the respective changes at positions 1256, 1378 and 1470 from the Af variant were introduced one by one into the E1-AsAi variant. With single mutations, nuclear signal intensity slightly increased in relation to that previously observed for E1-AsAi, Fig. 5(c). Double mutations were also tested and surprisingly, the changes at positions 1256 and 1470 resulted in greater E1 nuclear accumulation, similar to that obtained for E1-Af, Fig. 5(c).
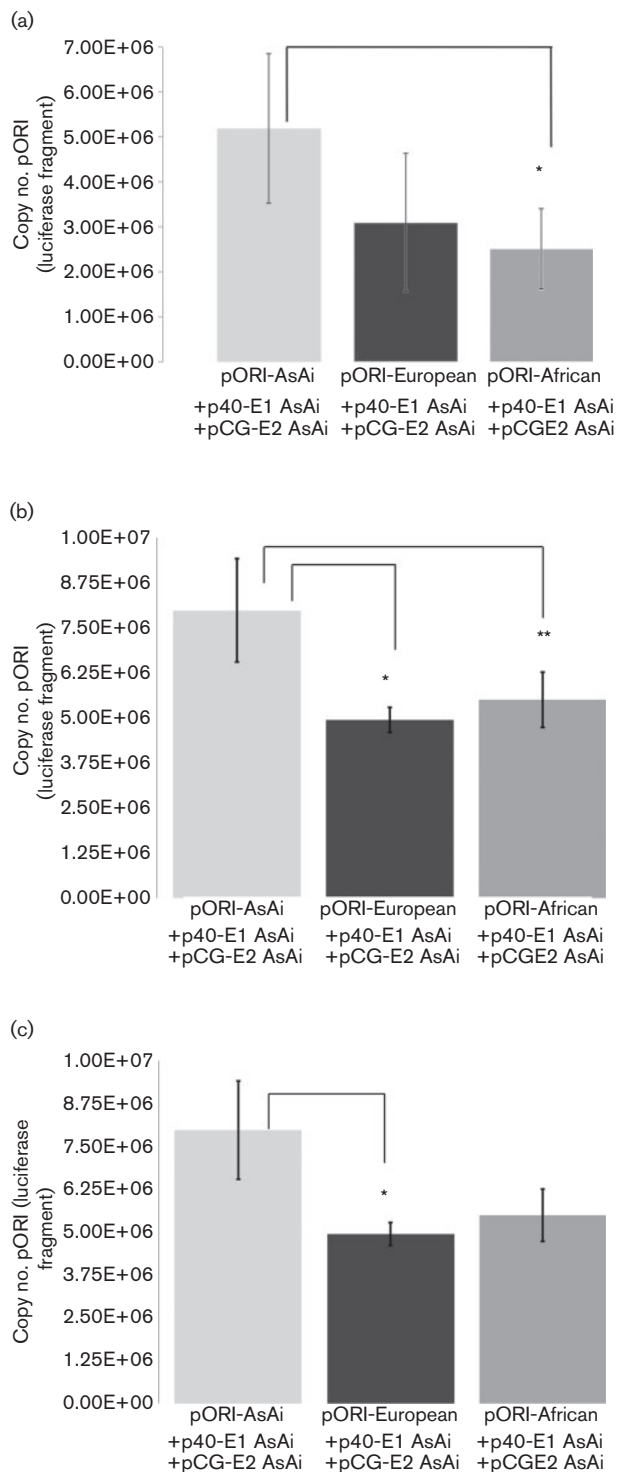
Fig. 1. HPV18 LCR variations affect pORI replication. (a) Plasmids with E1 and E2 of AsAi origin were maintained constant, while the variable was the pORI plasmid. The pORI-AsAi has the highest replication level, almost twofold compared with that of E and Af variants, *P=0.036. (b) A similar trend was observed for transfected C33 cell line, *P=0.0023 and **P=0215. (c) In HaCaT cell line a significant difference was observed only for AsAi and E variant, *P=000027.
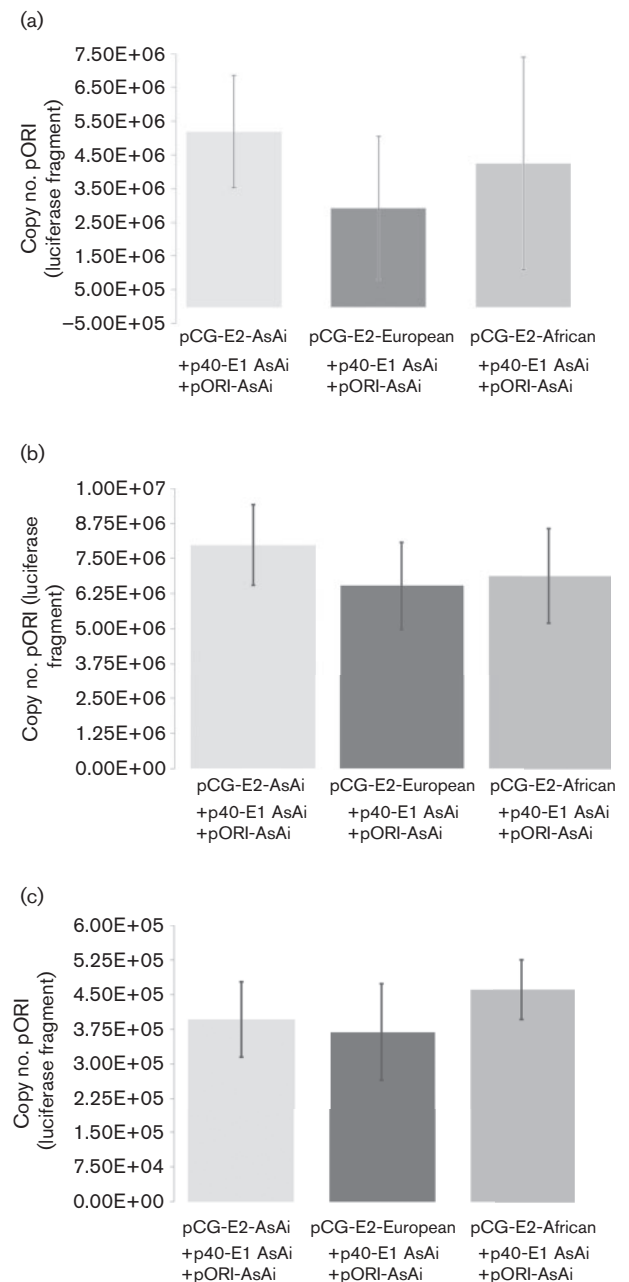

Fig. 2. Variations in the HPV18 E2 gene do not significantly affect replication. Transfections were performed where the variable was the E2-variant gene, while E1-AsAi and pORI-AsAi were maintained constant. No significant changes in pORI replication were observed, with similar data obtained with transfected HEK-293 (a), C33 (b) and HaCaT cell line (c).

DISCUSSION

Several lines of evidence suggest that HPV intratype variations may affect viral biological behaviour potentially altering the prognosis of HPV infections. To examine this possibility further, it is important to identify whether intratype variations may affect viral functions. The identification
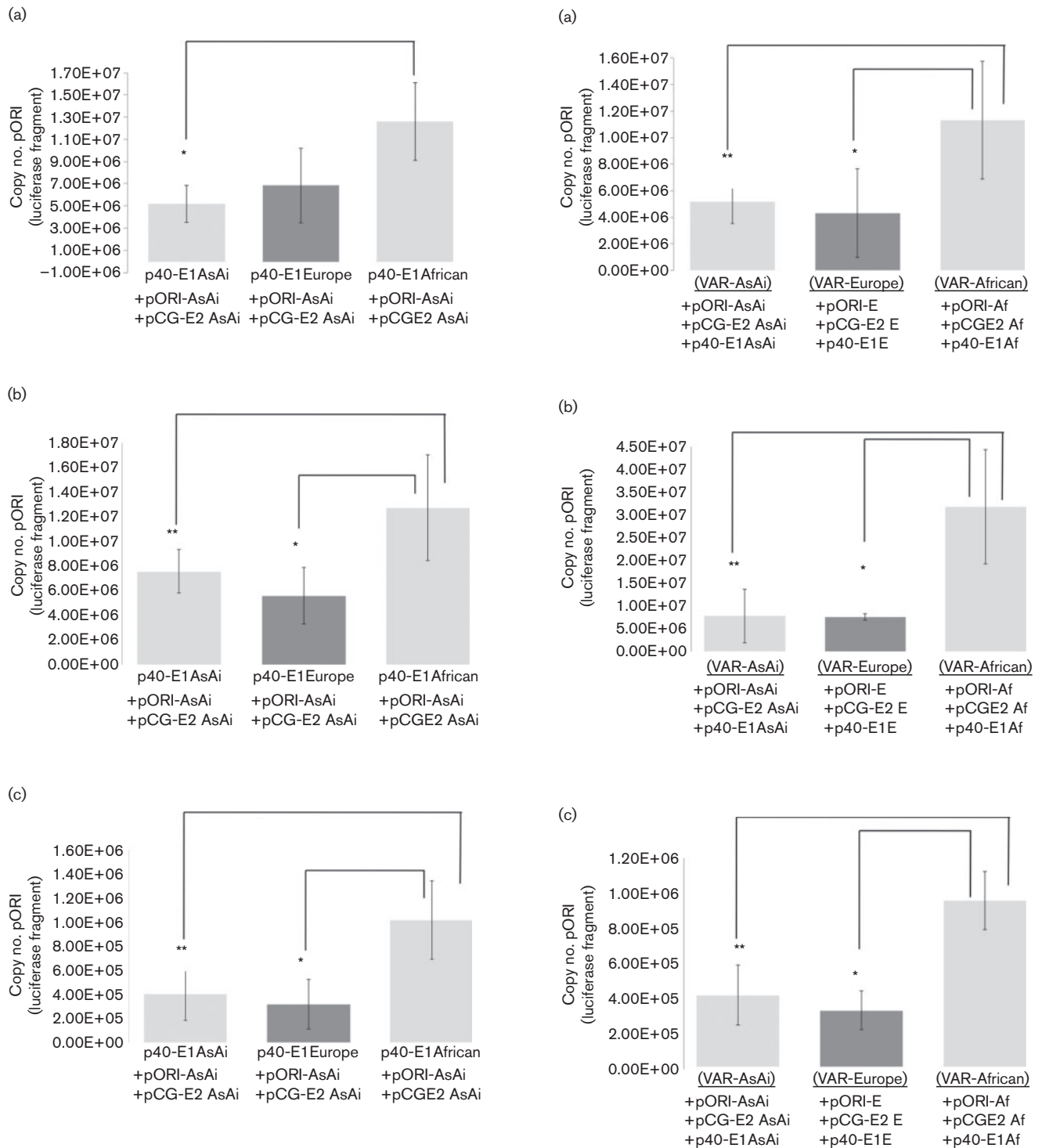
(a)

(a)

(b)

(b)

(c)

(c)

Fig. 3. E1 variations of HPV18 affect replication in different cell lines. (a) E1-Af promotes the highest plasmid amplification level, compared with E1-E and E1-AsAi in HEK-293 cell line (a), being nearly twice that observed for the AsAi, *P=0.01; (b) C33 cell line, *P=0.0091, **P=0.0171; and (c) HaCaT cell line, with differences for almost threefold related to both, E1-E *P=0.0103 and E1-AsAi **P=0.0188.

Fig. 4. The HPV18 Af variant has the highest replication level in different cell lines. pORI replication in the presence of homologous E1 and E2 from each variant were tested. (a) The Af variant had the strongest pORI replication level in HEK-293. *P=0.0413, **P=0.0235; (b) transfected C33 cell line, with approximately fourfold pORI replication level for the Af variant than that observed for E and AsAi variants, *P=0.0058 and **P=0.0026, respectively; and (c) HaCaT cell line, with approximately threefold pORI replication level for the Af variant, *P=0.00129 and **P=0.00120.
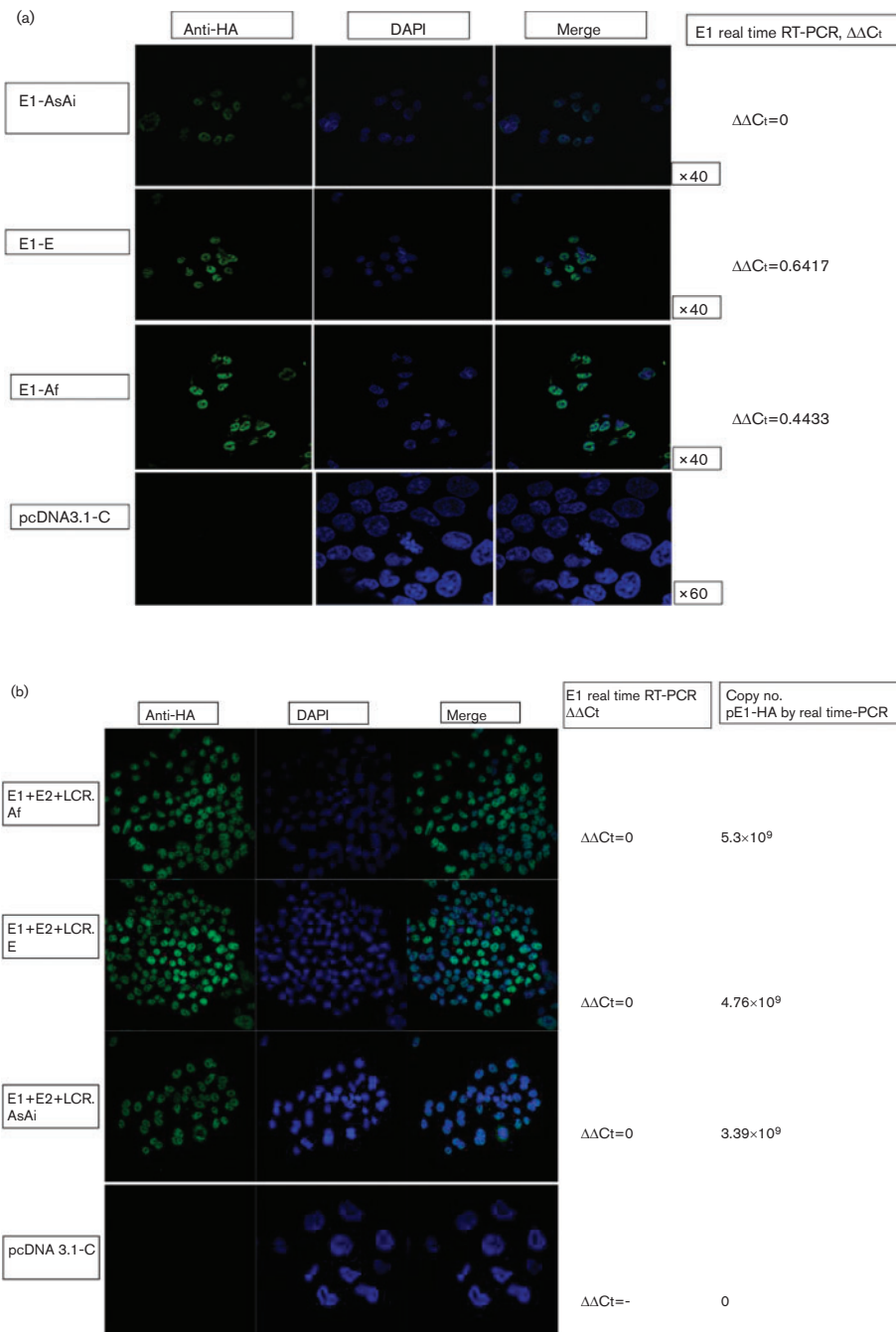
Fig. 5. Differences in nuclear amounts of E1 variants in C33 cell line. (a) Cells were separately transfected with the three HA-tagged E1 variants. E1 recombinant proteins were identified with anti-HA antibody; nuclei were stained blue with DAPI. HA-E1-Af shows the highest signal in the nucleus; pcDNA 3.1-C, empty vector. E1 real-time PCR was performed in transfectants; $\Delta\Delta C_t$ showed no difference in expression. (b) A comparable E1 signal was observed when E1 was transfected with both E2 and LCR from each variant. Copy number of the input plasmid was analysed by real-time PCR. (c) Analysis of mutations at nucleotide positions 1256, 1378, 1470 performed on E1-AsAi sequence. The effect on E1 nuclear signal was analysed in single and double mutants.

of the potential effects of HR-HPV intratype variations could help us to understand the evolution of HPV infections.

Different biological behaviours have previously been proposed for HPV18 variants, where an Af variant has been associated with lesions with a better relative prognosis
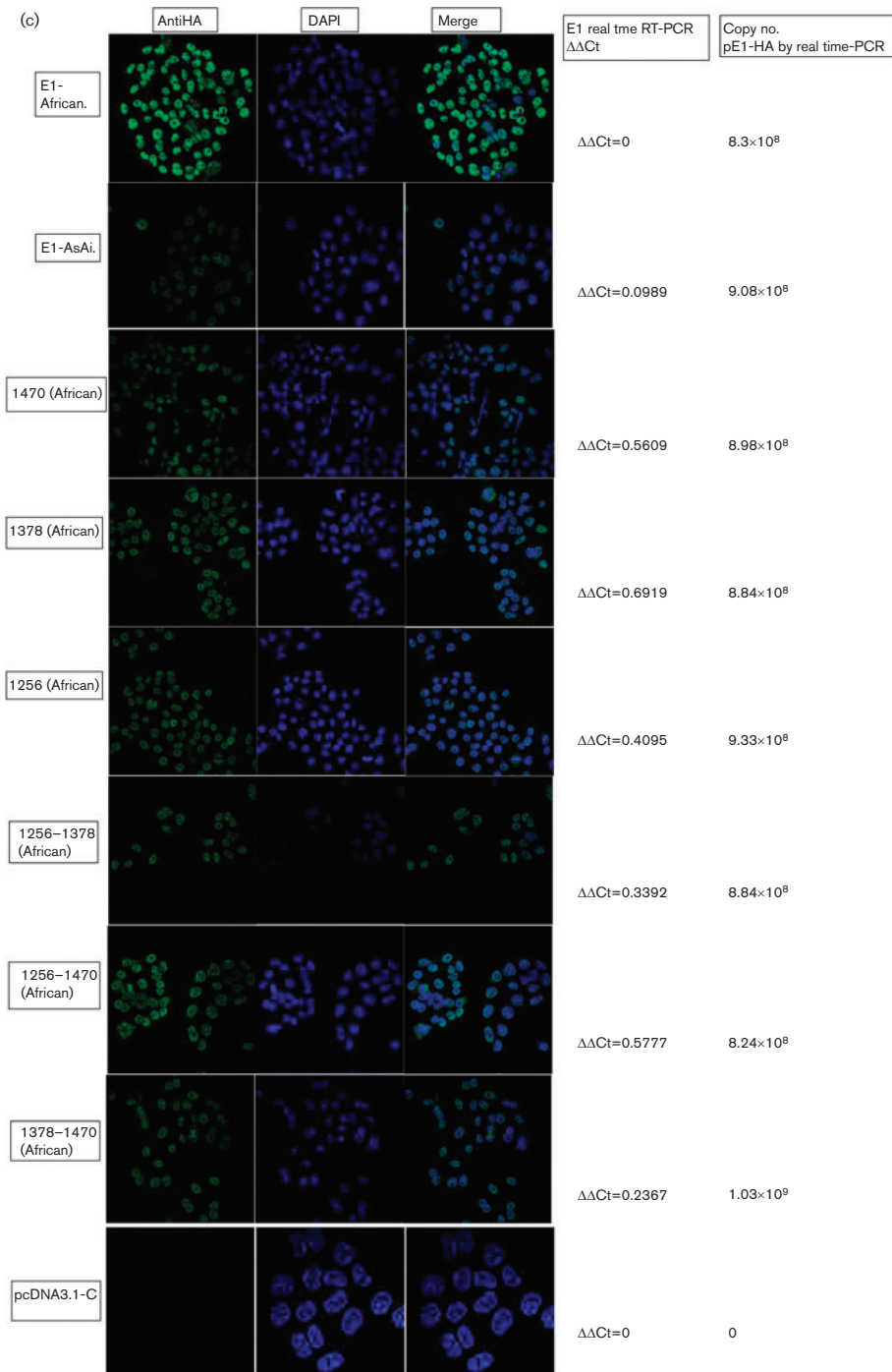
compared to those harbouring E and AsAi variants. (De la Cruz-Hernández *et al.*, 2005; Contreras-Paredes, *et al.*, 2009; Lizano *et al.*, 1997, 2006).

In the present study, it was examined whether intratype variations of E1, E2 or the LCR may affect viral *ori* function. We found that E1 intratype variations significantly impact *ori* function; the highest *ori* activity was found in the context of E1 Af variant.

Variations in the HPV18 LCR also affect *ori* function since a significant higher pORI amplification was obtained with

LCR-AsAi compared with the other LCR variants tested. This effect may be related to the changes found in the KE region as it has been reported that mutations in this domain affect HPV replication (Hubert *et al.*, 1999).

Even HPV18 E2 variant genes exhibit various changes within their sequences compared with the reference AsAi E2 gene, those changes did not affect *ori* function. It is noteworthy that variations in E2 are not located in key amino acids important for DNA binding or E1 protein interaction. It is possible that the E2 changes found in the

tested isolates do not alter E2 protein conformation in such a way as to affect its function in replication. As previously reported, variations in the HPV18 E2 gene did not affect LCR transcriptional activity (López-Saavedra et al., 2009), also suggesting that E2 DNA-binding performance is similar in these variants.

Interesting results were obtained with regard to E1 variants. The presence of Af and E E1 variants increased replication compared with E1-AsAi. Variations reside in the N-terminal region of the E1 predicted proteins, where nuclear localization (NLS) and export (NES) signals are located. On the other hand, it has been shown that changes in N-terminal, particularly in the amphipathic helix may alter replication (Morin et al., 2011).

After examining the importance of variations in each of the elements responsible for HPV replication, we then analysed the effect within a unique variant context, namely attesting the E1, E2 and LCRs of the same variants. It was demonstrated that replication variability was mainly due to changes in E1, even in the presence of homologous elements. This finding could be reproduced in distinct cellular contexts, since E1-Af also had the highest impact in ori function in C33 and HaCaT cell lines as in HEK-293.

We then analysed whether differences in replication level could be due to a disparity in variant E1 nuclear levels. Immunofluorescence results showed that E1-AsAi protein was moderately detected in the nucleus, while E1-Af had the strongest nuclear signal, correlating with the enhanced ori function. This trend was similar when immnunofluorescence was performed in cells transfected with E1, E2 and the LCR of each variant. When Af nucleotide changes at positions 1256, 1378 and 1470 were introduced in the AsAi E1 gene, E1 nuclear intensity augmented, particularly with the double mutant 1256–1470. The respective predicted amino acids (positions 115, 157 and 186) could be part of a domain that impact E1 nuclear stability. Nevertheless, even that mRNA E1 levels were similar; it is possible that the increased levels of Af E1 in the nucleus is due to higher steady-state levels of the protein.

On the other hand, even replication differences are clear, E E1 showed only a subtle difference in nuclear signal related to the Af E1. Therefore, even nuclear accumulation may have a main role in ori replication, other unknown mechanisms could also be participating. E1 was not detected in any case at the cytoplasm, probably evidencing that this protein is mainly stable in the nucleus.

The present data demonstrate that changes in the E1 gene affect ori function, and differences in replication among variants could be explained partially by its nuclear accumulation, but mechanisms such as post-translational modifications, enzymic cleavage, as other unknown mechanism could play an important role in this biological effect. However, our results suggest that E1 variations could impact the natural history of HPV infection, mainly affecting viral episome copy number.

In previous reports, we proposed that the HPV18 Af variant could exhibit a less aggressive behaviour (López-Saavedra et al., 2009; De la Cruz-Hernández, et al., 2005) based on data obtained through the analysis of the LCR activity and E6 oncogene function. The results obtained in this work show that the Af E1 has the highest impact on replication. Other authors proposed that a high viral load is a potential risk factor for the development of high-grade cervical lesions (Broccolo et al., 2009; Flores et al., 2006; Xu et al., 2009; Wanram et al., 2009;), someway contrasting with our data. The HPV18 Af variant has a lower oncogenicity for certain so it could not be discarded that a high number of HPV copies at initial infection, due to an overregulation of E1 function, could consequently be linked to a high expression of the E1 and E2 proteins. Moreover, it has been demonstrated that the E2 protein controls viral early gene expression and induces apoptosis (Demeret et al., 2003). Therefore, an HPV variant promoting an increase in viral replication could have a diminished transforming potential. Furthermore, Fradet-Turcotte et al. (2011) demonstrated that the nuclear export of E1 is required for the maintenance of the viral genome in undifferentiated keratinocytes but not for its amplification in differentiated cells, suggesting that the increased levels of E1 in the nucleus could create a favourable environment for viral DNA amplification by blocking cells in the S-phase. This blockage would induce DNA damage response by ATM-dependent pathway, promoting DNA repair or leading to apoptosis.

To closer define the impact of HPV intratype variations on the oncogenic potential, it would be necessary to explore the biological implication of other viral interactions with cellular targets.

METHODS

Plasmid construction. The pCG-E2 plasmids contain versions of the HPV18 E2 variant genes (E, AsAi and Af) cloned into pCG vector. Plasmids were named pCG-E2AsAi, pCG-E2E and pCG-E2Af according to each HPV18 E2 variant type. Variants of the HPV18 LCRs (E, AsAi and Af) were cloned into the pGL2-basic reporter vector (Promega), resulting in the pORI-AsAi, pORI-E and pORI-Af plasmids. The nucleotide sequences of the E2 genes and LCRs have been previously reported (López-Saavedra et al., 2009). The E1 AsAi gene was PCR amplified from pBR322-HPV18 (a kind gift from Professor H. zur Hausen, Deutsches Krebsforschungszentrum, Im Neuenheimer Feld 280, 69120 Heidelberg, Germany), which contains the entire genome of the HPV18 AsAi variant, using the following primers: forward: 5′-GGGGGATCCATGGCTGATCCAG-3′ (nt 914–926) and reverse: 5′-GGGAAGCTTCTAATCTGGACCA-3′ (nt 2783–2795). The resulting PCR product was cloned into the pXJ40 FT vector (p40), described by Xiao et al. (1991), to obtain p40-E1AsAi.

Recombinant pE1-HA plasmids containing E1-AsAi, -E or -Af variants were constructed from pcDNA 3.3 TOPO vector. E1 variant genes were PCR-amplified from the p-40-E1 vectors using the following primers: forward, 5′-GCCATGGGCTACCCATACGATGT-TCCAGATTACGCTGACGATGACGATAAGATGGCTGATCCAGAA-GGTACA-3′; reverse, 5′-CTATCTGGACCATGTCCTTTCAAA-3′.

The obtained product contained a haemagglutinin domain at the E1 N terminus. The plasmids were constructed with the pcDNA

3.3-TOPO TA Cloning kit (Invitrogen) and named pE1-HA-AsAi, pE1-HA-E and pE1-HA-Af.

HA–E1 recombinant genes were confirmed by sequencing.

Multi-site-directed mutagenesis assays. Plasmids expressing E1 E (p40-E1E) or E1 Af (p40-E1Af) were obtained through direct mutagenesis of p40-E1AsAi (QuikChange Multi-Site-Directed Mutagenesis kit; Stratagene) with the primers shown in Tables S1 and S2. Mutants were confirmed by direct sequencing (see Figs S5 and S6).

Single and double mutations at positions 1256, 1370 and 1470 were introduced in the plasmid pE1-HA AsAi, to obtain three AsAi mutants with an Af site (1256, 1378 or 1470) and three AsAi mutants with two Af sites (1256–1378, 1256–1470 and 1378–1470). The primers used were the same as those shown in Tables S1 and S2. Mutants were confirmed by direct sequencing (see Figs S7 and S8).

E1 gene sequences. E1 nt sequences were obtained from overlapping PCR products from pre-malignant lesions of the cervix containing HPV18 E or Af variants (Lizano *et al.*, 2006). Three samples for each variant were sequenced. The obtained sequence of the E1-AsAi gene from plasmid pBR322-HPV18 was confirmed using the published HPV18 AsAi sequence (HPV Sequence Database, http://www.stdgen.lanl.gov). Direct sequencing was performed from PCR products using the Big Dye Terminator v3.1 Cycle Sequencing kit (Applied Biosystems). Primers used to amplify the E1 genes are showing in Table S3.

Cell culture and transfection. HEK-293, C33 and HaCaT cells were grown in Dulbecco's modified Eagle's medium F12 supplemented with 10 % FBS. Then, 2×10^5 cells were plated in six-well plates (30 mm^2 each well) and transfected with Lipofectamine reagent and Plus reagent (Invitrogen) 24 h later. Co-tranfections with the E1 (1750 ng), E2 (55 ng) and LCR plasmids (12 ng) were performed. All transfections were carried out in triplicate in at least three independent experiments.

RNA extraction and expression analysis. To determine E1 and E2 expression, total RNA was extracted from transfected cells with TRIzol (Invitrogen Life Technologies) according to the manufacturer's instructions. Samples were treated with 1 U DNase I (Gibco-BRL). The amount of RNA was determined by UV spectrophotometry, and the RNA quality was confirmed using 2 % agarose gels. For cDNA preparation, 2 mg total RNA was reverse-transcribed with random hexamers using the SuperScript first-strand synthesis system for RT-PCR (Invitrogen Life Technologies). cDNA was PCR-amplified for E1 and E2-expression analysis.

Immunofluorescence. Duplicate assays were performed in C33 cells transfected with 800 ng of pE1-HA plasmids. At 24 h post-transfection one sample was fixed for 20 min at room temperature in 4 % paraformaldehyde. Then, cells were rinsed with PBS, and permeabilized for 5 min at room temperature with 0.2 % Triton X-100. Then, cells were incubated with 0.1 M glycine in PBS to quench free aldehyde groups. Primary antibody anti-HA [HA-probe (Y-11): sc-805, Santa Cruz Biotechnology] was incubated in PBS for 1 h at room temperature. After washing with PBS ($3 \times$, 10 min each), cells were incubated for 30 min at room temperature with anti-goat Alexa-488 secondary antibody diluted in PBS. Finally, cells were washed with PBS ($3 \times$, 10 min each), counterstained and mounted with Prolong Gold Antifade Reagent (Invitrogen). The second sample was used for real-time RT-PCR and real-time PCR E1 assays.

Confocal microscopy. Images were collected with an LSM710-DUO confocal laser system couple to an AxioObserver inverted scanning microscope (Zeiss) and were analysed using LSM Image Browser version 3.2.0.70 (Zeiss). Images were acquired with a $\times 40$ objective (E1-AsAi, E and Af) and $\times 60$ for the empty vector control.

E1 quantitative real-time PCR (qRT-PCR). E1 copy number (from DNA) and transcript levels (from cDNA) were measured in cells tested for E1 confocal microscopy. The quantity of E1 transcript was calculated by $\Delta\Delta C_t$. The primers used to amplified E1 and GAPDH genes were: E1-914-F: 5′-ATGGCTGATCCAGAAGGTACA-3′, E1-1125-R: 5′-TGGAACAATGCCTGTCGTGTC-3′ and GAPDH-F: 5′-TGCACCACCAACTGCTTAGC-3′, GAPDH-R: 5′-GGGATGGACT-GTGGTCATGAG-3′. E1 quantification was performed using a standard curve from pE1-HA with dilution series from 1×10^3 to 1×10^9 copy number.

cDNA was obtained by GeneAmp (RNA PCR kit; Applied Biosystems). E1 qRT-PCR was performed with SBYR Green (Applied Biosystems). PCR was optimized for 300 nM of reverse and forward E1 and GAPDH primers, on a StepOnePlus real-time PCR system (Applied Biosystems) with the following PCR conditions: 95 °C for 30 s and 60 °C for 1 min for 40 cycles.

DNA harvest. Low molecular mass DNA was extracted 72 h after transfection by using the Hirt method (Morgan & Taylor, 2005; Taylor & Morgan, 2003). Briefly, cells were lysed in 400 µl Hirt solution (0.6 % SDS, 10 mM EDTA) and scraped into a 1.5 ml microcentrifuge tube; 100 µl 5 M NaCl was added, and the samples were stored at 4 °C overnight. After centrifugation for 30 min at 4 °C, DNA was extracted once with phenol/chloroform-isoamyl-alcohol and precipitated with 100 % ethanol and ammonium acetate (pH 5.2, 3 M). Following centrifugation, the DNA pellet was washed with 70 % ethanol, dried and then suspended in 50 µl dH$_2$O. Plasmid replication was analysed using real-time PCR.

Plasmid replication assay. To test pORI plasmid replication, a 130 bp fragment of the luciferase gene contained in the pGL2-basic plasmid was amplified. This fragment contains two *Dpn*I sites, which are necessary to evaluate *de novo* replication in HEK-293 cells. The primers used to amplify the luc fragment were: Luc-Sense-5′-TCGTCACATCTCATCTACCTCC-3′ and Luc-Antisense-5′-CGAG-AATCTGACGCAGGCAGT-3′.

Real-time PCR assays were performed using SBYR Green (Applied Biosystems). PCR conditions were optimized to 50 nM Luc-Sense primer and 300 nM Luc-antisense primer. PCRs were performed on an ABI Prism 7700 detection system (Applied Biosystems) with the following PCR conditions: 95 °C for 30 s and 60 °C for 1 min for 40 cycles.

Harvested DNA was digested with either *Dpn*I or *Mbo*I. *Dpn*I can only digest GATC sites when both DNA strands are dam-methylated (dam positive, a bacterial-specific methylation at adenines), whereas *Mbo*I digestions are only possible when both strands are unmethylated at the adenines. Therefore, *Dpn*I will not digest DNA replicated in eukaryotic cells, and *Mbo*I will not digest input DNA (methylated in bacteria). The digestion conditions were previously described (Morgan & Taylor, 2005; Taylor & Morgan, 2003). To detect replicated pORI-(AsAi, E or AF), 25 µl sample were digested with *Dpn*I; to detect input plasmid, 25 µl of sample were digested with *Mbo*I. Exonuclease III digestion was performed for 30 min to reduce the amount of incompletely digested DNA (Taylor & Morgan, 2003). Two microlitres of each treated sample was analysed in triplicate using real-time PCR. Quantification was performed using a standard curve from pORI-AsAi (which contains the luciferase fragment to be amplified) with dilution series from 1×10^3 to 1×10^9 copy numbers.

Statistical analysis. Differences in plasmid replication levels were analysed with Student's *t*-test, expressing replication levels as copy number ± 1 SD.

ACKNOWLEDGEMENTS

REFERENCES

Abbate, E. A., Berger, J. M. & Botchan, M. R. (2004). The X-ray structure of the papillomavirus helicase in complex with its molecular matchmaker E2. *Genes Dev* **18**, 1981–1996.

Auster, A. S. & Joshua-Tor, L. (2004). The DNA-binding domain of human papillomavirus type 18 E1. Crystal structure, dimerization, and DNA binding. *J Biol Chem* **279**, 3733–3742.

Berumen, J., Ordoñez, R. M., Lazcano, E., Salmeron, J., Galvan, S. C., Estrada, R. A., Yunes, E., Garcia-Carranca, A., Gonzalez-Lira, G. & Madrigal-de la Campa, A. (2001). Asian-American variants of human papillomavirus 16 and risk for cervical cancer: a case-control study. *J Natl Cancer Inst* **93**, 1325–1330.

Bosch, F. X., Lorincz, A., Muñoz, N., Meijer, C. J. & Shah, K. V. (2002). The causal relation between human papillomavirus and cervical cancer. *J Clin Pathol* **55**, 244–265.

Broccolo, F., Chiari, S., Piana, A., Castiglia, P., Dell'Anna, T., Garcia-Parra, R., Maneo, A., Villa, A., Leone, E. B. & other authors (2009). Prevalence and viral load of oncogenic human papillomavirus types associated with cervical carcinoma in a population of North Italy. *J Med Virol* **81**, 278–287.

Chiang, C. M., Ustav, M., Stenlund, A., Ho, T. F., Broker, T. R. & Chow, L. T. (1992). Viral E1 and E2 proteins support replication of homologous and heterologous papillomaviral origins. *Proc Natl Acad Sci U S A* **89**, 5799–5803.

Contreras-Paredes, A., De la Cruz-Hernández, E., Martínez-Ramírez, I., Dueñas-González, A. & Lizano, M. (2009). E6 variants of human papillomavirus 18 differentially modulate the protein kinase B/phosphatidylinositol 3-kinase (AKT/PI3K) signaling pathway. *Virology* **383**, 78–85.

Côté-Martin, A., Moody, C., Fradet-Turcotte, A., D'Abramo, C. M., Lehoux, M., Joubert, S., Poirier, G. G., Coulombe, B., Laimins, L. A. & Archambault, J. (2008). Human papillomavirus E1 helicase interacts with the WD repeat protein p80 to promote maintenance of the viral genome in keratinocytes. *J Virol* **82**, 1271–1283.

De la Cruz-Hernández, E., García-Carrancá, A., Mohar-Betancourt, A., Dueñas-González, A., Contreras-Paredes, A., Pérez-Cardenas, E., Herrera-Goepfert, R. & Lizano-Soberón, M. (2005). Differential splicing of E6 within human papillomavirus type 18 variants and functional consequences. *J Gen Virol* **86**, 2459–2468.

Demeret, C., Goyat, S., Yaniv, M. & Thierry, F. (1998). The human papillomavirus type 18 (HPV18) replication protein E1 is a transcriptional activator when interacting with HPV18 E2. *Virology* **242**, 378–386.

Demeret, C., Garcia-Carranca, A. & Thierry, F. (2003). Transcription-independent triggering of the extrinsic pathway of apoptosis by human papillomavirus 18 E2 protein. *Oncogene* **22**, 168–175.

Flores, R., Papenfuss, M., Klimecki, W. T. & Giuliano, A. R. (2006). Cross-sectional analysis of oncogenic HPV viral load and cervical intraepithelial neoplasia. *Int J Cancer* **118**, 1187–1193.

Fradet-Turcotte, A., Moody, C., Laimins, L. A. & Archambault, J. (2010). Nuclear export of human papillomavirus type 31 E1 is regulated by Cdk2 phosphorylation and required for viral genome maintenance. *J Virol* **84**, 11747–11760.

Fradet-Turcotte, A., Bergeron-Labrecque, F., Moody, C. A., Lehoux, M., Laimins, L. A. & Archambault, J. (2011). Nuclear accumulation of the papillomavirus E1 helicase blocks S-phase progression and triggers an ATM-dependent DNA damage response. *J Virol* **85**, 8996–9012.

Hegde, R. S. & Androphy, E. J. (1998). Crystal structure of the E2 DNA-binding domain from human papillomavirus type 16: implications for its DNA binding-site selection mechanism. *J Mol Biol* **284**, 1479–1489.

Hubert, W. G. (2005). Variant upstream regulatory region sequences differentially regulate human papillomavirus type 16 DNA replication throughout the viral life cycle. *J Virol* **79**, 5914–5922.

Hubert, W. G., Kanaya, T. & Laimins, L. A. (1999). DNA replication of human papillomavirus type 31 is modulated by elements of the upstream regulatory region that lie 5′ of the minimal origin. *J Virol* **73**, 1835–1845.

Koonin, E. V. (1993). A common set of conserved motifs in a vast variety of putative nucleic acid-dependent ATPases including MCM proteins involved in the initiation of eukaryotic DNA replication. *Nucleic Acids Res* **21**, 2541–2547.

Lizano, M., Guido, M. C., Garcia-Carranca, A., Berumen, J. & Casas, L. (1997). Association between human papillomavirus type 18 variants and histopathology of cervical cancer. *J Natl Cancer Inst* **89**, 1227–1231.

Lizano, M., De la Cruz-Hernández, E., Carrillo-García, A., García-Carrancá, A., Ponce de Leon-Rosales, S., Dueñas-González, A., Hernández-Hernández, D. M. & Mohar, A. (2006). Distribution of HPV16 and 18 intratypic variants in normal cytology, intraepithelial lesions, and cervical cancer in a Mexican population. *Gynecol Oncol* **102**, 230–235.

López-Saavedra, A., González-Maya, L., Ponce-de-León, S., García-Carrancá, A., Mohar, A. & Lizano, M. (2009). Functional implication of sequence variation in the long control region and E2 gene among human papillomavirus type 18 variants. *Arch Virol* **154**, 747–754.

Morgan, I. M. & Taylor, E. R. (2005). Detection and quantitation of HPV DNA replication by Southern blotting and real-time PCR. *Methods Mol Med* **119**, 349–362.

Morin, G., Fradet-Turcotte, A., Di Lello, P., Bergeron-Labrecque, F., Omichinski, J. G. & Archambault, J. (2011). A conserved amphipathic helix in the N-terminal regulatory region of the papillomavirus E1 helicase is required for efficient viral DNA replication. *J Virol* **85**, 5287–5300.

Taylor, E. R. & Morgan, I. M. (2003). A novel technique with enhanced detection and quantitation of HPV-16 E1- and E2-mediated DNA replication. *Virology* **315**, 103–109.

Titolo, S., Brault, K., Majewski, J., White, P. W. & Archambault, J. (2003). Characterization of the minimal DNA binding domain of the human papillomavirus E1 helicase: fluorescence anisotropy studies and characterization of a dimerization-defective mutant protein. *J Virol* **77**, 5178–5191.

Wanram, S., Limpaiboon, T., Leelayuwat, C., Yuenyao, P., Guiney, D. G., Lulitanond, V. & Jearanaikoon, P. (2009). The use of viral load as a surrogate marker in predicting disease progression for patients with early invasive cervical cancer with integrated human papillomavirus type 16. *Am J Obstet Gynecol* **201**, e1–e7.

Wilson, V. G., West, M., Woytek, K. & Rangasamy, D. (2002). Papillomavirus E1 proteins: form, function, and features. *Virus Genes* **24**, 275–290.

Xiao, J. H., Davidson, I., Matthes, H., Garnier, J. M. & Chambon, P. (1991). Cloning, expression, and transcriptional properties of the human enhancer factor TEF-1. *Cell* **65**, 551–568.

Xu, Y., Dotto, J., Hui, Y., Lawton, K., Schofield, K. & Hui, P. (2009). High grade cervical intraepithelial neoplasia and viral load of high-risk human papillomavirus: significant correlations in patients of 22 years old or younger. *Int J Clin Exp Pathol* **2**, 169–175.

zur Hausen, H. (2002). Papillomaviruses and cancer: from basic studies to clinical application. *Nat Rev Cancer* **2**, 342–350.